



Peoples Democratic Republic of Algeria
Ministry of Higher Education and Scientific Research
Larbi Tébessi University -TEBESSA-
Faculty of Science and Technologies
Civil Engineering Department



**3D NUMERICAL INVESTIGATION OF THE LINEAR AND
NON-LINEAR BEHAVIOUR OF STEEL STRUCTURES
HAVING WEB OPENINGS UNDER DIFFERENT LOADING
CONDITIONS.**

BOUDJADJA Marwa

Master Academic Dissertation

Speciality: Structural Engineering

Academic year: 2019/2020

Presented on -September the 22^{sd} 2020:

Examination committee

Dr. SOLTANI Mohammed Redha

President Examiner

Dr. HAMIDANE H'mida

Member Examiner

Dr. LABED Abderrahim

Member Supervisor

بِسْمِ اللَّهِ الرَّحْمَنِ الرَّحِيمِ

Acknowledgment

الحمد لله

First of all, I thank ALLAH, the One who gave me the strength and the commitment to achieve this after months of hard work.

I want to dedicate this modest work to the light of my life my parents, and all my brothers and sisters

I pay my deep sense of gratitude to my supervisor Abderrahim LABED to encourage me to the highest peak, and gave me the golden opportunity to do this project. And I came to now about so many new things. I am thankful to him

To all those who, by a word gave me the courage to continue. also to all the staff of the department and faculty and to all the professors who have taught us and shared their vast knowledge over the past 5 years.

Boudjadja.M

Table of contents	
AKNOWLEDGMENT	
LIST OF TABLES	i
LIST OF FIGURES	ii
LIST OF SYMBOLES	vi
ABSTRACT	A
INTRODUCTION	D
MOTIVATION AND AIMS OF THIS RESEARCH	E
OBJECTIVES	F
METHODOLOGY	F
CHAPTER I: GENERAL ABOUT PERFORATED STEEL BEAMS	
1.1 Introduction	1
1.2 Structural elements with web openings	1
1.2.1. Application area	2
1.2.2. Advantages	3
1.3 Opening shapes	5
1.3.1: Common types of web openings with and without reinforcement	5
1.3.2: Advanced types	7
1.3.3. Geometry	9
1.4 Manufacturing	10
Bibliography	12
CHAPTER II: STRUCTURAL PERFORMANCE OF ELEMENTS WITH WEB OPENINGS.	
2.1 Introduction	14

2.2 Literature review	14
2.3 Current research status	15
2.4 Perforations in steel beams effect on their behaviour	16
2.4.1. Global bending action	17
2.4.2. Global shear action	17
2.4.3. Local Vierendeel action	17
2.5 Failure modes of steel structures with web openings	18
2.5.1 Strength failure modes.	19
2.5.2 Instability related modes	20
2.6 Summary of failure modes of WOB's to EC3	24
2.7 Guidelines for web openings and stiffeners	24
2.7 Overview of Experimental Studies in the Literature.	25
2.7.1 General	25
2.7.2 Overview	26
Bibliography	31
CHAPTER III: DESIGNING RECOMMENDATIONS FOR WOB's	
3.1 Introduction	34
3.2 Influence of opening on the carrying capacity of beams	34
3.3 Classification of the cross-section of the web-openings beams	34
3.4 Design of beams with web openings	36
3.4.1 Design rules for openings	37
3.4.2 Design of sections strength	39
Bibliography	54
CHAPTER VI: PORTAL STEEL FRAMES	
4.1 General	57

4.2 Types of portal frame and characteristics	57
4.2.1 Definition	57
4.2.2 Categories	58
4.3 Portal frame with WOB structures as lateral resisting systems.	58
Bibliography	60
CHAPTER V: OVERVIEW ON USED SOFTWARE AND FEA	
5.1 General	61
5.2 Introduction to ABAQUS	61
5.3 Modelling sequence	62
5.4 Elements in ABAQUS	65
5.4.1 Element types	65
5.4.2 Element Shapes	68
5.5 Numerical Techniques used for Solving Nonlinear Problems with ABAQUS	69
5.5.1 Non-linear numerical modelling tools	70
Bibliography	73
CHAPTER VI: MODELLING	
6.1 Introduction	74
6.2 modelling properties of tested beams	74
6.2.1 Beams tested by Redwood and Mccutcheon	75
6.2.2 Beams tested by warren. J	76
6.3 Numerical simulations	78
6.3.1 The applied loads	79
6.3.2 Boundary conditions	80
6.3.3 Meshing	81

6.4 Validation of the results and discussion of the primary studies	82
6.4.1 Study of single WOB tested by Redwood and Mccutcheon	82
6.4.2 Study of beams tested by Warren.J	89
6.4.3 Summary of the obtained results	95
Bibliography	97
CHAPTER VII: ANALYSIS OF KEY PARAMETERS ON THE NONLINEAR BEHAVIOURS OF WOB'S.	
7.1 General and scope	98
7.2 Parametric study and modelling of isolated beam	99
7.2.1 Properties of modelled beams	99
7.2.2 Cases studied model geometrical features	100
7.2.3 Boundary conditions and meshing for isolated beams	102
7.2.4 Results and discussion of isolated beam cases	103
7.3 Parametric study and modelling of portal frames	113
7.3.1 Model description	113
7.3.2 Boundary conditions and meshing for the portal frames	113
7.4 Summary of the obtained results	121
Bibliography	123
SUMMARY, CONCLUSIONS AND RECOMMENDATIONS FOR FUTURE WORK	

List of tables	
Title	Page
Table 6.1: steel sections yield and ultimate stresses.	76
Table 6.2: steel sections geometrical properties.	76
Table 6.3: steel sections yield and ultimate stresses.	77
Table 6.4: steel sections geometrical properties.	78
Table 7.1: Profile details.	99
Table 7.2: Perforated profile details.	99
Table 7.3: parametric modelling variables	100
Table 7.4: portal frames models	113

List of figures	
Title	page
Figure 1.1: Various web-opening shapes in floor beams.	2
Figure 1.2: Opening's applications.	4
Figure 1.3: Example of castellated beams.	5
Figure 1.4: Example of cellular beams.	5
Figure 1.5: Beam with rectangular shape openings.	6
Figure 1.6: cellular beam with circular reinforcements.	6
Figure 1.7: rectangular shape with large reinforcement.	7
Figure 1.8: Ellipse openings.	8
Figure 1.9: Angelina beams.	9
Figure 1.10: geometry details of openings.	9
Figure 1.11: Profile geometry of perforated cross section.	10
Figure 1.12: fabrication process of perforated steel beams.	11
Figure 2.1: Location of the plastic hinges.	20
Figure 2.2: rupture of welded web joints.	20
Figure 2.3: Buckling of a typical cross section with LTB.	21
Figure 2.4: Lateral-torsional buckling due to (vertical) shear.	21
Figure 2.5: Buckling of a typical steel cross section with LDB.	22
Figure 2.6: compression and tension locations at the inclined edge of an opening	23
Figure 2.7: Local forces and position of the critical sections in the intermediate web-post.	23
Figure 3.1: Portion of the web opening forming the stem of an unstiffened tee.	36
Figure 3.2: Position of tee section and web post.	37
Figure 3.3: Position and dimension of isolated openings.	38
Figure 3.4: Position and dimension of multiple rectangular openings.	38
Figure 3.5: Position and dimension of multiple circular openings.	39
Figure 3.6: Cubic Diagram of Moment-shear force Interaction	43
Figure 3.7: Interaction Curve Moment-shear force	44
Figure 3.8: Beam with multiple polygonal openings	46
Figure 3.9: Beam with multiple circular and oval openings.	47
Figure 3.10: Stress resultant at critical section.	48

Figure 3.11: Vierendeel bending either by an ‘equivalent rectangular opening’ or by inclined section verifications.	50
Figure 3.12: equivalent diameter for a rectangular opening.	50
Figure 3.13: internal stress distribution.	52
Figure 3.14: Local forces and position of the critical sections in the intermediate web-pos.t	53
Figure 4.1 typical one bay portal frame; (a) flat-roofed portal frame and (b) pitched-roof portal frame.	57
Figure 5.1: ABAQUS Modules.	64
Figure 5.2: Family of element in ABAQUS.	65
Figure 5.3: Number of nodes of element in ABAQUS	66
Figure 5.4: Displacement and Rotational degrees of freedom.	66
Figure 5.5: Elements Shapes in ABAQUS.	68
Figure 5.6: Resolution methods using implicit formulation.	70
Figure 6.1: Beam models geometry	75
Figure 6.2: Typical test beam setup	77
Figure 6.3: Stress vs strain curves used for FEA material properties.	77
Figure 6.4: Creating of a shell element for modelling of beams	78
Figure 6.5: creating part element for modelled Redwood and Mccutcheon beams	79
Figure 6.6: creating part element for modelled Warren.J beams.	79
Figure 6.7: loading position for (a) 2A and (b) 3A beams.	80
Figure 6.8: loading position for (a) beam 1A and (b) beam 3B.	80
Figure 6.9: Meshing type example for (a) Redwood and Mccutcheon, (b) Warren.J and (c) flanges mesh generation for both.	82
Figure 6.10: Finite element results (a) Beam 2A (b) Beam 3A .	84
Figure 6.11: Von Mises equivalent stress contour distribution for 5 % strain hardening.	85
Figure 6.12: Von Mises equivalent stress distribution contour for 2 % strain hardening.	85
Figure 6.13: Von Mises equivalent stress distribution for 5 % strain hardening.	86
Figure 6.14: Comparison of finite element and experimental model results beam 2A (b) beam3A	87

Figure 6.15: Comparison of several finite element and experimental model result (a) beam 2A (b) beam3A.	87
Figure 6.16: Von Mises stress distribution contour in Beam 2A (a) Chung, (b) Flavio.R and (c) present study.	88
Figure 6.17: Shear stress distribution contour in Beam 2A (a) Present study (b) Chung	89
Figure 6.18: Beam 1A finite element model results.	90
Figure 6.19: Beam 1A finite element and experimental model results comparison.	91
Figure 6.20: Von mises stress distribution contour at last stage.	92
Figure 6.21: Beam 3B finite element model results.	92
Figure 6.22: Comparison of finite element and experimental model results for Beam 3B.	93
Figure 6.23: Von Mises stress distribution contour for beam 3B.	95
Figure7.1: Plain web beam geometry	99
Figure7.2: Basic geometry models layout without reinforcements cases 1 and2	101
Figure 7.3: Basic geometry models layout without reinforcements cases 3 and 4	102
Figure 7.4: Load-deflection curves for case1	104
Figure 7.5: Von Mises combined stress distribution contour for case 1.	105
Figure 7.6: Load-deflection curves associated to case 2.	106
Figure 7.7: Von Mises combined stress distribution contour for case 2.	107
Figure 7.8: Deformed shape and Von Mises stress distribution for case 3	108
Figure 7.9: Von Mises stress distribution for configuration 3.	110
Figure 7.10: Load-deflection curve associated to case 4.	111
Figure 7.11: Deformed shape and Von Mises stress distribution for case 4.	112
Figure 7.12: Load-deflection comparative curves.	114
Figure 7.13: Basic geometry layouts of models of the portal single storey one bay with cellular beams.	114
Figure 7.14: Load-deflection curve for model 1.	114
Figure 7.15: Deformed shape and Von Mises Equivalent Stress contour for model 1 with some other details in different interesting sections.	116

Figure 7.16: Load-deflection curve for model 2	116
Figure7.17: Deformed shape and Von Mises Equivalent Stress contour for model 2with some other details in different interesting sections.	118
Figure 7.18: Load-deflection curve for model 3.	118
Figure7.19: Deformed shape and Von Mises Equivalent Stress contour for model 3 with some other details in different interesting sections.	119
Figure 7.20: Load-deflection curve for model 4.	120
Figure7.21: Deformed shape and Von Mises Equivalent Stress contour for model 4with some other details in different interesting sections.	121

List of symbols	
Symbol	Designation
A	Cross sectional area of the original beam
A_v	shear area of the unperforated cross-section
d_w	overall height of the web
d_c	Distance between the elastic neutral axes of the tee-sections
d_0	Circular opening diameter.
e_0	Eccentricity between the centre of the opening and the mid-height of the beam web.
E	Elastic modulus of steel
f_y	Material yield stress.
f_{yw}	elastic limit of the web
h_0	height of the opening
I_y	moment of inertia of the unperforated cross-section;
k	Factor indicates the reserve provided by the Tees for openings beyond the appearance of instability of the web post.
l_o	Opening length
$l_{o, \text{eff}}$	Effective length of the opening for stability of the web.
$M_{o, \text{sd}}$	load moment
$M_{pL, \text{Rd}}$	Plastic moment of resistance of the unperforated cross-section
$M_{eL, \text{Rd}}$	Elastic moment of resistance of the unperforated cross-section.
$M_{o, \text{rd}}$	moment resistance capacity
$M_{v, \text{sd}}$	Design value of Vierendeel bending
$M_{v, \text{rd}}$	Design Vierendeel moment resistance of the perforated section.
$M_{pLC, \text{Rd}}$	Moment resistance of the top tee section in compression.
$M_{pLt, \text{Rd}}$	Moment resistance of the bottom tee section in tension.
$M_{\phi, \text{sd}}$	Internal moment.
$M_{\phi, \text{Rd}}$	Reduced moment of resistance for shear force.
$M_{eL, \text{Rd}}$	Elastic moment of resistance of the critical cross-section in the web post.
M_{sd}	Applied global moment at the mid-length of the opening.
$N_{m, \text{sd}}$	Applied axial force due to global bending action.
$N_{\phi, \text{sd}}$	Normal force perpendicular to the section.
$N_{\phi, \text{Rd}}$	Reduced normal shear stress resistance.
r	Fillet radius of the rolled section.
t_w	Web thickness.
t_f	Flange thickness.
$V_{opL, \text{Rd}}$	Plastic shear strength of the net cross section at an opening.
V_{h_i}	Longitudinal shear force at the welding joint of the web post.
$V_{h, \text{sd}}$	Horizontal shear stress at web post.
$V_{0, \text{Rd}}$	Resistance to the pure shear in the middle of the perforated section.
$V_{0, \text{sd}}$	Shear force in the middle of the perforated section

$V_{T,pl,Rd}$	plastic shear resistance of the tee section
$V_{T,sd}$	Applied shear force.
$V_{Oba,Rd}$	Resistance to shear buckling of a perforated cross section.
V_{sd}	Shear force.
$V_{PL,Rd}$	Plastic shear strength of the unperforated section.
W_{pl}	plastic module of the unperforated cross section
W	Minimum width of the web post.
y_t	Distance from the elastic neutral axis of the upper Tee to the upper edge of the flange.
γ_{M_0}	Partial safety coefficient
η	Coefficient that takes into account the influence of the eccentricity of the opening on the shear strength
ϕ	angle (of inclined section to the vertical through the hole).
σ_{wEd}	Main compressive stress in the half web post studied.
σ_{wRd}	Principal resistive stress with a post-critical reserve factor.
ε	coefficient for section classification

ABSTRACT

The main aim described in this master dissertation was to investigate the mechanical linear and nonlinear behaviours of steel isolated beams having web openings with an emphasis on load carrying capacities, failure mode and stress distribution at the opening's edges and its effects in the web regions. Several 3D numerical simulations using ABAQUS software were performed taking into account material and geometric nonlinearities. Firstly, the simulations were built-up to validate some available data obtained from two experimental investigations on single and multiple openings in steel beams designed as simply supported excluding any LTB effect. By comparison with experimental data the numerical models developed in this work have predict with good accuracy the linear and nonlinear behaviours and to some extent the failure modes of models. Furthermore, the outcomes obtained in this investigation were favourably compared to others simulations using different software. in terms of strain hardening inputs. Then, In the purpose to investigate the influence of the geometrical parameters on the load capacity and failure modes, a comprehensive through 16 simulations parametric study on isolate beams with variable shapes and sizes equipped or not stiffeners was carried out together with a series of one bay single storey portal frames in which multiple cellular beams associated to columns. A detailed discussion of the results will be provided and, accordingly, interesting conclusions will be derived based on the results obtained for the evaluation of each parameter studied on the non-linear WOB's behaviour.

Key words:

Web opening beams, 'Vierendeel' Mechanism, Linear and Non-linear FEM, Plastic Hinges, Critical opening sections, Stress Concentration.

Résumé

Le principal objectif décrit dans ce mémoire de maîtrise est d'étudier les comportements mécaniques linéaires et non linéaires des poutres isolées en acier ayant des ouvertures dans l'âme en mettant l'accent sur les capacités portante, le mode de rupture et la répartition des contraintes aux bords des ouvertures et leurs effets dans les régions de l'âme. Plusieurs simulations numériques en 3D ont été réalisées en tenant compte des non-linéarités matérielles et géométriques en via le logiciel ABAQUS. Tout d'abord, les simulations ont été développés pour valider certaines données expérimentales disponibles dans la littérature. Ces données expérimentales sont issues de deux études expérimentales sur des poutres isolées à ouvertures simples et multiples comme simplement appuyées aux extrémités en excluant tout déversement respectivement. Les résultats obtenus dans cette étude des modèles numériques développés ont correctement prédit, avec une bonne précision les comportements linéaires et non linéaires des courbes expérimentales et dans une certaine mesure les mêmes modes de ruptures observés lors de l'expérimentation. En outre, les résultats obtenus dans cette étude ont été favorablement comparés à d'autres simulations, utilisant des logiciels différents, des mêmes données expérimentales avec différentes valeur de l'écroutissage. Ensuite, une étude paramétrique a été engagée pour étudier l'influence des paramètres géométriques sur la capacité portante et les modes de rupture à travers 16 simulations sur des poutres isolées de formes et de tailles variables, équipées ou non de raidisseurs, Ajouter à cela une série de portiques à un seul étage dans lesquels de multiples poutres cellulaires sont associées à des colonnes a été menée pour voir l'influence des conditions d'appuis notamment les assembles sur le comportement des mêmes poutres analysées précédemment. Une discussion détaillée des résultats est donnée et, en conséquence, des conclusions intéressantes seront tirées sur la base des résultats obtenus.

Mot clés

Poutres avec ouverture dans l'âme (poutres ajourées), mécanisme de Vierendeel, MEF linéaire et non linéaire, rotules plastique, sections critiques des ouvertures, concentration des contraintes.

ملخص

الهدف الرئيسي الموصوف في هذه الرسالة الرئيسية هو التحقيق في السلوكيات الميكانيكية الخطية وغير الخطية للعوارض الفولاذية المعزولة التي لها فتحات مع التركيز على قدرات تحمل الأحمال ووضع الفشل وتوزيع الضغط عند حواف الفتحة وتأثيراتها في مناطق الويب. تم إجراء العديد من عمليات المحاكاة الرقمية ثلاثية الأبعاد باستخدام برنامج ABAQUS مع مراعاة المواد وغير الخطية الهندسية. أولاً ، تم إنشاء عمليات المحاكاة للتحقق من صحة بعض البيانات المتاحة التي تم الحصول عليها من تحقيقين تجريبيين حول فتحات مفردة ومتعددة في عوارض فولاذية مصممة على أنها مدعومة ببساطة باستثناء أي تأثير LTB. بالمقارنة مع البيانات التجريبية ، فإن النماذج العددية التي تم تطويرها في هذا العمل قد تنبأت بدقة جيدة بالسلوكيات الخطية وغير الخطية وإلى حد ما تمدد أنماط فشل النماذج. علاوة على ذلك ، تمت مقارنة النتائج التي تم الحصول عليها في هذا التحقيق بشكل إيجابي مع عمليات المحاكاة الأخرى باستخدام برامج مختلفة. من حيث إجهاد المدخلات تصلب. بعد ذلك ، من أجل التحقق من تأثير المعلمات الهندسية على سعة التحميل وأنماط الفشل ، تم إجراء دراسة شاملة من خلال 16 دراسة حدودية على عوارض معزولة ذات أشكال وأحجام متغيرة مجهزة أو غير مجهزة مع سلسلة من خليج واحد إطارات بوابة من طابق واحد حيث ترتبط حزم خلوية متعددة بالأعمدة. سيتم تقديم مناقشة مفصلة للنتائج ، وبالتالي ، سيتم استخلاص استنتاجات مثيرة للاهتمام بناءً على النتائج التي تم الحصول عليها لتقييم كل معلمة تمت دراستها على سلوك الغير الخطي للعوارض الفولاذية.

INTRODUCTION

In recent decades, a new engineering practice in modern architecture by introducing single or multiple openings in beams, which can assume different shapes. To allow the passage of services within the depth of the beam instead of underneath the beam. It is in this context, beams with web openings were increasingly used in steel constructions and since the introduction of castellated beams in the 1940's and cellular beams in the 1990's, attention has largely shifted to these types of beam as alternative means for Mechanical and Electrical services integration within the floor depth and for esthetical reasons. This helps to reduce the floor height of the building and optimizes the available space. Although, the primary purpose of these beams was to improve the structural efficiency of rolled I-section beams particularly in terms of the flexural bending capacity. In general, castellated and cellular beams are ideal for long span applications with moderate uniform distributed loading (UDL). A new elliptically based web opening shapes as the sinusoidal openings, were presented in literature to enhance the structural behaviour of the perforated beams as well as lead to economic design in terms of both manufacture and usage.

Creating an opening in web may have a significant drawback on the load carrying capacities and failure modes of structural members, depending on shapes, sizes, and locations of the openings as reported by Chung. While the presence of web perforations in steel beams generate three different modes of failure at the perforated sections:

- flexural failure due to reduced moment capacity,
- shear failure due to reduced shear capacity,
- the 'Vierendeel' mechanism, associated with transferring of lateral shear force across a web opening with the formation of four plastic hinges in the tee-sections above and below the web openings.

Numerous numerical and experimental investigations on beams with web openings have been developed throughout the world and some are available in literature. This were attempts to better understand and examine the structural behaviour under some key parameters by optimizing the shapes, sizes and positions of web openings to provide a better understanding of the stress distribution in the vicinity of web openings. Many other works can be cited concerning a

development of studies on local instabilities by means of lateral-torsional buckling (LTB) and local buckling (LB) accompanied with the presence of stiffeners with its various configurations.

In this dissertation and in order to obtain the actual behaviour of WOB's, it is necessary to perform a more sophisticated nonlinear analysis including the load positions, the entire load deflection curve and the plastic location of plastic hinges properties of the structure. An elaborate finite element model has been established, with both material and geometric non-linearity plotted with ABAQUS software. This investigation therefore focuses on three main categories, beams with single web opening, beams with multiple web openings and those associated with columns. towards an analysis of two important parts where the first one is involved with the validation of number of experimental data on cellular beams. Hence, importance of the parameters that affect the structural performance of beams is illustrated by a parametric study in the second part dealing with the variation of opening shapes, size, presence of different stiffeners configurations and where connected to columns.

- **MOTIVATION AND AIMS OF THIS RESEARCH**

Structural engineers have always tried to find new methods to improve the design and construction performance of steel and composite buildings in order to increase strength and reduce overall cost. Open web beams are some of these options. For many years, web openings with various geometric properties have been used to pass conduits or utilities through web holes to reduce floor heights and the cost of constructing large-scale buildings.

The subject of beams with web openings caught my attention mainly because of their popularity, as they are being used for structures such as industrial buildings and high-rise buildings has turned out to be extensive use in recent years. In addition, some heavy-mass structures, such as bridges, have been constructed using perforated beams for the full span.

- **OBJECTIVES**

The objective of this work is to study and compare, by means of a finite element (FE) study and experimental data respectively, the behaviour of perforated steel beams with single and multiple openings. Therefore, the sub-objectives of this research are as follows:

- Investigate the structural behaviour of single and multiple web openings in steel beams.
- Correlate the experimental results with FE models, and to study in details their complexity structural behaviour in terms of stress distribution and failure modes.
- Examine both the load capacities and failure modes of the perforated sections.
- Analyse the positions of the high stress concentration points near the openings.
- Conduct a parametric finite element study on single web opening sections with different shapes, sizes and stiffeners configurations.
- To evaluate the behaviour of multiple cellular beams when connected to columns in steel MRFs.

- **METHODOLOGY**

This dissertation has been structured into seven chapters as follows:

- An introduction providing a brief information on the work undertaken in this study and its objectives.

-**Chapter 1:** This chapter presents an overview on beams with web opening, their common and advanced shapes, furthermore a historical order and a practical application of cellular beams are shown with some pictures.

-**Chapter 2:** This chapter is aimed at giving a brief account with the main characteristics of steel beams with web openings used in constructions, highlighting their operating method and the complexity of their elastic and inelastic behaviour; furthermore, their failure modes in order to mention it both with isolated and multiple holes.

-**Chapter 3:** The state of the art inevitably starts with an inventory of the usual methods and design equations used dealing with beams with web openings (BWO). In this chapter, the modelling approaches proposed in the literature are reviewed to assess their relevance and the limits of their applicability including those approved by the EUROCODES3 in (ENV 1993-1-1:1992/A2:1998: steel structure design rules).

-**Chapter 4:** Brief background on MRF's portal frame structures and its performance.

-**Chapter 5:** This chapter is divided into two main topics: First, a presentation of some

generalities concerning ABAQUS programme capabilities, which were used in this study. Secondly, a discussion of the use of finite element analysis and nonlinearities by its fields for the beams that implemented and tested in the ABAQUS in terms to validate the results of the experimental tests.

-Chapter 6: The objective of this chapter is to develop and describe numerical models that is able to simulate as accurately as possible the behaviour of cellular beams. Furthermore, is to carry out non-linear finite element analysis of (BWO) that were considered in the experimental study.

-Chapter 7: The chapter deals with a parametric study which investigates the influence of the geometrical parameters.

- Conclusions and suggestions for further work: Main conclusions are drawn with some suggestions for further work.

C ***HAPTER I:***

GENERAL ABOUT PERFORATED STEEL BEAMS

1.1 Introduction

In Modern architecture, solutions that can minimize the cost and increase the strength are available, indeed, over the past several years or maybe three decades, extensive theoretical, numerical and experimental research has been carried out on the structural behaviour of steel beams with web openings considering various shapes, although the use of cellular columns is less common, examples in literature are available. However, in research publications less attention is paid to this topic. [6]to find new ways to reduce the cost of steel structures due to limitations on maximum allowable deflections the high strength properties of structural steel cannot always be utilized to the best advantage; as a result several new methods have been aimed at increasing the stiffness of steel members without any increase in the weight of steel, required web openings steel beams have been used extensively in recent times. [7]

1.2 Structural elements with web openings

A perforated steel beam is an I-shaped beam section with a variety in shape opening in the web, so that the opening can be hexagonal, rectangular, circular, diamond or oval in shape. [1] The use of perforated steel beams has resulted in longer span floors. Their popularity has also increased because of an architectural emphasis on exposed structures [3], In the 1960s, 1970s, and 1980s, studies on different web opening configurations were completed in the United States and Canada, including square, rectangular, circular, concentric, and eccentric openings in both non-composite and composite steel beams. In the late 1980s, Darwin and Donahey (1988), Darwin and Lucas (1990) and Darwin (1990) demonstrated that it is possible to produce a unified procedure embodying the different cases that are frequently used in steel building structures. When used as floor beams, open-web sections on their turn are a part of the group of floor systems which provide a means to incorporate building services within the structural depth of the floor, Nowadays, in most cases the design of floor beams with web openings is carried out recognizing the composite action between the steel beam and the concrete slab on top of it.[6]

Some national designing standards, i.e. the British Standard (BSI, 2000) and the Canadian Standard (CSA, 2001), provide some simplified rules for opening design. These rules are provided in order to avoid the weakening of the beam. However, these rules cover a wide range of possibilities, and,

therefore, they are very conservative and, in general, restrict the openings to the middle third of the beam depth and to the two central quarters of the beam span. By fixing some parameters, it would be possible to get more flexible and economical results for typical situations in the floors of buildings.[2]

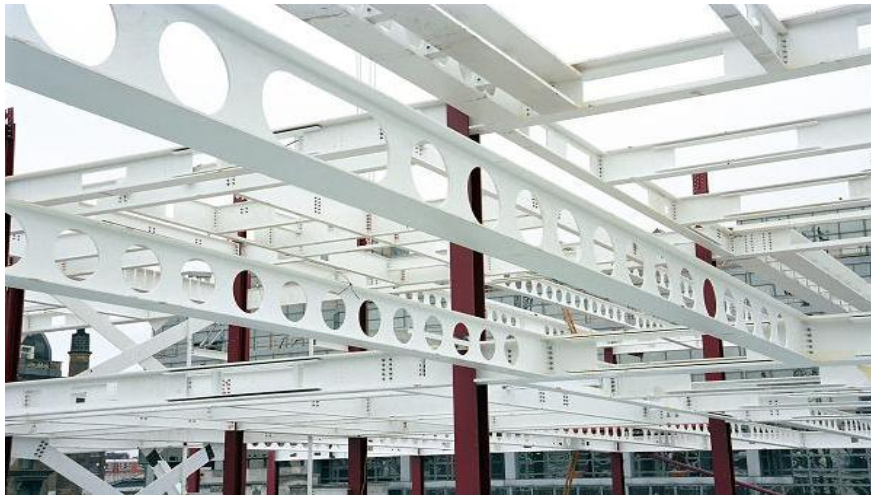


Figure1.1: various web opening shapes in floor beams.

1.2.1. Application area

Open web expanded steel beams were firstly used in structures during World War II to reduce the cost of steel structures (Altifillisch, Cooke, and Toprac 1957; Toprac and Cooke 1959; Sherbourne 1966; Bazile and Texier 1968). Cellular beams were first used in Switzerland in the 1970s [Stahlbau 1970s], but application became common not before the 1990s. Increasing the stiffness and strength of the original beam has been the main purpose of the selection of these beams from designers. This is achieved by cutting the web of the root beam in a certain pattern and then welding two parts to each other. First, in the Netherlands multi-storey buildings with more than four floors are traditionally the domain of concrete [BmS2002]. Second, the price of individual cellular beams is indeed higher than that of standard rolled profiles. It has however been shown by many success-full designs (especially in the UK, but among others also in Germany and France) that steels really a viable alternative, Castellated beams were used in the 1930s already.

Cellular beams can be used as floor beams or roof beams. They are most economical when used in long spans or when inclusion of services is a consideration. The Westok brochure14 advises that

cellular beams are most economical when used as long span secondary members. Additional benefits are column free floor space, fewer foundations and faster erection.

1.2.2. Advantages

The initial idea was to create single web openings in steel beam in order to incorporate services within the floor-ceiling zone of the structure [13]; like pass heating, ventilation and air conditioning (HVAC) system through the web of beam. Since the first decade of the twentieth century, the improved automation in fabrication has resulted in the use of castellated beams and cellular beams. In comparison with traditional steel beam, castellated beams and cellular beams have more advantages such as light weight and long span capability. One of its great advantages is the ability to run utilities directly through the web openings. By integrating the HVAC system into the floor structure, the clear height of floor will be increased.[12] the annex N of EC3 summarize that the individual web openings are formed to allow for easy installation of buildings services through the webs of beams. Multiple web openings can be formed for the same purpose but are also formed to increase the overall depth of a beam to enhance its moment resistance. In other words, and as a result there are several advantages of steel beams with web openings:

- In addition to the aesthetic aspect; beams with web openings increase the stiffness of steel members without any increase in the weight of steel required.
- Used for Passing of utilities and services such as ventilation ducts, air condition ducts, electrical and data communication systems, fire protection systems, heating and cooling systems and instrumentation cables. (11)
- Satisfy economic requirements and minimize floor height. (11)
- To reduce the material volume without affecting the structural strength or serviceability requirements.[13]
- To alleviate the beam column joints from high stresses. [13]

1.3 opening shapes

Perforated beams are generally classified on the basis of type or shape of perforation made in the web of the beam; hence the shape of the web openings will depend upon the designer's choice

and the opening purpose (4), however Steel members can be equipped with single or multiple web openings, which can take different shapes. When these openings are circular and regularly spaced, the members are designated cellular. Depending on the fabrication process other opening shapes are possible, including square, rectangular, hexagonal (standard castellated section) and octagonal shapes.[6]but can include irregular openings that are employed under certain circumstances where a modification is necessary, With the rapid development of fabrication technology, more complex profiles of the perforated beams have become possible including elongated openings, tapered sections and curved beams.[14]



Figure1.2: opening's applications

1.3.1 Common types of web openings with and without reinforcement

1.3.1.1 web with centrally placed hole without reinforcement

a-web with hexagonal hole (Castellated beams): castellated beams were originally developed in Europe in 1930's to help ease steel shortage and high cost of steel, first produces in U.S early 1960's prior to domestic mills being able to produce deep wide flange sections. (5)



Figure 1.3: Example of castellated beams

b- Web with centrally placed circular hole (cellular): cellular beam is the modern version of the traditional castellated beam (5), so they have been used as beams for more than 30 years now. However, in certain countries, like the Netherlands and Belgium, application seems to lack behind. This can probably be attributed to a combination of factors: unfamiliarity with these beams, the present concrete-minded practice for multi-story buildings, and a lack of localized design guides. (6) However Cellular beams are available in different steel grades, usually floor beams require higher steel grades like S355 and S460, where the standard grade S235 suffices for roof beams.



Figure 1.4: Example of cellular beams

c- Web with centrally placed rectangular hole: generally, the use of this shape is more commonly in bridges, so when investigating the effect of web openings on the behaviour of steel I-girder bridge, both square and rectangular web openings are considered. (9)



Figure 1.5: Beam with rectangular shape openings

1.3.1.2 Web with centrally placed hole with reinforcement

When the chosen section with web opening fails to perform satisfactorily, the beam can locally be reinforced. In high shear areas in the vicinity of the supports, it may be necessary to fill or reinforce one or more openings. Buckling of a web-post can be avoided by adding two-part hoops or a simple (vertical) flat. (6)

A-Web with centrally placed circular hole with reinforcement:



Figure 1.6: cellular beam with circular reinforcements

B-Web with centrally placed rectangular hole with reinforcement

Figure 1.7: rectangular shape with large reinforcement

1.3.2 Advanced types**1.3.2.1 Ellipse web opening**

A new study was carried out and presented on the optimization of novel elliptically based web opening shapes which enhance the structural behaviour of the perforated beams as well as lead to economic design in terms of both manufacture and usage, This novel shape have a narrow opening length at the top and bottom tee sections these web opening shapes consist of a combination of semicircles with straight lines elliptical shapes the width is independent of the depth and many deep web openings can be fitted adjacent to each other along the length of a beam in comparison with the perforated beams with circular web openings.

An overall study of many standard and non-standard web opening shapes it was shown that perforated beams with vertical and inclined classic elliptical web opening behave more effectively compared to perforated beams with conventional circular and hexagonal web openings mainly in terms of stress distribution and local deflection.

To define the various web opening configurations with different web opening areas two main parameters are varied the angle (θ) of the straight lines and the radius (R) of the semicircles at the top and bottom tee sections Four θ angles (10o, 20o, 30o and 40o) as well as four R radii (0.15do,

0.2do, 0.25do and 0.3do) and their combinations were modelled for now the elliptical form of these web openings was investigated in both the vertical and inclined configurations. (7)

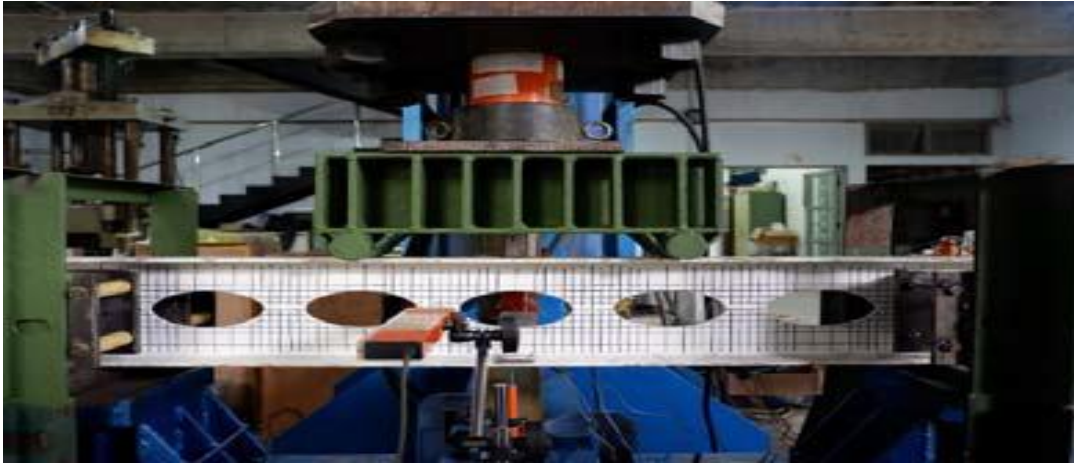


Figure 1.8: Ellipse openings.

1.3.2.2 Sinusoidal web opening

This shape offers a new architectural dimension within an environmentally friendly approach, the ANGELINA beam is manufactured from H or I beam, cut through the web along a unique sinusoidal line. The two T sections are offset and welded together providing a beam one and a half times deeper than the original profile. Moreover the aesthetic advantages of the softer gentle lines of the sinusoidal shape, there are other economic and environmental advantages of using the ANGELINA beam which is Reduced fabrication and waste, the single longitudinal cut along the beam is more efficient, whereas a traditional cellular beam requires 2 cuts resulting in additional waste and scrap material and also the sections are made from recycled material and are 100% recyclable.(8)



Figure 1.9: Angelina beams

1.3.3. Geometry

- The geometry and dimensions of a perforated section according to the Eurocodes (annex N) are covered as bellow:
 - Rectangular opening defined by its d_0 , and length a_0 ;
 - Circular opening defined by its radius r_0 ;
 - Extended circular opening defined by its depth d_0 , and end radius r_0 ;
 - Hexagonal opening defined by its depth d_0 and length a_0 , and the tee length $a_{0,eff}$;
 - Octagonal opening defined by its depth d_0 and length a_0 , the tee length $a_{0,eff}$, and the extension plate dimension d_0 .

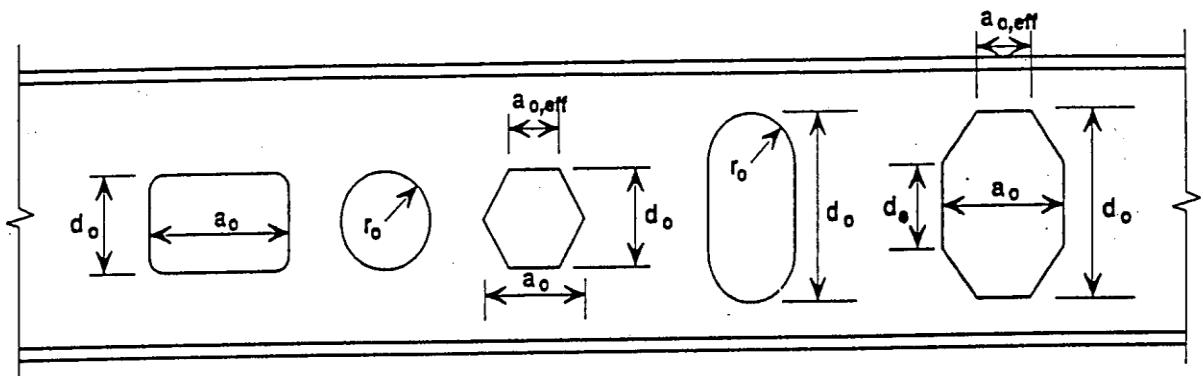


Figure 1.10: geometry details of openings.

- cross section of perforates beam

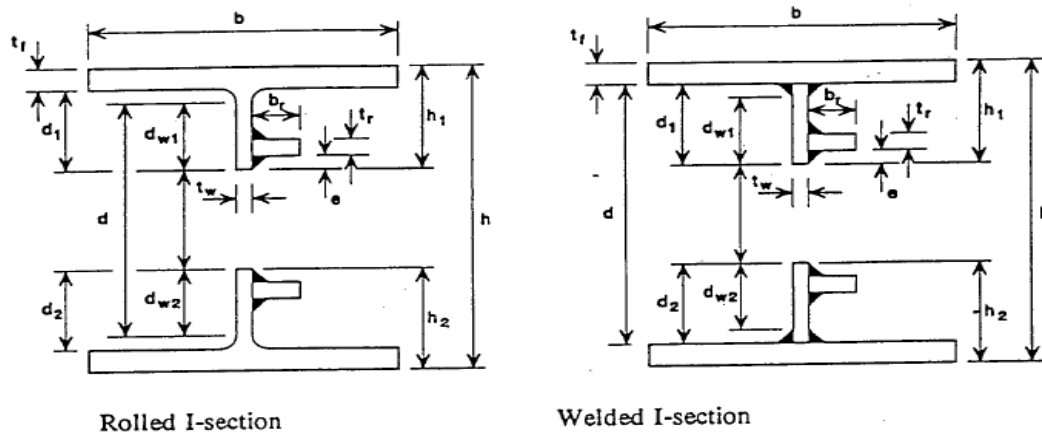


Figure 1.11: Profile geometry of perforated cross section

1.4 Manufacturing

The manufacturing method of beams with web openings is a very important factor as it affects the cost and the structural behaviour of the final product. Many advantages are gained by using the profile cutting procedure to manufacture a perforated steel beam but this process needs to be optimized to keep costs down(7); Cellular beams and castellated beams are generally classified as beams with regular web openings. As opposed to the conventional technique of perforating holes in the webs, these types of beam are fabricated by single zig-zag cutting (for castellated beams) or double cutting (for cellular beams) of the parent I-sections into two halves, and re-welding the two components back together in a shifted position. This produces new I-beams with increased depth and regular holes in the webs (BSSPC, 1995), which is both convenient and efficient. Moreover, the two half-components can be from the same original beam to generate a typical form of symmetric cellular or castellated beams. And they can also be from different parent sections leading to asymmetry in the cross-section of the new fabricated beams. The latter configuration is more beneficial for composite beam applications. [14]

So, we can resume this in three methods of manufacture of a beam with web openings:

- Individual openings are cut in the web of a hot-rolled section. In the steel section is symmetric in shape, this method is used for beams with isolated openings.
- A fabricated section is formed from three plates that are welded together to form an I-section. The section can be asymmetric (one of the flanges is larger than the other) and the beam can be tapered in depth along their length openings are cut in the web either before or after forming the I-section. This method is used both for isolated openings and for regularly spaced openings.
- A hot-rolled section is cut to a profile along the web, the resulting tee sections are repositioned and re-welded to form a series of regular openings in a deeper section. (10)



Figure 1.12: fabrication process of perforated steel beams.

Recent rapid development in manufacturing sector has been facilitated by the enhancement in computing technology, which has encouraged innovations of modern automated fabrication, where sophisticated profiles of beams with web openings can now be produced within reasonable operation time and cost. [14]

Bibliography

- [1] **S. Tudjono¹, Sunarto² and A L Han**; Master program in Civil Engineering; Analysis of castellated steel beam with oval openings; Department of Civil Engineering, Diponegoro University, Semarang-Indonesia.
- [2] **Gustavo de souza veríssimo**; Design Aids for Unreinforced Web Openings in Steel and Composite Beams with W-Shapes. Federal University of Viçosa, Viçosa, MG.
- [3] **Konstantinos Daniel TSAVDARIDIS**; Detailed Study of Perforated Beams with Closely Spaced Novel Web Openings; Academic Fellow City University, London, United Kingdom.
- [4] [/http://www.steelinsdag.org/TeachingMaterial/chapter28.pdf](http://www.steelinsdag.org/TeachingMaterial/chapter28.pdf) STEEL BEAMS WITH WEB OPENINGS.
- [5] AISC Design Guide 31 Castellated and Cellular Beam Design.
- [6] **J.G. Verweij**; Master thesis ‘‘CELLULAR BEAM-COLUMNS IN PORTAL FRAME STRUCTURES’’; Delft University of Technology Civil Engineering Section Steel and Timber Structures; November 2010.
- [7] **Konstantinos Daniel Tsavdaridis, Cedric D’Mello**; Optimization of Novel Elliptically Based Web Opening Shapes of Perforated Steel Beams.
- [8] / <https://jsteel.com.au/products/structural-sections/angelina-beams/>
- [9] **Mohamed Abdel-Basset Abdo**; ‘‘analysis of steel bridges with rectangular web openings: finite element investigation’’; Journal of Engineering Sciences, Assiut University, Vol. 38, No. 1, pp. 1-17, January 2010.
- [10] **R.M. Lawrson, Stephen james hicks**; design of composite beams with large web openings; jan 2011.
- [11] **Fattouh M. F. Shaker¹ and Mahmoud Shahat**; Strengthening of web opening in non-compact steel girders, Civil Eng. Department, Faculty of Eng. Mataria, Helwan University, Cairo. ²Graduate student.

[12] **Nguyen Tran Hieua**, simplified design method and parametric study of composite CELLULAR BEAM; Journal of Science and Technology in Civil Engineering NUCE 2018. 12

(3): 34–43 Faculty of Building and Industrial Construction, Vietnam Article history: Received 28 February 2018, revised 22 March 2018, Accepted 27 April 2018.

[13] **Lagaros***, **Lemonis D. Psarras**, **Manolis Papadrakakis**; optimum design of steel structures with web openings; Institute of Structural Analysis & Seismic Research National Technical University of Athens Zografou Campus, Athens 15780, Greece (PDF) Optimum design of steel structures with web openings. Available from: <https://www.researchgate.net/publication/222327933> Optimum design of steel structures with web openings [accessed Dec 22 2019].

[14] **Ahmad Razin Zainal Abidin**; modelling of local elastic buckling for steel beams with web openings; MSc,thesis submitted in fulfilment ofthe requirements for the degree ofDoctor of Philosophy ofImperial College LondonDepartment of Civil and Environmental EngineeringImperial College LondonLondon SW7 2AZ.jan 2013.

C ***HAPTER II:***

STRUCTURAL PERFORMANCE OF ELEMENTS WITH WEB OPENINGS

2.1 Introduction

Details On web with openings have been developed in the previous chapter. In the present section, a succinct review over last decades, on the elastic and inelastic behaviour of BWO including the stress distribution.

For more than 100 years, different researchers (Verweij 2010) have studied the influence of creating openings on the elastic and plastic stress distribution. Given the widespread application of beams with web openings in steel construction and the great variety in structural parameters, numerous studies have been conducted on the ultimate strength of these elements both experimentally and analytically. In the 1970s, a large number of tests on steel beams with discrete rectangular and circular openings were conducted (Redwood and McCutcheon 1968; Bower 1968; Congdon and Redwood 1970; Redwood et al. 1978; Clawson and Darwin 1980). These studies showed that the stress state at the opening area is very complex, leading to a complicated behaviour of these elements.[1]

Design procedures and programs are available nowadays, which enable easy calculation for a wide range of possibilities. Composite and non-composite designs, symmetric and asymmetric designs, stiffened and unstiffened openings, regular and irregular web openings are all covered.[2]

2.2 Literature review

Additionally, to what has been said in section 2.1; the increasing the stiffness and strength of the original beam has been the main objective of the selection studied beams with web openings from designers. These beams are being current research as they have been a popular research theme over the past few decades [1]. Since the 1950s, the high strength to weight ratio of castellated beams has been a desirable item to structural engineers in their efforts to design lighter and more cost-efficient steel structures (Husain and Speirs 1971, 1973; Galambos, Husain, and Spin 1975; Kerdal and Nethercot 1984; Zaarour and Redwood 1996). [3].

Many research projects, comprising both theoretical and experimental investigations. Usually, WOB can be subdivided into two main categories that is with multiple or regularly spaced web openings beams. When the spacing between the openings is sufficiently large along with ensuring that adjacent openings do not interact, these openings may be treated as individual to ensure that adjacent openings do not interact. Furthermore, it is possible to distinguish between

taking into account the composite action the concrete floor slab or not, and whether opening reinforcement is dealt with. In the past all these categories were approached as separate design problems.

For over 100 years the influence of creating openings on the elastic stress distribution has been studied, e.g. by Chan & Redwood [1974] [2]. However, the design and specifications for such beams are either inadequate or difficult to use. This may be due to the fact that the behaviour of I-Beams with web openings is complex to understand, analysed and difficult to simplify the design procedures. Therefore, it is imperative that more elaborative investigations are required to provide sufficient information to understand the behaviour so that a simple design method could be developed. Few experimental and analytical studies related to steel beams with web openings have been reported in the past. For steel beams with circular web openings, most of the design rules are applicable using an equivalent rectangular opening of modified dimensions, as suggested by Redwood (1969). However, due to the simplistic approach, the load carrying capacity of steel beams are always underestimated significantly. Elastic stress distribution in the beams with large circular web openings have been examined by Chan and Redwood (1974) using the theory of elasticity and the curved beam analysis. In order to assess the load-carrying capacity of steel beams with several circular web openings in an explicit manner, a design method Ward (1990) based on the research works of Olander (1953) was developed at the Steel Construction Institute in 1990. The method was later incorporated into Amendment A2 of EUROCODE3 (1998): Part 1.1: Annex N, in 1998 with minor modification. However, for steel beams with individual circular web openings, the use of a different set of approximate design rules was recommended in Annex N.

2.3 Current research status

Previously, researchers Redwood and Uenoya (1979) have treated the problem of webs as a stability problem of a perforated plate with simplified edge loadings and support conditions. Based on their experimental studies Coull and Alvarez (1980), have proposed an empirical method for determining the lateral buckling capacity of beams with a number of openings, either circular or rectangular [9]. Nethercot and Kerdal (1982) and Kerdal and Nethercot (1984) investigated the performance and stability of castellated beams, in which they provided quantitative data on the lateral torsional buckling strength of castellated sections, and the similarity in the behaviour of castellated and plain-webbed beams was shown. The results of their study showed that web opening

has a slight influence on the overall lateral torsional buckling behaviour of these beams. Thevendran and Shanmugam (1991), Shanmugam and Thevendran (1992) proposed a numerical method to calculate the elastic lateral buckling load of narrow rectangular and I-beams containing web opening and subjected to single concentrated load applied at the centroid of the cross-section using the principle of minimum total potential energy. In an additional study by Mohebkhah (2004), the numerical procedure has been conducted to investigate the inelastic lateral torsional buckling behaviour of castellated beams; Corresponding information may be found in Sweden (2011), where propositions for the determination of the critical bending moment M_{cr} in cellular and castellated beams are given.

Other investigations associated to instabilities in cellular or castellated beams may also be found in Sweden (2011) and Verweij (2010), such as for flexural buckling behaviour. Main difficulties that have arisen with the use of perforated beams relate to the position of openings along the span of the beam, the shape the openings should have, how large the openings should be, and the closeness of the openings to each other. Chung *et al.* (2003), Tsavdaridis and D’Mello (2011, 2012) and Morkhade and Gupta (2015) has made significant experimental and theoretical research on steel beams with web openings in the last decade with the aim to maximize the web opening area and minimize the self-weight of the beam.[10]

2.4 Perforations in steel beams effect on their behaviour

The existence of openings in a beam means that the beam’s mechanical behaviour will not be the same as a plain one and therefore implies specific failure modes in addition to the common solid web beams [17], hence these openings could lead to a significant decrease of the beam load carrying capacity depending on the adopted openings shape, size and location. Usually an increase of the web opening height reduces the beam shear and bending capacities. Alternatively, an increase on the web opening length do not significantly affect the beam shear and bending capacities but increases the local Vierendeel bending moment acting on the “Tees”, reducing the perforated section Vierendeel collapse capacity [7]. In the following a succinct summary will be given on the behaviour of perforated sections which is characterized by three actions, that is global bending action, global shear action and local Vierendeel action [8]

2.4.1. Global bending action

One of the most noticeable actions that characterise the behaviour of sections with holes under bending stress, which is in fact, the normal compressive/tensile stress induced in a beam by a bending action, and which is typically referred to the global bending moment. It attains a maximum value at mid-span for a simply supported beam under a transverse load. Nevertheless, due to the existence of openings, the bending stress is rather different from that in the original beam. By considering the analogy with a Vierendeel girder, the global bending stress is assumed constant along the tee-components [11], which means in fact, that the global bending moment capacity is, to a large extent, determined by the flanges and hence will be resisted predominantly by tension in the bottom tee and compression in the upper tee [2]. However, this will depend mainly on the geometry of the openings by assuming a linear stress distribution due to global bending as suggested by Boyer (1964) [11].

2.4.2. Global shear action

For the basic case of a simply supported beam, the position of the maximum shear (V) is located at the supports, which becomes critical always especially in the area of reduced web-sections. In other words, the shear capacity at an opening location may be calculated by addition of the respective shear capacities of the top and bottom tee. Moreover, due to the nature of the tees in perforated beams which stand as a beam with two fixed ends, the action of vertical shear across the component leads to linearly varying local bending stress. When the bending and the shear mechanisms are considered separately, they can rarely form the critical modes of failure in cellular beams. In the other hand, for the region in openings where both shear force and bending moment are acting an additional bending is created due to the transfer of the shear force across the opening [2].

In the particular case of composite beams, some of the applied shear is transferred to the concrete slab, depending on the type of concrete slab and shear connector (Lawson, 1987).[11]

2.4.3. Local Vierendeel action

The term ‘Vierendeel’ comes from an analogy with Vierendeel girders in steel constructions, which are the type of structural system consisting of relatively long and slender chords that are connected to each other, by rigid joints. Mainly, when subject to transverse loading

causing global bending, all the individual local members of the V-girders are subjected to shear forces and local bending moments in addition to commonly tensile/compressive forces arising from the global bending. The behaviour of beams with regular openings are considered to be similar to Vierendeel girders (Gibson and Jenkins, 1957; Kolosowski, 1964), where individual sub-elements in the beam are exposed to global tension/compression, shear forces and local ‘Vierendeel’ moments. This can be illustrated by the action of shear forces at the mid-span of the tees and Vierendeel moments at both ends in a static equilibrium state, where the points of inflection of Vierendeel moments are often assumed to be at the mid-length of the tees (Kerdal and Nethercot,1984). Obviously, for a long tee member, for example in the presence of elongated openings, Vierendeel moments become more significant. This often leads to critical local failure of the tee, especially due to Vierendeel bending, or plastic collapse (Liu and Chung, 2003).[11]

2.5 Failure modes of steel structures with web openings

As previously mentioned, the existence of openings in steel beams introduces typical failure modes depending on geometry of the beams, size of web openings, between openings, web slenderness, type of loading, quality of welding, and lateral restraint conditions [13].In the literature, web-opening shapes are mainly of hexagonal shape, in some cases with an extra mid-depth plate, which then creates an octagonal shape, circular; rectangular; square or elongated (i.e. ‘extended’). Accordingly, the octagonal web openings behave better than hexagonal ones and that they are easier to manufacture than circular web openings. Published results of FE modelling studies show that web openings with rhomboidal shapes lead to lower stresses (but concentrated at the sharp corners) than circular ones, due to the narrower opening length at the top and bottom tee-sections. The majority of the previous studies were carried out based on global analyses with a combination of forces acting on the perforated beams. Therefore, many parameters were included simultaneously and so unpredicted failure modes were obtained, without being able to affirm which one of the parameters studied affect the results in every particular case [12]. They are presented as potentially being critical regarding the structural resistance evaluation and to the stability assessment. Under applied load conditions, failure is likely to occur due to one of the two following modes.

2.5.1 Strength failure modes

2.5.1.1 Flexural mechanism

Formation of a flexural mechanism mode of failure is most likely to occur in laterally supported I-shaped beams with stocky cross-sections subjected to significant bending moment and negligible shear. Under these conditions, the failure due to global or local instabilities, namely LTB, is eliminated due to the existence of adequate lateral restraint and the low width-to-thickness ratio of the cross-section elements. In such a case, the tee sections above and below the web openings yield in tension and compression until they become fully plastic [Toprac and Cooke (1959), Halleux (1967)] and thus, the beam can reach its maximum in-plane moment carrying capacity. Ward (1990) recommended that the maximum moment capacity of the beam should not exceed the plastic moment capacity of the reduced section taken through the vertical centreline of the hole.[15]

2.5.1.2 Vierendeel mechanism

Local failure modes occur as a Vierendeel mechanism (or as shear force mechanism), when the total resistance of the tee sections around an opening against the local normal forces and secondary bending moments is reached so the beam will fail by a Vierendeel mechanism with four plastic hinges surrounding this opening, as shown in Figure 2.1. In other words, the Vierendeel mechanism associated with high shear forces acting on beams, hence it is clear that this type of mechanism is more likely to develop in beams with some combination of a short span, the tee sections above and below the web opening must carry the shear and moment applied to the beam. Additionally, the tee sections also carry the secondary moments on the beam resulting from the action of the shear force over the horizontal length of the opening. As a result, secondary moments are more pronounced in beams with bigger opening size [16] and [15]; means that with increasing opening length the Vierendeel moment will further increase, reducing the ultimate load capacity.

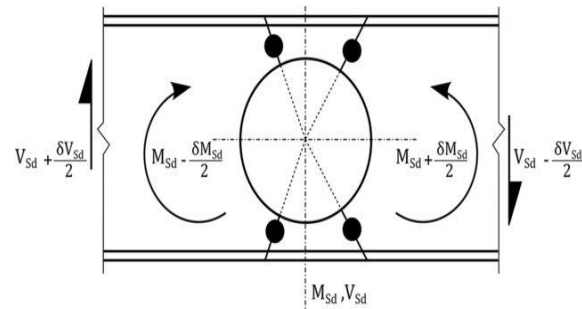


Figure 2.1: Location of the plastic hinges

2.6.1.3 Rupture of welded web joints:

In this mode of failure, the mid depth weld joint of the solid web post between two consecutive openings may rupture when horizontal shear stresses exceed the yield strength of the welded joint, Hosain and Speirs (1973) conducted experimental investigation on six beams with short welded joints. Results indicated that beams with shorter width of web posts are more vulnerable to this failure mode. Thus, it should be noted that reducing the spacing between the openings (i.e., reducing the width of the web-posts) may cause the web post to become more susceptible to weld rupture in the web joints.[15]

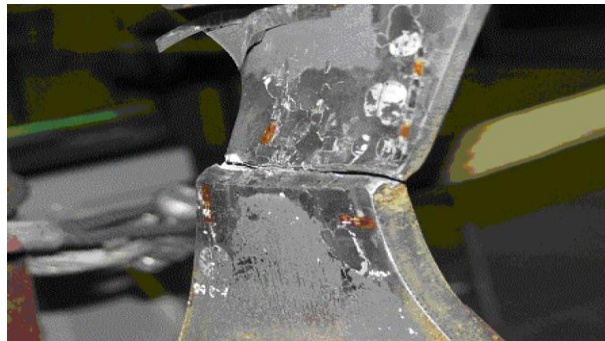


Figure 2.2: Rupture of welded web joints

2.5.2 Instability related modes

2.5.2.1: lateral-torsional buckling

The lateral-torsional buckling (LTB) presented as a global buckling mode, which is a collapse mechanism that occurs when the in-plane bending capacity of a member exceeds its resistance to out-of-plane lateral buckling and twisting. [14]. It is characterized by combined rigid

body lateral translation and rotation of the cross section of the beam affecting longer span beam with inadequate lateral support to the compression flange.

Nethercot and Kerdal (1982) who concluded that failure by lateral torsional instability of castellated beams is similar to that of solid web beams previously investigated response of castellated beams to LTB experimentally. However, a more recent study conducted by Mohebkhah (2004) has shown that a significant influence of beam's slenderness on the moment-gradient factor of castellated beam in the resistance against LTB, such influence was more apparent in beams that buckle inelastically, see figure 2.3.

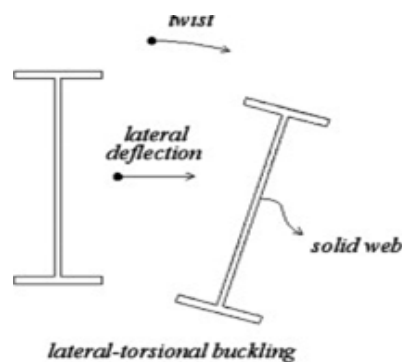


Figure 2.3: Buckling of a typical cross section with LTB



Figure 2.4: Lateral-torsional buckling due to (vertical) shear.

2.5.2.2: Lateral-Distortional Buckling

Unlike lateral torsional buckling mode of failure, lateral distortional buckling mode (LDB) involves localized distortion of the cross section leading to unequal angle of twist for the two flanges. Additionally, the final buckling mode combines lateral displacement and twist, together with localized web distortion. This interaction usually occurs in intermediate length I-beams with slender webs, figure 2.5.

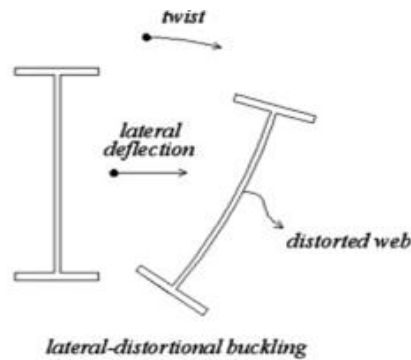


Figure 2.5: Buckling of a typical steel cross section with LDB

In beams with perforated web existence of web openings results in a reduction in the stiffness of the web plate, which increases the level of web deformations. As a result, local web distortions are more likely to accompany the lateral torsional buckling deformation leading to the occurrence of lateral distortional buckling mode. Recently, Zirakian and Howkati (2006) and Zirakian (2008) have conducted experimental investigations of the distortional buckling of castellated beam. Test results indicated that all beams underwent lateral torsional buckling accompanied by localized web distortion. Experimental outcomes were then used to develop several extrapolation techniques that have been reported to provide accurate predictions of critical buckling load of castellated beams undergoing lateral distortional buckling.

2.5.2.3 Shear buckling of the web post

In case of failure of the web post due to shear buckling mode, the horizontal shear force in the web post is associated with double curvature bending over the height of the post. One inclined edge of the opening will be stressed in tension, and the opposite edge in compression and buckling will cause a twisting effect of the web post along its height, as shown in (figure 2.5). Several cases of web post buckling have been reported in the literature [Herbourne (1966), Haileux (1967), Bazile and Texier (1968)]. Furthermore, many analytical studies on web post buckling have also been reported to predict the web post buckling load due to shearing force. Based on finite difference approximation for an ideally elastic-plastic-hardening material, Aglan and Redwood (1974) produced some graphical design approximations for a wide range of beam and hole geometries. Some correlations between experimental and non-linear finite element analysis (FEA) estimations were found in the works of Redwood and Zaarour (1996). Redwood and Demirdjian (1998)

conducted elastic finite element analysis to identify buckling loads. They found a good agreement between their numerical predictions and the experimental counterpart available in literature. The study by Redwood and Demirdjian concluded that the results of Aglan and Redwood (1974) should not be used for very thin web.

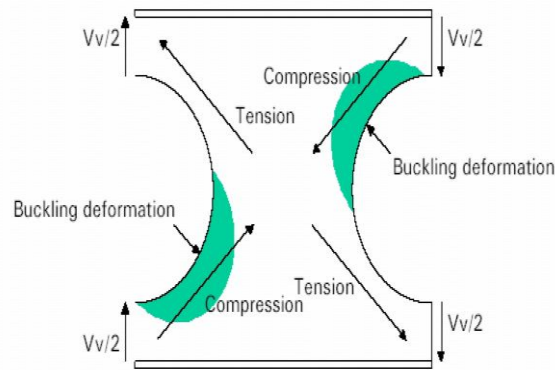


Figure 2.6: Compression and tension locations at the inclined edge of an opening [2]

2.5.2.4: Compression buckling of the web Post:

Compression buckling of web post results from direct application of a concentrated load/reaction over the web post. This mode was reported in the experiments conducted by Toprac and Cooke (1959), Hosain, and Speirs (1973). This mode is similar to crippling failure of web plates in solid beams [Kerdal and Nethercot (1984)]. Unlike webs of solid beam, this buckling mode is not considerably sensitive to the size of the loaded area [Okubo and Nethercot (1985)]. In general, this failure mode could be prevented if adequate web stiffeners are provided. A strut approach was proposed by Dougherty (1993) to apply standard column equations to determine the strength of the web post under the effect of concentrated load.

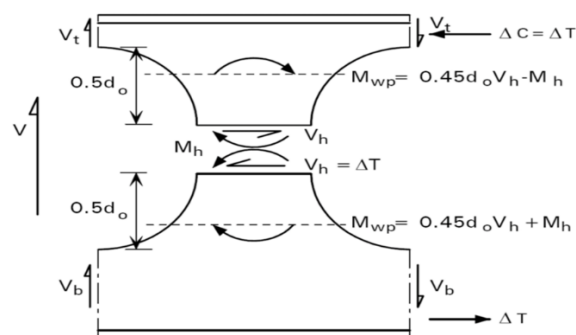


Figure 2.7: Local forces and position of the critical sections in the intermediate web-post.

2.6 Summary of failure modes of WOB's to EC3

It is worth to point out that failure modes are affected by the geometry and slenderness of the web, the shape and the dimensions of the openings, loading methods and the lateral supports provided.

- The different modes of failure that can occur at or near large, isolated openings are as follows:
 - Overall bending of the perforated cross section;
 - Pure shearing of the perforated cross section;
 - Vierendeel bending around the web opening;
 - Buckling of the compressed Tee.
- For beams with multiple web openings, additional failure modes must be considered:
 - Buckling of the web post between two adjacent openings;
 - Bending of the web post;
 - Shear failure of the web post or the web post weld;
 - Compressive buckling of the web;
 - Overall instability of the beam caused by LTB.

2.7 Guidelines for web openings and stiffeners

Available design guidelines in British Standards and the Eurocodes are then reviewed along with other available design-oriented models proposed by several researchers; should be considered as follow:

- The hole should be centrally placed in the web and eccentricity of the opening is avoided as far as possible.
- Unstiffened openings are not always appropriate, unless they are located in low shear and low bending moment regions.

- Web opening should be away from the support by at least twice the beam depth, D or 10% of the span (L), whichever is greater
- The best location for the opening is within the middle third of the span.
- Clear Spacing between the openings should not be less than beam depth, D .
- The best location for opening is where the shear force is the lowest.
- The diameter of circular openings is generally restricted to $0.5D$.
- Depth of rectangular openings should not be greater than $0.5D$ and the length not greater than $1.5D$ for un-stiffened openings. The clear spacing between such openings should be at least equal the longer dimension of the opening.
- The depth of the rectangular openings should not be greater than $0.6D$ and the length not greater than $2D$ for stiffened openings. The above rule regarding spacing applies.
- Corners of rectangular openings should be rounded
- Point loads should not be applied at less than D from side of the adjacent opening.
- If stiffeners are provided at the openings, the length of the welds should be sufficient to develop the full strength of the stiffener. Various types of stiffeners are shown in
- If the above rules are followed, the additional deflection due to each opening may be taken as 3% of the mid-span deflection of the beam without the opening.[6]

2.7 Overview of Experimental Studies in the Literature

2.7.1 General

Beside the theoretical investigations undertaken including analytical and numerical ones on the behaviour of castellated beams, lot of experimental effort has been made to understand their behaviour as well as their mode of failures of this kind of structures. Indeed, this chapter is devoted to present succinctly the chronology of the experimental investigations, available in literature, dealing with the mode of failure observed and focusing on the major parameters involved which will, certainly, helps to a better understanding of this type of structures when comparing the numerical results also and to follow the evolution of the actual parameters investigated during the experimental works.

2.7.2 Overview

Sherbourne (1966) has performed a series of tests on alveolar beams, with the objective of studying the influence of loading conditions on the behaviour of this type of beam. Seven specimens, stressed to only simulate on the beams the conditions of pure bending, simple bending and pure shear, were tested. The results of experimental program have shown that for the beam subjected to a concentrated load failed by excessive plasticization at mid-height of the first web post between the first and second openings, while the second one, designed to study the effect of pure bending, was tested under four-point bending loading, in which has failed because of excessive plasticization in the areas in the vicinity of the concentrated loads with highly stressed by bending and shear stress.[18]

Bazile and Texier (1968) tested two series of beams based on hot-rolled beams, 4 HEA 360 with spans of 8,064 m and 3 IPE 270 with spans of 6,624 m, 8,064 m and 10,08 m. The openings of two beams of the first series were fitted with intermediate plates. These were supported at one end on a cylindrical roller and at the other end on a half-cylinder. The loads are applied by means of two identical cylinders powered by the same hydraulic system. For all beams, strain gauge and deflection measurements were taken. The deflections were measured at mid-span of the beam. For all the beams tested, the experimental load-deflection curves showed three load zones P1, P2 and P3.

Husain and Speirs (1971) studied the resistance of web post welds by conducting 6 tests on alveolar beams, 4 of which were subjected to the three-point bending. The other two were subjected to four-point bending. The tested beams included vertical stiffeners at concentrated loads and supports. At the end of the beam an arrangement of lateral support was placed to avoid failure by local buckling or by lateral torsional buckling of the specimen tested. All the beams have collapsed by the breaking of the weld on the web post. The tests have also showed that, in all cases, the longitudinal shear obtained experimentally was higher than the computational approach prediction. This demonstrates that the approach values were conservative and the reserves of the weld joints before failure. [20]

S. Shrivastava and R. Redwood (1977) conducted studies on web reinforcement near rectangular openings. Using horizontal stiffeners, the dimensions of which are often determined by a fracture design. In order to valid the method, it is necessary to previously determine when web

buckling occurs prior to failure near the opening. An experimental study was devoted to determine the premature buckling of beam sections normally considered in the plastic design of structures. From this study, some recommendations were presented for the design taking into account the effect of placing stiffeners, which prevent beams from premature buckling [21].

Okubo and Nethercot (1985) carried out tests on 16 alveolar beams having 1 to 4 openings. To evaluate the buckling resistance of unstiffened web posts under compression at concentrated loads and support reactions, the ends of the beams were restrained laterally by supports arranged at the level of the upper flanges, except two beams, for which a concentrated load was applied at the mid-span of the beams. One of the beams was loaded eccentrically to the middle, the single-opening beam was subjected to two loads applied to the upper and lower flanges of the web post. All the tested beams failed by buckling of the web posts under concentrated loads.[22]

R. Lupien and R. Redwood (1996) tested six beams containing mid-height rectangular openings equipped with welded horizontal stiffeners to one side of the web reinforced. The objective was to evaluate the effect of unilateral reinforcement on the ultimate strength. Particular attention was paid to beams with slender webs and the effect of the moment to shear ratio. The effectiveness of unilateral reinforcement was evaluated on the basis of the expected capacity of a symmetrically reinforced beam with the same reinforcement zone. It was found that, due to strain hardening, the ultimate strength obtained was in some cases equal to this predicted capacity force. And based on these results, design suggestions are made. [23]

Zirakian and Showkati (2006) tested six simply supported beams with web opening with a special intention to study the behaviour of beams with hexagonal openings with respect to LTB. The test specimens were manufactured from the two profiles IPE120 and IPE140 in accordance with the Current German Code Estahl Standard [19]. A concentrated load is applied in the middle of the beam by a hydraulic cylinder. Using a non-deformable steel cube arranged on the upper part of the beam. Four lateral restraints were used along the beam to prevent lateral movements during the tests. [24]

Tsavidaridis and D'Mello (2011) studied analytically and experimentally the performance, failure modes and load carrying capacity of different types of cellular beams. In particular, they considered narrowly spaced web openings. The beams were stiffened at the supports as well as in

the middle of the beam to prevent from lateral torsional buckling LTB effect. The beams restrained with single supports with three-point bending. High shear was observed at the web post with strong distortion of the openings associated to additional deformation at the loading point location. The researchers concluded that no absolute studies were carried out on the stability of the stiffeners and balance problems. [25]

Wakchaure and al (2012) carried out an experimental study on beam with hexagonal openings with simple supports under two loading points. Failure modes were studied for different opening heights. Following the experiment, the researchers concluded that the perforated beam behaves satisfactorily up to a maximum height of 0.6 times the height of the beam (0.6D). The researchers recommended that the presence of a stiffener is necessary to avoid Vierendeel effects caused by the existence of openings. [26]

Durif and al (2012) carried out tests on three cellular beams with sinusoidal openings. In order to obtain three different modes of failure, three configurations of openings corresponding to standard, small and large openings were used. The elastic limits of each beam were deliberately chosen to obtain one failure mode rather than another. The flatness defects of each intermediate web post were measured and being put in the numerical model. The following failure modes were observed during the tests: (i) For beams with large openings, collapse occurs by Vierendeel bending as for rectangular openings, (ii) For the smaller openings, the failure mode combines both local buckling and plasticization of certain areas around the opening. [27]

Erdal and Saka (2013) tested three series of cellular beams with circular openings using 3-point bending. Each of the rolled sections NPI_CB_240, NPI_CB_260 and NPI_CB_280 was used to fabricate the four cellular beams of each series. All specimens are of 3 m span. The cellular beams tested were optimally dimensioned for specific loads in accordance with the British Standard BS 5950. The aim of the study is to determine the carrying capacity of the beams and to examine the modes of failure in order to validate the numerical model proposed by the authors. The beams of the first series each have eight openings. The two beams of the first series perished by lateral torsional buckling due to the absence of lateral supports. The two other beams of the first series, restrained laterally, perished by buckling of the web post due certainly to the small spacing between the openings. The beams of the second series each have seven openings. [28]

SONCK and al (2014) carried out experimental studies to study the influence of residual stresses on the behaviour of open web beams with circular and hexagonal openings. Four alveolar beams and two cellular beams made from IPE 160 steel base profile S275 have been tested. Three geometrical configurations were used; each of them describes the geometry of two identical beams. Before the flame cutting operation of the 1m sections of the six basic profiles used were cut to determine the distribution of residual initial stresses. The manufacturing process of the cellular beam used in this study differs from the conventional method, which consists of make a double cut in the web by flame cutting before offset and welding of the two halves obtained. This different process consists, in the first place, of manufacturing the alveolar beam by the conventional method, and then make the hexagonal and circular openings. Residual stresses were measured at the base plates of six basic profiles (called PS), two open-web beams after flame cutting (AC) and seven open-web beams (AW).[29][30]

More recently, **A. Jamadar and D. Kumbhar** (2015) carried out an experimental programme along with a numerical study using Abaqus (CAE 6.13) in order to valid by mean of comparison the experimental results on openwork beams with circular and rhomboid openings following the guidelines given in Eurocode 3. The results of the software with experimental results. The result indicates that the rhomboid alveolar beam with the opening suffers less local instability, which can attribute to the mobilization of a larger shear transfer surface compared to a circular opening. In addition, the load carrying capacity is greater for the rhomboid shape in comparison to the circular opening. Based on the results of the analysis, it was found that the increased height of the beam leads to a significant reduction in lateral displacement. Moreover, the bending stresses are close to those of a flat web beam. The stress values obtained from the analysis show that stress concentration occurs near the corner and web portion, which can cause local failures. [31]

Morkhade and al (2015) carried out an experimental of test programme tests consisting of seven tested beams with five open web beams having circular openings and two others open web beams with rectangular openings. The aim of these tests was to obtain the load-deflection curves at mid-span of the beams until the collapse. The open-webbed beams tested were subjected to a monotonically increasing concentrated load applied at mid-span. The results of the tests were compared with the results of numerical simulations carried out using the ANSYS software. [32]

Zaher and al (2018) performed an experimental programme concerns curved cellular beams. In fact, four curved cellular beams. One of the tested beams with solid web, the 3 others are open web beams with circular openings. The ratio of the diameter of the opening to the overall height of the web is 0.67. Three of the tested beams, including the one with a solid web have a span of 2.59 m, the fourth tested beam with span of 2.19 m. The purpose of these tests is to study the effects of web openings, opening and angle at the centre of the arch on the behaviour up to the failure of curved cellular beams. The tested beams are hinged at both ends and subjected to a concentrated transverse load at mid-span. Some concluding remarks were drawn from these tests, among which the curved cellular beams have a lower strength than the curved beam with a solid web. Also, the increase in the angle at the centre of the average fibre of the curved cellular beam results in an increase in its ultimate strength. On the other hand, the reduction in the span of the curved cellular beam is inversely proportional to the ultimate strength of the beam. [33]

Feng and al (2018) The objective of these tests is to study the bending behaviour of beams with web openings made of high-strength steel. As a function of the ratio of web overall height (h)/thickness of web (t_w) and the number of web openings. They performed tests on 12 cellular beams made from high-strength steel Wide Flange H- shape beams. The steels used have a yield strength of 550 and 690 MPa. The beams consist of two basic sections: H125×225×6×6 and H210×210×6×6, according to the American standard AISC 360-16 [37]. The tested cellular beams made from the narrow flange profile H125 have a span of 2.65 m and those made from the wide flange profile H210 have a span of 2.3 m. The circular openings have a diameter equal to 3/10 of the overall height of the web. The tested beams were loaded through two bending modes (3-point and 4-point bending). The obtained test results consist of the failure modes, load-deflection curves at mid-span, ultimate loads and distribution of relative deformations in the perforated mid-section. The results showed that the ultimate loads and the corresponding curvatures of cellular beams loaded at a variable moment (3-point bending), are higher than those of cellular beams loaded essentially at a constant moment (4-point bending). Despite the mode of loading, the failure of all the beams occurred by local buckling in association of a bending over of the upper flange, thus preventing plasticisation of the perforated section. [34][35]

Bibliography

- [1] **Akrami and Saeed Erfani**: Review and Assessment of Design Methodologies for Perforated Steel Beams. Feb2011.
- [2] **J.G. Verweij**; Master thesis ‘‘CELLULAR BEAM-COLUMNS IN PORTAL FRAME STRUCTURES’’; Delft University of Technology Civil Engineering Section Steel and Timber Structures; November 2010.
- [3] **Samadhan. G. Morkhade & L. M. Gupta Australian**; Ultimate load behaviour of steel beams with web openings Journal of Structural Engineering.
- [4] **Alpsten, G.A. and Tall, L.** Residual Stresses in Heavy Welded Shapes. Welding Journal (AWS), 49, 93-105.
- [5] **Sherif Elsayaf**: Behaviour Of Structural Subassemblies Of Steel Beams With Openings / article April 2017/
- [6] BS5950
- [7] **Pedro C g da s Vellasco**; Finite Element Modelling of Steel Beams with Web Openings/Conference Paper *in* Engineering January 2014.
- [8] **Konstantinos Daniel Tsavdaridis**; Finite element investigation of perforated steel beams with different web opening configurations; Conference Paper January 2009.
- [9] **Samadhan G. Morkhade and Laxmikant M. Gupta**; Experimental investigation for failure analysis of steel beams with web openings *in* Steel and Composite Structures · April 2017/DOI: 10.12989/scs.2017.23.6.647
- [10] **Ko, C.H. & Chung, K.F.** *A review of recent developments on design of perforated beams.* Advanced in Steel Structures, Vol. 1. 2002.
- [11] **Ahmad Razin Zainal Abidin**; modelling of local elastic buckling for steel beams with web openings; MSc,thesis submitted in fulfilment ofthe requirements for the degree ofDoctor of Philosophy ofImperial College LondonDepartment of Civil and Environmental Engineering Imperial College London SW7 2AZ.jan 2013..
- [12] **Tsavdaridis, KD and D'Mello, C**; Vierendeel Bending Study of Perforated SteelBeams with Various Novel Web Opening Shapes, through Non-linear Finite ElementAnalyses. Journal of Structural Engineering, 138 (10). 1214 - 1230. ISSN 0733-9445.2012
- [13] **LAURSEN. T. A.**, " Computational Contact and Impact Mechanics: Fundamentals of Modeling Interfacial Phenomena in Nonlinear Finite Element Analysis. " , Springer- Verlag Berlim Heidelberg ,2002.

- [14] **Matthew J. Vensko**; Lateral-Torsional Buckling Of Structures With Monosymmetric Cross-Sections. Msc or PhD Thesis Pennsylvania State University, 2003
- [15] **Mohammad Iqbal Mohammad Hesham Martini**; Elasto-Plastic Lateral Torsional Buckling of Steel Beams with Perforated Web. Msc or PhD thesis; United Arab Emirates University Scholarworks.
- [16] **Delphine Sonck**; Global Buckling of Castellated and Cellular Steel Beams and Columns // Faculties Ingenious wetenschappen en Architecture Academiejaar 2013 – 2014.
- [17] **Sébastien Durif , Abdelhamid Bouchaïr ; Claude Bacconnet**; Elastic Rotational Restraint Of Web-Post In Cellular Beams With Sinusoidal Openings. Clermont Université, Université Blaise Pascal, Institut Pascal, BP 10448, F-63000 Clermont-Ferrand, France 2 CNRS, UMR 6602, Institut Pascal, F-63171 Aubière, France (Received August 02, 2012, Revised June 13, 2014, Accepted June 29, 2014).
- [18] **A.N. Sherbourne**. The plastic behavior of castellated beams. Proceeding 2nd Commonwealth Welding Conference Institutional of Welding, No. C2, pages 1-5, London, 1966.
- [19] **A. Bazile and J. Texier**. Essais de poutres ajourées. Revue construction métallique CTICM No.3, pages 12-25, 1968.
- [20] **M.U. Husain and W.G. Speirs**. Failure of castellated beams due to rupture of welded joints. Acier-Stahl-Steel, No. 1, 1971.
- [21] **R. Shrivastava and S. Redwood**, “Web instability near reinforced rectangular holes web instability near reinforced rectangular holes,” IABSE proceedings, vol. 1, no. 6, pp. 1-17, 1977.
- [22] **T. Okubo and D.A. Nethercot**. Web post strength in castellated steel beams. Proceedings Institution of Civil Engineers, Part 2, Vol. 79, , pages 533-557, 1985.
- [23] **R. Lupien and R. Redwood**, “Steel beams with web openings reinforced on one side,” Canadian Journal of Civil Engineering, vol. 5 no. 4, pp. 451-461, December 1978.
- [24] **Zirakian. T., Showkati. H.** " Distortional buckling of castellated beams". Journal of Constructional Steel Research. Vol n° 62, pp: 863–871, 2006.
- [25] **K. Tsavdaridis and C. D’Mello**, “Web buckling study of the behaviour and strength of perforated steel beams with different novel web opening shapes,” Journal of constructional steel research, vol. 67, no. 10, pp. 1605–1620, 2011.
- [26] **M. Wakchaure, A. Sagade, and V. Auti**, “Parametric study of castellated beam with varying depth of web opening,” International Journal of Scientific and Research Publications, vol. 2, no. 8, pp. 1–6, 2012.
- [27] **Durif, S., Bouchaïr, A., Vassart, O.**, "Experimental tests and numerical modeling of cellular beams with sinusoidal openings", Journal of Constructional Steel Research, vol n°82 (1), pp:72–87, 2013.

- [28] **Erdal. F, Saka. M.P.**, " Ultimate load carrying capacity of optimally designed steel cellular beams", Journal of Constructional Steel Research, Vol n° 80, pp:355-368, 2013.
- [29] **British Standards, BS 5950**. "Structural use of steelworks in building. Part 1. Code of Practice for design in simple and continuous construction, hot rolled sections". London, U.K: British Standard Institution; 2000.
- [30] **Sonck. D, Belis. J.**, " Experimental investigation of residual stresses in steel cellular and castellated members", Journal of Construction and Building Materials, vol n° 54, pp: 512 519,2014.
- [31] **A. Jamadar and D. Kumbhar**, "Parametric study of castellated beam with circular and diamond shaped openings," International Research Journal of Engineering and Technology, vol. 02, pp. 715–722, 2015
- [32] **Morkhade. S. G., Gupta L. M.**, "An experimental and parametric study on steel beams with web openings", Int J Adv Struct Eng, vol n°7, pp:249–260,2015.
- [33] **Zaher.O. F, Yossef. N.M, El-Boghdadi. M.H, Dabaon. M.A.**, "Structural behavior of arched steel beams with cellular openings", Journal of Constructional Steel Research, vol n°148, pp :756–767,2018.
- [34] **Feng. R, Zhan. H, Meng. S, Zhud. J.**, " Experiments on H-shaped high-strength steel beams with perforated web", Engineering Structures, vol n°177, pp: 374–394, 2018
- [35] **Soltani. M.R.** " modélisation numérique du comportement des Poutres métalliques avec des ouvertures dans l'âme. Thèse de doctorat, université de Mantouri de Constantine, Algérie, 2012.

C **CHAPTER III:**

DESIGNING RECOMMENDATIONS FOR WOB's

3.1 Introduction

Designing perforated steel beams (BWO) is always a practical challenge in steel construction. There are a number of design methods available in the literature for designing these structural members. Some theoretical methods to predict failure loads and failure modes as the British Steel Construction Institute (SCI) design method from the SCI publication by Ward, A plastic analysis method, non-linear finite element analysis (FEA), The plastic analysis methods check for Vierendeel bending, primary bending, horizontal shear of the web post and vertical shear failure. However, the range of and accuracy of these methods in estimating the resistance of perforated beams is not known precisely [1] which means that the available design guides and specifications for such structural elements are either inadequate or difficult to use. This may be due to the fact reported in previous studies, like what it has been already discussed in chapter II, the complexity of the stress distribution in the vicinity of the opening area with a high stress concentration leading consequently to a very complicated behaviour of an I-beam with web openings. Therefore, these design approaches formulated in analytical terms still prove their value. Even when performing an advanced analysis, the use of simplified methods of computation is essential to check out the outcomes. Because of the interaction between bending and shear forces, these beams are calculated according to several parameters: the applied load combinations, the opening dimensions, the distance between openings, and number of openings.

3.2 Influence of opening on the carrying capacity of beams

According to Chung et al, for steel beams and Chung and Lawson [13] for composite beams, stated that for services that requires web openings up to 75% of the beam height are not uncommon. These openings could lead to a significant decrease of the beam load carrying capacity depending mainly on the adopted openings shapes, sizes and locations. Frequently, circular and rectangular openings are used and likely to be equipped with stiffeners welded neighbouring the web openings in order to improve the beam load carrying.

3.3 Classification of the cross-section of the web-openings beams

The role of cross-section classification is to identify the extent to which the resistance and rotation capacity of cross-sections is limited by its local buckling resistance [3]. Steel beams with web openings, one of its great advantages is that with almost the same quantity of steel as the original beam, due the increased height of the cross section a much higher inertia moment of the section and consequently the larger moment strength capacity can be achieved. Detailed analysis

of the beam with the web openings leads to the conclusion that the distribution of the bending moments being induced in the critical beam-cross-section. As a result of such situation the beam behaviour is based on the plastic reserve being the consequence of the redistribution of the bending moment is not available.

As what has been treated in Eurocodes 3, for each wall subjected to compression the class is determined depending on the its slenderness that is width-to-thickness ratio. In the same way, cellular beams made from hot-rolled sections, the flange may usually be treated as class 2 or higher. At an opening location additional classification rules are applicable, which were taken from Annex N [4]. The outstand of the web of the tee is classified depending on the ratio of the effective length of the opening for stability of the web, $l_{o, \text{eff}}$ to the outstand depth $d_t = (h_t - t_f)$. Note that webs with an opening that satisfies the lower limit on $l_{o, \text{eff}}$ (so for small openings) are classified independently of d_t . Because of the magnitudes of the required plastic hinge rotations for the development of the Vierendeel mechanism are small, it is sufficient for the unstiffened or stiffened tee-sections above and below web openings to be classified as class 1,2 or 3 cross-sections classification established by EC3. The portions of the web forming the stems of unstiffened tee-sections above and below unstiffened web openings may be classified allowing for the restraint of the adjacent portions of the web, as follows: [5]

- For class 2: Either $l_0 \leq 32 \varepsilon t_w$ or $d_w \leq \frac{10 \varepsilon t_w}{\sqrt{1 - \left(\frac{32 \varepsilon t_w}{l_0}\right)^2}}$
- For class 3: Either $l_0 \leq 36 \varepsilon t_w$ or $d_w \leq \frac{14 \varepsilon t_w}{\sqrt{1 - \left(\frac{36 \varepsilon t_w}{l_0}\right)^2}}$
- All class 4 webs may be treated as class 3 if $l_0 > 32 \varepsilon t_w$

Where:

- d_w is the outstand d_{w1} or d_{w2} defined in figure (3-1)
- l_0 is as defined in figure (3-1)
- $\varepsilon = \sqrt{\frac{235}{fy}}$ And fy is the material yield stress in MPa.

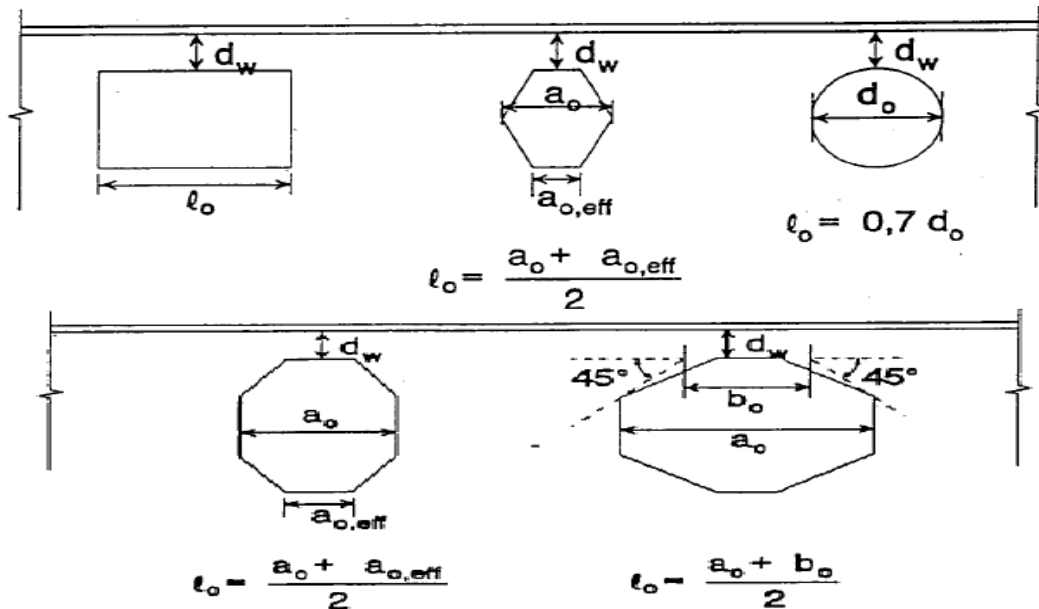


Figure 3.1: Portion of the web opening forming the stem of an unstiffened tee.

The cross-sections subjected to a bending belonging to class 2 (compact) which are able to develop a full plastic behaviour with a limited rotation capacity. Class 3 (semi-compact) are those in which only the stress in the extreme fibres can reach its yielding stress because local buckling prevents development of the full plastic stress distribution. Class 4 (slender) are those in which local buckling occurs in the elastic range and bending resistance is determined based on an effective cross-section [6]

3.4 Design of beams with web openings

Beams must be sufficiently strong to carry the bending moments and shear forces generated by the applied loads. The performance of any beam depends upon the cross-section geometry, the dimensions layouts, and the openings shape. Several authors i.e. Chung and Ko [12], Chung and Lawson [13], Lawson [14], Darwin [15], Redwood and Cho [16], Oehlers and Bradford [17] have indicated that two approaches can be used for Tee Section and Perforated Section for the design of steel and composite (with associated slab) beams having web openings. An interesting procedure, based on plastic section analysis methods, is reported by Chung *et al.* [18] to design these girders. Other numerical and experimental investigations on the design recommendations for steel and composite beams with web openings [19] are available in the literature but led to specific rules or empirical formulae for general design [20]. For the time being, there is no consensus on a accepted design method due to the complexity of the behaviour of beams with web openings and their

associated modes of failure. In the design of beams with web openings, these criteria should be considered:

3.4.1 Design rules for openings

3.4.1.1 General

The design rules given in this section are relate to the situations of beams with regular shape openings such as rectangular, circular or elongated circular, in addition to a uniform web thickness. The basic geometric parameters are illustrated in figures 3.2 to 3. The eccentricity of the centreline of the opening is defined relatively to the centreline of the web. The design principles are based on the development of the elastic or plastic resistance of the element, depending on the section classification.

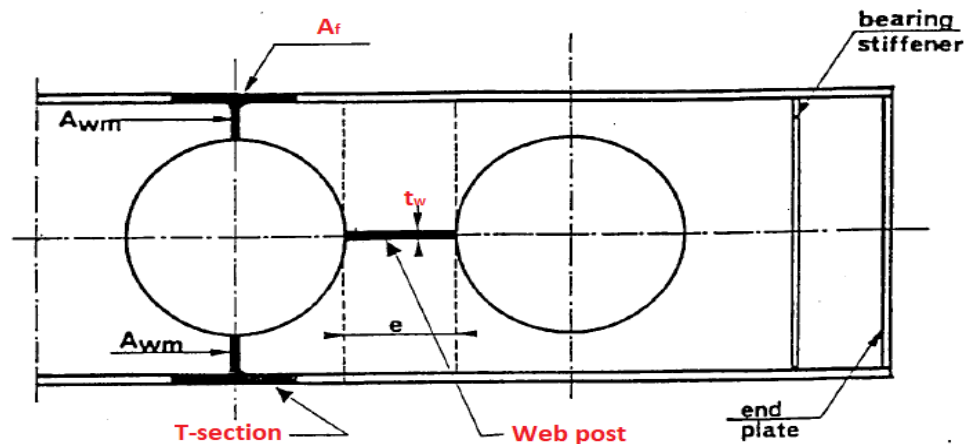


Figure 3.2: Position of tee section and web post.

3.4.1.2 Beams with isolated openings

$$d_1 + d_2 \geq 0,25d$$

$$d_1 \text{ or } d_2 \geq 0,16d$$

$$a_r \geq 0.5d$$

$$a_0 \leq d_0 r_0 \geq 2t_w \quad \text{but } r_0 \geq 15 \text{ mm}$$

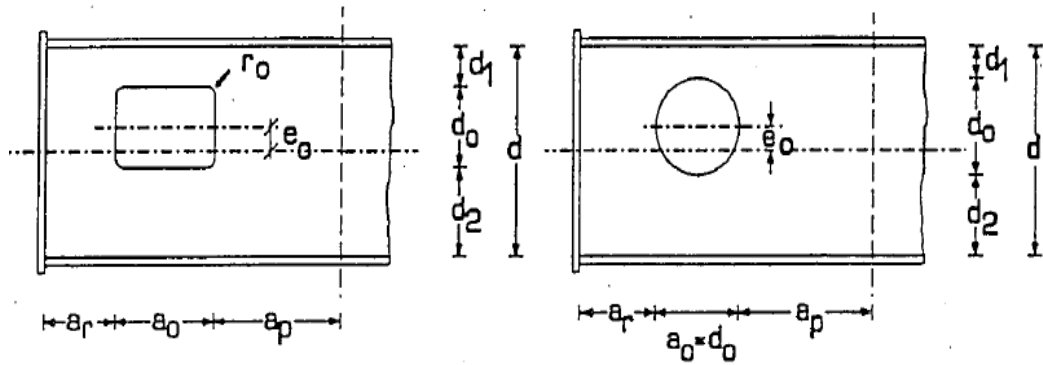


Figure 3.3: Position and dimension of isolated openings.

3.4.1.3 Beams with multiple openings without stiffeners

The following rules can only be applied if the dimensions of the openings are limited as follows:

$$r_0 \geq 2tw \text{ but } r_0 \geq 15 \text{ mm}$$

- **For rectangular openings**

$$d_0 \leq 0.7 h$$

$$d_t \text{ And } d_b \geq 0.1 h$$

$$d_t \geq 0.1 l_0 \text{ if the opening is unstiffened.}$$

$$d_b / d_t \leq 2 \text{ and } d_b / d_t \geq 1$$

$$s_0 \geq 0.5 l_0$$

$$s_e \geq h \text{ and } s_e \geq l_0$$

$$l_0 \leq 2 d_0$$

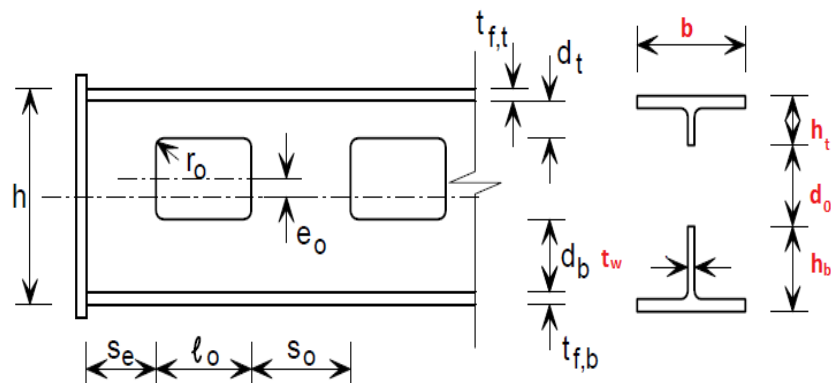


Figure 3.4: Position and dimension of multiple rectangular openings

- **For circular openings**

$$d_o \leq 0.8 h$$

$$d_t \text{ and } d_b \geq t_f + 30 \text{ mm}$$

$$d_b / d_t \leq 3 \text{ and } d_b / d_t \geq 0.5$$

$$s_o \geq 0.3 d_o$$

$$s_e \geq 0.5h$$

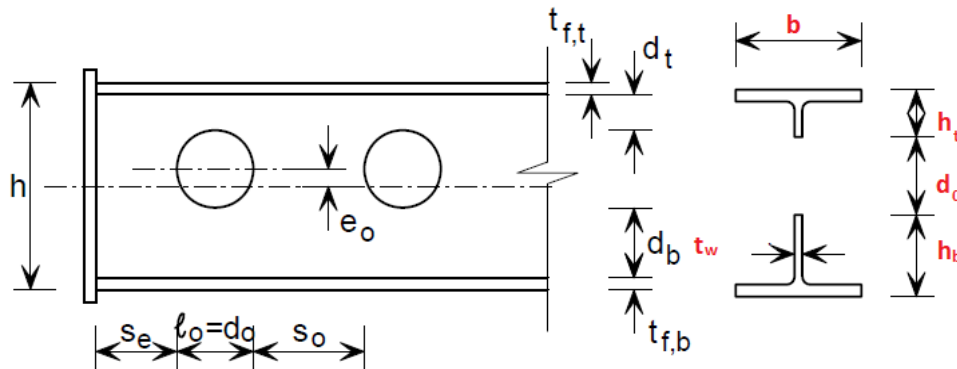


Figure 3.5: Position and dimension of multiple circular openings.

3.4.1.4 Beams with multiple openings with stiffeners

For beams with stiffeners, the rules given for beams without stiffeners apply.

- Reinforcement and stiffeners of web openings:

Due to web opening, stiffness and strength of steel beam decrease significantly. The common reinforcing method is setting reinforcement and stiffeners around the opening section. Therefore, the use of stiffeners is to avoid buckling. While reinforcement where used to increase the resistance of the beam web, and may be single sided or double sided.

3.4.2 Design of sections strength

3.4.2.1 Beams with isolated openings

Openings can be considered as isolated when their edge-to-edge spacing is greater than the diameter d_o of the circular openings, or the width l_o of the rectangular openings or oblong for which the interaction effects in the web post can be ignored. In addition, Annex N (clause N.2.1.5) proposes formulae for the calculation of shear forces and moments of resistance, under certain conditions, for beams with reinforced web openings

- **Resistance to pure bending**

Under a simple bending in an opening, it must be checked that the load moment $M_{o,sd}$ in the centre of the opening remains lower than the moment resistance capacity $M_{o,rd}$ of the perforated section: [8]

$$M_{o,sd} \leq M_{o,rd} \quad (3.1)$$

The resistance to pure bending in the presence of an opening, and without shear force, is written under the form:

$$M_{o,rd} = \frac{A_T \times f_y}{\gamma_{M_0} \times d_c} \quad (3.2)$$

Where:

- $A_T = \min\{A_{Upper T}, A_{lower T}\}$

* $A_{Upper T}, A_{lower T}$: are the areas of the upper and lower Tees respectively;

- **Shear resistance:**

For I- or H-beams, the vertical shear strength in the middle of an opening is essentially provided by the beam web. Redwood [8] proposes to calculate the plastic shear strength of the net cross section at an opening through the formula:

$$V_{opl,Rd} = \frac{(d_w - h_0) \times t_w}{\sqrt{3}} f_{yw} \quad (3.3)$$

Where:

- d_w : is the overall height of the web.
- h_0 : is the height of the opening, in the case of a circular opening h_0 is replaced by its diameter d_0 ;
- t_w : is the thickness of the web;
- f_{yw} : is the elastic limit of the web.

To take into account the role played by the flanges in vertical shear strength, K.F. Chung, T.C.H. Liu and A.C.H. Ko proposed the following formula:

$$V_{opl,Rd} = \frac{(A_v - h_0 \times t_w)}{\sqrt{3}} f_y \quad (3.4)$$

Where:

A_v : is the shear area of the unperforated cross-section determined by the below formula:

$$A_v = d_w \times t_w + 2 \times [(0,75t_f + t_w) \times t_f] \quad (3.5)$$

t_f : is the thickness of the flanges, and t_w : is the thickness of the web.

In Annex N of the ENV-1993-1-1 version of Eurocode3 [6], the resistance to the shear is calculated in two steps. The first step deals with the calculation of the shear buckling, the second concerns the computation of the pure shear strength obtained by the summation of the shear strengths of the two Tees. Then, it should be checked:

- **For rectangular openings:**

$$V_{opl,Rd} = \left(V_{PL,Rd} - \frac{h_0 t_w f_{yw}}{\gamma_{M_0} \sqrt{3}} \right) \sqrt{\frac{\eta}{\eta+1}} \quad (3.6)$$

Where: $V_{PL,Rd}$: plastic shear strength of the unperforated section calculated according to EC3-1.1 (clause 5.4.6) [18] by the formula:

$$V_{PL,Rd} = \frac{f_{yw}}{\gamma_{M_0} \sqrt{3}} A_v \quad (3.7)$$

$$A_v = A - 2b_f t_f + (t_w + 2r)t_f \quad (3.8)$$

γ_{M_0} : Partial safety coefficient = 1.0

A : Cross sectional area of the original beam;

r : Fillet radius of the rolled section;

η : Coefficient that takes into account the influence of the eccentricity of the opening on the shear strength, determined from the formula:

$$\eta = 0,75 \left[\frac{(dw-h_0)^2 + 4e_0^2}{a_0(dw-h_0)} \right] \quad (3.9)$$

e_0 : The eccentricity between the centre of the opening and the mid-height of the beam web.

-for circular openings

$$V_{opl,Rd} = \left(V_{PL,Rd} - \frac{0.9d_0 t_w f_{yw}}{\gamma_{M_0} \sqrt{3}} \right) \sqrt{\frac{\eta}{\eta+1}} \quad (3.10)$$

Where:

$$\eta = 0,75 \left[\frac{(dw-0.9d_0)^2 + 4e_0^2}{a_0(dw-0.9d_0)} \right] \quad (3.11)$$

And:

$$V_{oba,Rd} = V_{ba,Rd} \left(1 - \frac{d_0 + 0,3a_0}{d} \right) \quad (3.12)$$

The resistance to shear buckling $V_{oba,Rd}$ of a perforated cross-section is calculated by the following expressions:

-For a rectangular opening:

$$V_{oba,Rd} = V_{ba,Rd} (1 - h_0 / d_w + 0,3a_0 / dw) \quad (3.13)$$

- For a circular opening:

$$V_{oba,Rd} = V_{ba,Rd} (1 - d_0 / d_w) \quad (3.14)$$

Where $V_{ba,Rd}$ represents the shear buckling strength of the cross-section not perforated as defined by Eurocode3 (clause 5.6.3)

The mid-opening check is therefore to ensure that:

$$V_{0,sd} \leq V_{0,Rd} = \min\{V_{opl,Rd}, V_{oba,Rd}\} \quad (3.15)$$

$V_{0,sd}, V_{0,Rd}$: represent respectively the shear force and the resistance to the pure shear in the middle of the perforated section.

- **Resistance to local bending (Vierendeel)**

The verification of the transfer of the shear force over the length of an opening, also known as the Vierendeel effect, is the important purpose of local checks. Hence, the Vierendeel effect is actually due to the fact that the shear force has to pass through and be transmitted via the opening that obstructs that transmission. Furthermore, the efforts in the Tees depend on:

- The shape of the opening;
- The relative dimensions of openings ratio to the dimensions of the beam;
- The location with respect to those of the supports;
- The height position as regard to the axis of the beam.

Two categories of methods dealing with resistance verification of the Vierendeel effect are available in literature. The first one, states that the resistance to the Vierendeel effect at a perforated section is determined by taking the ultimate resistances of the upper and lower tees separately. The ultimate strength of each tee is evaluated by considering the interaction effect between moment, shear force and normal force. This process leads to a long and tedious iterative calculation. Simplifying assumptions are often made, herding naturally to less accurate results, but on the safety side. This type of approach is mainly used in the case of composite beams. In the second kind of methods, an M-V interaction diagram is formulated defining the limits of the resistance range at the centre or edges of the opening subjected to a combination of bending moment and shear force.

Any combination $(M_{o,sd} - V_{o,sd})$ located either inside or on the boundary of the resistance curve is permissible with respect to the Vierendeel resistance. Currently, interaction diagrams are constructed in a simpler way to facilitate dimensioning. The procedure is to calculate the pure bending moment as well as the pure shear moment in the middle of the opening and then connect these points by a curve. [9] Darwin and Donahey [21] used a cubic resistance criterion by expressing as dimensional the relationship between the bending moment and the resistant shear force (M_n and V_n , according to Darwin's notations) in the centre of the opening as a function of the moment of resistance in pure bending M_m , and pure shear strength in shear stress V_m , as shown in (Figure 3.4). This criterion is adopted for steel or composite beams with rectangular openings that can be offset from the mid-height of the beam web.

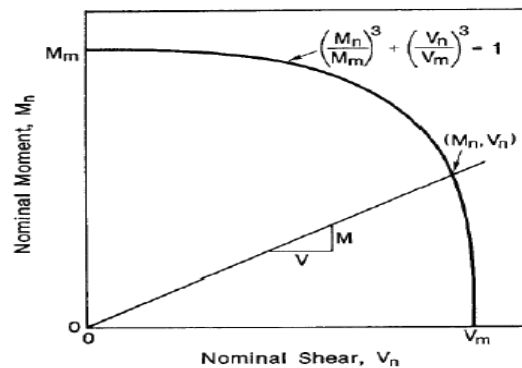


Figure 3.6: Cubic Diagram of Moment-shear force Interaction [21]

Redwood [22] proposed an interaction diagram depicted in Figure 3.5, where the dimensionless parameters controlling the interaction between the bending moment M and the shear force V in the middle of a centred rectangular opening are the ratio M/M_p and V/V_p , where M and V are respectively the pure bending moment and the pure shear force at the assumed section without opening. It may be worth to mention that the relationship was established by assuming a perfect elasto-plastic behaviour following the Von Mises criterion of plasticity.

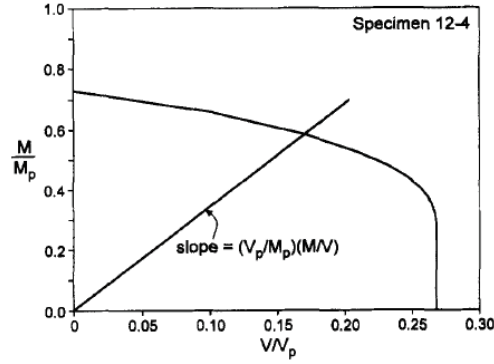


Figure 3.7: Interaction Curve Moment-shear force [22]

In the presence of a circular opening centred at mid-height of the web, the resistance criterion proposed by Chung [9] is written as follows:

$$\left(\frac{M_{o,sd}}{M_{o,Rd}}\right)^{2.5} + \left(\frac{V_{o,sd}}{V_{opl,Rd}}\right)^{2.5} \leq 1 \quad (3.16)$$

Where:

$V_{opl,Rd}$ And $M_{o,Rd}$ are respectively the capacity shearing and bending moment resistances of the perforated section respectively.

It is worth recalling that verifications proposed in Annex N consider the class of unperforated sections. The moment of resistance $M_{o,Rd}$ of a beam at the mid-height of a web opening, taking into account the effects of the shear force V_{sd} occurring in a given section, can be determined, depending on the shape of the opening and the class of the section, by means of the following approximate formulae:

a) Rectangular openings:

- For Class 1 and 2 cross sections:

$$M_{o,sd} \leq M_{o,Rd} = M_{pl,Rd} \left(1 - 0,25t_w h_0 (h_0 + 4e_0) / W_{pl} - \mu_1 V_{sd}'\right) \quad (3.17)$$

-For class 3 cross section:

$$M_{o,sd} \leq M_{o,Rd} = M_{el,Rd} \left(1 - \frac{t_w (h_0 + 2e_0)^3}{12I_y} - \mu_1 \frac{V_{sd}}{V_{0,Rd}}\right) \quad (3.18)$$

Where:

$$\mu_1 = 0,25t_w d_w^2 [1 + 3(0,7 - h_0 / d_w) a_0 / dw] / W_{pl} \quad (3.19)$$

b) Circular openings:

- For Class 1 and 2 cross sections:

$$M_{o,sd} \leq M_{o,rd} = M_{pl,Rd} \left\{ 1 - 0,225 t_w d_0 (0,9 d_0 + 4 e_0) / w_{pl} - \mu_1 V_{sd} / V_{0,Rd} \right\} \quad (3.20)$$

-For class 3 cross section:

$$M_{o,sd} \leq M_{o,rd} = M_{el,Rd} \left(1 - \frac{t_w (0,9 d_0 + 2 e_0)^3}{12 I_y} - \mu_1 \frac{V_{sd}}{V_{0,Rd}} \right) \quad (3.21)$$

With:

$$\mu_1 = 0,25 t_w d_w^2 [1 + 1,35 (0,7 - 0,9 d_0 / dw) a_0 / dw] / w_{pl} \quad (3.22)$$

Where:

I_y : moment of inertia of the unperforated cross-section;

$M_{el,Rd}$: Elastic moment of resistance of the unperforated cross-section according to EC3 (clause 5.4.5.1);

$M_{pl,Rd}$: Plastic moment of resistance of the unperforated cross-section according to EC3 (clause 5.4.5.1);

$V_{0,Rd}$: shear strength of the perforated cross section, according to Annex N (clause N.2.1.3);

W_{pl} : plastic module of the unperforated cross section.

The reduction of the moment of resistance caused by an insulated web opening may be overlooked for cross sections located at a distance from the opening greater than a_p defined by the following expressions:

-If $dw / t_w \leq 90\varepsilon$:

-for a rectangular opening: $a_p = h_0$

-for a circular opening: $a_p = d_0$

- If $dw / t_w > 90\varepsilon$:

-for q rectangular opening: $a_p = \left(\frac{d_w / t_w}{90\varepsilon} \right) h_0$ but $a_p \leq d_w$

-for a circular opening: $a_p = \left(\frac{d_w / t_w}{100\varepsilon} \right) d_0$ but $a_p \leq d_w$

3.4.2.2 Beams containing multiple web openings

In Annex N of EC3, a design method is given for steel beams with multiple web openings providing some assumptions:

(i) Web openings must be regularly spaced at a regular pitch and located concentrically to the centerline of the web

(ii) Made from expanding rolled I-sections or by forming a series of holes in the webs of welded I-section.

(iii) It includes concludes openings that are either polygonal or circular in shape or have a circular end and two straight sides.

- Geometrical layout for multiple openings:

Polygonal openings:

The geometrical layout for polygonal openings is defined by two parameters, that is (a) and (s) as shown in the figure below. Furthermore, the following relations are determined:

- $e = 2s$
- $P = 6s$
- $H_n = 2H - 2a$
- $H_m = 2H - 2a + h$

Circular openings:

The geometrical layout for circular openings is defined by two parameters (a) and (g) as shown in the figure below. The following relations are determined:

- $R = H - (2a + g)$
- $e = 2\sqrt{g(2R - g)}$
- $p = 2R + e$
- $H_n = 2(R + a)$
- $H_m = 2(R + a) + h$

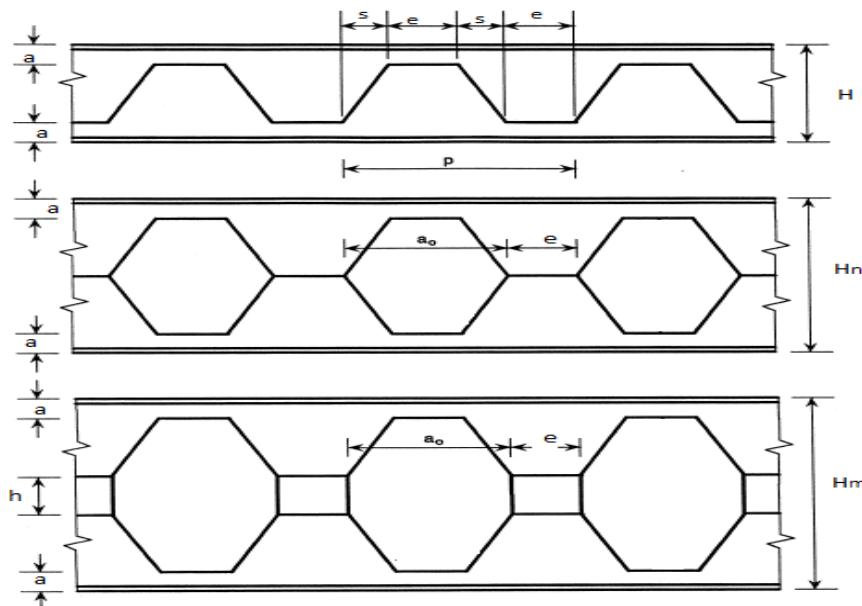


Figure 3.8: Beam with multiple polygonal openings

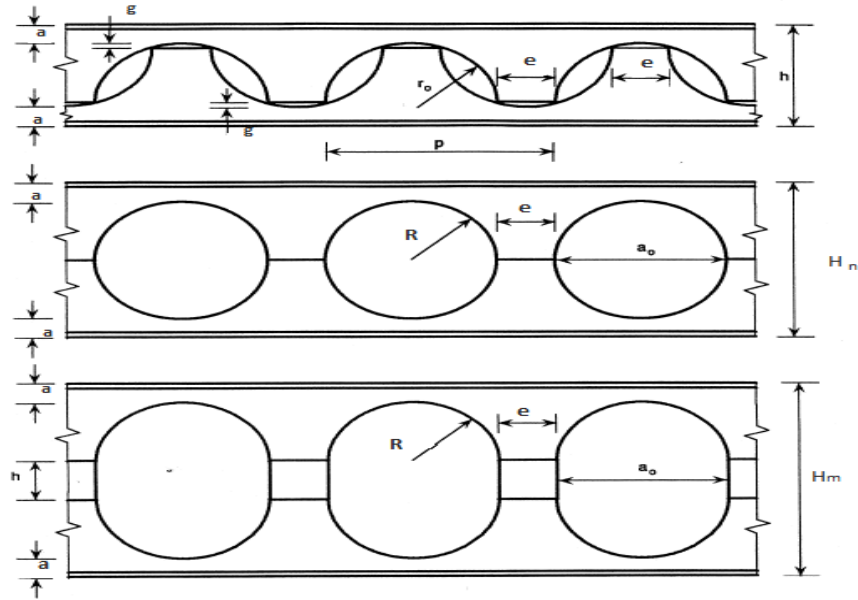


Figure 3.9: Beam with multiple circular and oval openings.

- **Overall flexural strength.**

The overall bending strength at mid-length of an opening is calculated as follows similar to that used in the middle of an insulated openings. As mentioned in paragraph 3.4.1.1.

• **Flexural Vierendeel strength**

- **Polygonal openings:**

As what has been mentioned in Annex N.3.4.2.3, the ‘Vierendeel’ moment resistance of the perforated cross-section depends on the sum of the moment resistance of the top and the bottom tee sections. So, the design value of Vierendeel bending $M_{v,sd}$ should satisfy the following:

$$M_{v,sd} \leq M_{v,Rd}$$

Where:

$$-M_{v,sd} = V_{sd} \times b_0$$

$$-M_{v,Rd} = M_{pLC,Rd} + M_{pLt,Rd} + M_{pLC,Rd} + M_{pLt,Rd}$$

With:

- $M_{v,Rd}$: design Vierendeel moment resistance of the perforated section.

- b_0 : the minimum length of the opening or $a_{0,eff}$ tee length

- $M_{pLC,Rd}$ and $M_{pLt,Rd}$: the moment resistance of the top and the bottom tee section in compression and tension respectively.

Hence, in determining the moment resistance of the tee section it should be allowed for the interaction of the co-existing axial force due to the global bending action. Also, it depends on the presence of co-existing shear force due to the applied lateral load.

-Shear resistance and buckling in bending

The horizontal shear force action at the web post will stress the web post in bending. One edge of the web post will be stressed in compression while the other will be stressed in tension. Consequently, this can occur web post buckling. Furthermore, for both the top and the bottom tee section

- ✓ If: $V_{T,sd} > 0,5 V_{T,Rd}$ the design resistance of the cross section to combination of moment and axial force should be calculated using a reduced yield strength of $(1 - \rho)fy$. For the

$$\text{shear area, with } \rho = \left(\frac{2V_{T,sd}}{V_{T,p1,Rd}} - 1 \right)^2$$

Where:

- $V_{T,p1,Rd}$: plastic shear resistance of the tee section.

- $V_{T,sd}$: applied shear force

- ✓ Or: $V_{T,sd} \leq 0,5 V_{T,Rd}$, so no reduction to the strength of the shear area is necessary.

*For beams with multiple polygonal openings the shear strength is checked as follows:

$$V_{h,sd} \leq \frac{e t_w f_y}{\sqrt{3} \gamma_M}$$

Where:

- $V_{h,sd}$: is the horizontal shear stress at web post.

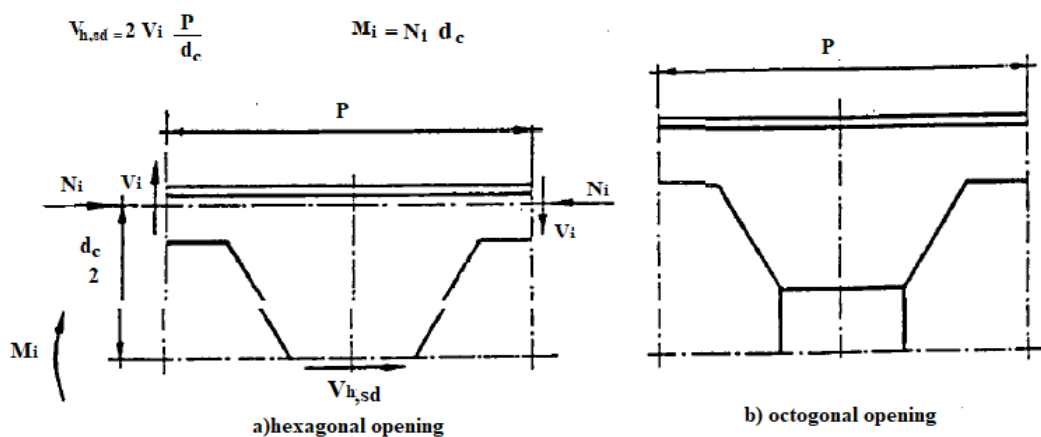


Figure 3.10: Stress resultant at critical section.

- The effect of the axial force on the flexural strength of the Tees

In determining the moment resistance under the axial force due to global bending action the following expressions are considered:

- For beams with unstiffened or unreinforced web openings

$$M_{m,N,Rd} = M_{m,Rd} \left(1 - \left(\frac{N_{m,sd}}{N_{m,Rd}} \right)^2 \right)$$

- For beams with stiffened or reinforced openings

$$M_{m,N,Rd} = M_{m,Rd} \left(1 - \frac{N_{m,sd}}{N_{m,Rd}} \right)$$

Where:

$$-N_{m,sd} = \frac{M_{sd}}{d_c}$$

- $N_{m,sd}$: is the applied axial force due to global bending action.
- M_{sd} : applied global moment at the mid-length of the opening.
- d_c : distance between the elastic neutral axes of the tee-sections.

- **Circular openings:**

The method developed by Ward for circular openings is based on the work of Olander [24] and Sahmel [23]. This approach was subsequently introduced and adopted in Annex N [6] after that some modifications have been made.

The principle of this method is to transfer the reduced forces at the opening to inclined, and flat sections [23] or curved [24], the angle is $\pm\phi$, as shown in the Figure below. The critical angle ϕ varies in the range of 20 and 30° [25]. The strength of each section inclined by an angle ϕ is checked by varying this angle from 25° to ϕ_{max} by increments of 5° for manual calculations and only 1° in when using a computer program. A commonly used rule is to multiply the diameter of a circular web opening by a favourable reducing factor of 0.45- 0.50 to determine the length of an 'equivalent rectangular opening'. This rule was first proposed by Redwood [1973], and it provides a safe though conservative approximation [Ko & Chung 2002].

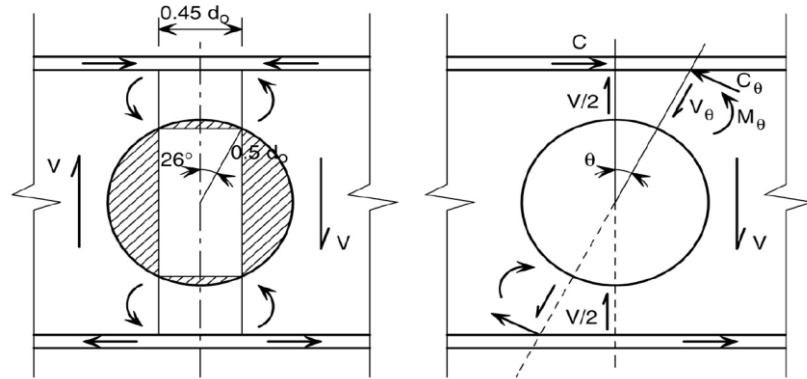


Figure 3.11: Vierendeel bending either by an ‘equivalent rectangular opening’ or by inclined section verifications.

To explain the equivalent diameter D for a non-circular hole, the figure below is analyzed:

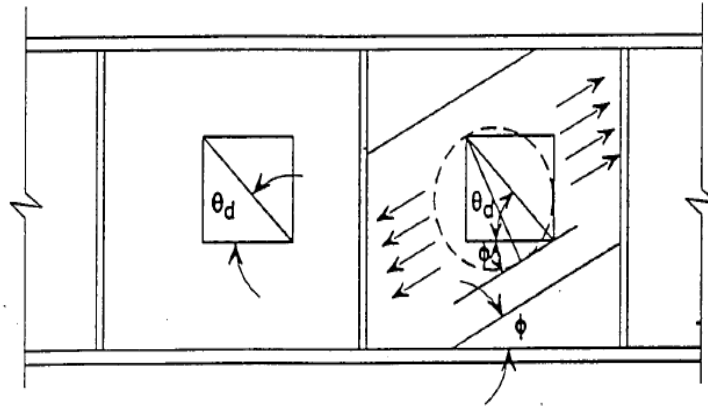


Figure 3.12: equivalent diameter for a rectangular opening.

The verification of the critical section is carried out by the following interaction formula:

$$\frac{N_{\phi, sd}}{N_{\phi, Rd}} + \frac{M_{\phi, sd}}{M_{\phi, Rd}} \leq 1 \quad (3.23)$$

Where:

- $N_{\phi, sd}$: is the normal force perpendicular to the section;
- $N_{\phi, Rd}$: is the reduced normal shear stress resistance;
- $M_{\phi, sd}$: is the internal moment;
- $M_{\phi, Rd}$: is the reduced moment of resistance for shear force.

* **Web post buckling resistance:**

The uprights of the cellular beams are loaded at half height by shear force. Longitudinal V_{hi} due to the variation of the normal stresses in the Tees. The shear stress in the upright side causes bending that induces tensile stresses in a side of the post and compressive stresses in the other as shown in the figure 2.13. Under the effect of compressive stresses, the studs may be unstable and may undergo out-of-plane deformations that resemble local buckling. The resistance of the upright to buckling depends on several parameters of which the main ones are:

- The openings spacing of characterized by the parameter $\alpha = p / h_0$;
- The opening slenderness of $\beta = \frac{h_0}{t_w}$;
- The steel grade and the symmetry or asymmetry of the cross-section. [26]

The buckling resistance is satisfied when the bending moment $M_{wp,sd}$ at the critical cross-section in the web post satisfies the following criterion:

$$M_{wp,sd} \leq (C_1\alpha - C_2\alpha^2 - C_3)M_{el,Rd} \quad (3.24)$$

With:

- $M_{wp,sd} \leq 0.6 M_{el,Rd}$
- $C_1: 5.097 + 0.1464 \beta - 0.00174\beta^2$
- $C_2: 1.441 + 0.0625 \beta - 0.000683\beta^2$
- $C_3 : 3.645 + 0.0853\beta - 0.00108\beta^2$
- $M_{el,Rd}$: is the elastic moment of resistance of the critical cross-section in the web post.

The horizontal shear force at mid-height of the web post V_{hi} is calculated by considering the following hypotheses:

- (i) The shearing force is constant over the opening pitch p ($V_{t,sd,i} = V_{t,sd,i+1}$), i.e. the loads applied to 'p' are being neglected;
- (ii) There is an inflection point of the out-of-plane deformation at mid-height of the amount, so the moment is zero in this section.

From where:

$$V_{hi} = \frac{2V_{T,sd,i} \times P}{(h_n - 2y_t)} \quad (3.25)$$

- y_t : is the distance from the elastic neutral axis of the upper Tee to the upper edge of the flange.

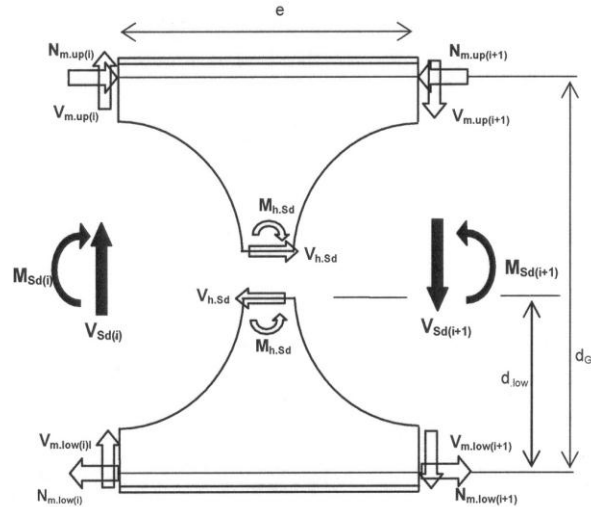


Figure 3.13: internal stress distribution

In order to calculate the resistance of cellular beams to the buckling of the web post, Bitar et al [39] proposed an analytical model based on experimental observations. The area of instability of the web post depends on its width, that's to say, the thinner the web post, the closer the critical section is to the weld joint. Inversely, the larger the web post, the further away the critical section is from this joint. The point of maximum out-of-plane deformation is located at an approximate distance from the weld line of the members, varying from 1/3 of the radius of the openings for thin web post to 1/2 of that radius for large one.

The distance d_w of the critical section (according to the notations in (Figure 3.8)) is plotted according to the geometrical characteristics of the opening from the formula:

$$d_w = \frac{d_0}{2} \sqrt{\frac{\sqrt{\alpha^4 + 8a^2} - 2 - a^2}{2}} \quad (3.26)$$

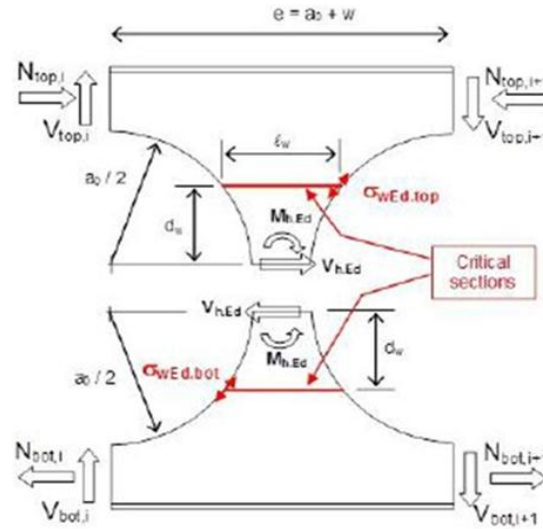


Figure 3.14: Local forces and position of the critical sections in the intermediate web-post [27]

- The buckling resistance of the web post is verified by the following relation:

$$\sigma_{wEd} \leq k\sigma_{wRd} \quad (3.27)$$

Where:

- σ_{wEd} : is the main compressive stress in the half web post studied;
- σ_{wRd} : is the principal resistive stress with a post-critical reserve factor, which takes into account the mechanical failure after the local buckling of a web post.
- k : factor indicates the reserve provided by the Tees for openings beyond the appearance of instability of the web post. It reflects the fact that the global collapse of the beam can occur after the local collapse by the development of plastic hinges in the Tees around the openings. This coefficient has been calibrated from the results of numerical simulations.

- Longitudinal shear strength

The longitudinal shear force at the welding joint of the web post shall be satisfy the following condition:

$$V_{hi} \leq \frac{w t_w f_{yw}}{\sqrt{3} \gamma_{M0}} \quad (3.28)$$

Where:

- W : is the minimum width of the web post.

Bibliography:

- [1] LAURSEN. T. A., SIMO. J. C., " A Continuum-Based Finite Element Formulation for the Implicit Solution of Multibody, Large Deformation Frictional Contact Problems. ", International Journal for Numerical Methods in Engineering, vol n° 36, pp:3451-3485, 1993.
- [2] Ferhat Erdal; Osman Tunca, Serkan Tas; Ultimate Load Capacity of Optimal Designed Angelina;Beams, Serdar Carbas4; *Smart Construction Research* Volume 2 Issue 1 | 2018 | 1
- [3] A. BADKE-NETO^a,A. F. G. CALENZANI^a; Study of methods for the design of cellular composite steel and concrete beams; jan 2014.
- [4] hicks.R.jamzs; Cross-section classification of elliptical hollow sections/Article in Steel and Composite Structures · June 2007/Leroy Gardner.
- [5] ENV 1993-1-1:1992/A2:1998, Eurocode 3: Annex N, web openings.
- [6] Soltani, M. R., Bouchair, A. & Mimoune, M. (2012). Nonlinear FE analysis of the ultimate behavior of steel castellated beams. *Journal of Constructional Steel Research*.
- [7] A. Kaveh and Farnoud Shokohi/; Cost optimization of castellated beams using charged system search algorithm/Article in Iranian Journal of Science and Technology - Transactions of Civil Engineering · February 2014.
- [8] I. E. Bower.; Design of beams with web openings. *Journal of the Structural Division ASCE*, vol. 94, No. ST 3, pages 783-807,1968.
- [9] K.F. Chung, T.C.H. Liu and A.C.H. Ko; Steel beams with large web openings of various shapes and sizes: An empirical design method using a generalised moment–shear interaction curve. *Journal of Constructional steel Research*, vol. 59, pages 1177–1200, 2003.
- [10] K.F. Chung, T.C.H. Liu and A.C.H. Ko. Investigation on Vierendeel mechanism in steel beams with circular web openings. *Journal of Constructional steel Research*, vol. 57, pages 467–490, 2001.
- [11] T.C.H. Liu and K.F. Chung. Steel beams with large web openings of various shapes and sizes: finite element investigation. *Journal of Constructional steel Research*; vol. 59, pages 1159–1176, 2003.
- [12] Chung, K.F. and Ko, C.H; Harmonization on Practical Design of Steel and Composite Beams with Large Web Openings for Full Integration with Building Services. *Proceedings of the Second Structural Engineering World Congress*, Yokohama, 9-12 October 2002 (CD Publication).

- [13] **Chung, K.F. and Lawson, R.M.** Simplified Design of Composite Beams with Large Web Openings to Eurocode4. *Journal of Constructional Steel Research*, **57**, 135-163
- [14] **Lawson, R.M.** Design for Openings in the Webs of Composite Beams. CIRIA/Steel Construction Institute, CIRIA Special Publication and SCI Publication 068, Ascot.
- [15] **Darwin, D.** Steel and Composite Beams with Web Openings. Steel Design Guide Series, Vol. 2. AISC-American Institute of Steel Construction, Chicago.
- [16] **Redwood, R.G. and Cho, S.H.** Design of Steel and Composite Beams with Web Openings. *Journal of Constructional Steel Research*, **25**, 23-41.
- [17] **Oehlers, D.J. and Bradford, M.A.** Composite Steel and Concrete Structural Members: Fundamental Behaviour. Kidlington, Oxford.
- [18] **Chung, K.F., Ko, C.H. and Wang, A.J.** Design of Steel and Composite Beams with Web Openings—Verification Using Finite Element Method. *Steel and Composite Structures*, **5**, 203-233.
- [19] **Ko, A.C.H. and Chung, K.F.** A Review of Recent Developments on Design of Perforated Beams. *Proceedings of the Third International Conference on Advances in Steel Structures*, Hong Kong, 9-11 December 2002, 121-128.
- [20] **Wang, A.J. and Chung, K.F.** Advanced Finite Element Modelling of Perforated Composite Beams with Flexible Shear Connectors. *Engineering Structures*, **30**, 2724-2738.
- [21] **D. Darwin, R.C. Donahy.** LRF; composite beams with unreinforced web openings. *Journal of the Structural Division ASCE*, vol. 114(3), 1988.
- [22] **R. G. Redwood.** Design of I-beams with web perforations. Beams and beam-column-stability and strength. Narayanan editions, Applied Science Publishers, Barking, England, 1983;
- [23] **P. Sahmel.** **Konstruktive Ausbildung und Na'herungsbenechaung**; The design, construction and approximate analysis of weld beams and torsion members having large web openings]. *Schweissen und Schneiden 1969*, 21(3),
- [24] **H.C. Olander.** A method of calculating stress in rigid frame corners. *Journal of the Structural Division ASCE*, vol. 1953.
- [25] **D. Mateesco et G. Mercea.** Un nouveau type de poutres ajourées. *Revue construction métallique CTICM No.3*, pages 3-14, 1981.
- [26] **D. Bitar, P.O. Martin, Y. Galéa, T. Demarco.** Poutres cellulaires acier et mixtes : Partie 1 Proposition d'un modèle pour la résistance des montants. *CTICM n°1*, 2006.

[27] **Sébastien Durif/Abdelhamid Bouchair/Olivier Vassart.** Validation of an analytical model for curved and tapered cellular beams at normal and fire conditions/January 2013/Periodica Polytechnica Civil Engineering 57(1):83.

C *HAPTER IV:*

PORTAL STEEL FRAMES

4.1 General

Steel portal frames are used in the most common form of single-story construction in the industry. The design of portal frames is well covered in EC3 and BS 5950-1, supported by extensive guidance in other publications. Steel portal frames are appreciated as a highly efficient and cost-effective way to support an envelope, enclosing a usable volume. They are highly suited to carrying relatively modest loads. Also, by their very nature they are relatively flexible; less onerous deflection limits are generally applied to portal frames than for other forms of steel construction. [1]

4.2 Types of portal frame and characteristics

4.2.1 Definition

Steel moment resistant portal frame is a rectilinear assemblage of beams and columns, in which the beams are rigidly connected to the columns. The basic structural form of portal frames was developed during the Second World War, driven by the need to achieve the low-cost building envelope [2]. Nowadays they are the most commonly used structural forms for single-storey industrial structures. With a better understanding of the structural behaviour of slender plate elements under combined bending moment, axial load and shear force, many fabricators now offer a structural frame fabricated from plate elements. [3]

4.2.2 Categories

There are two main configurations of a frame; flat-roofed portal frame and pitched-roof portal frame. An illustration of the two different frames can be seen in Figure 1.4.[4]

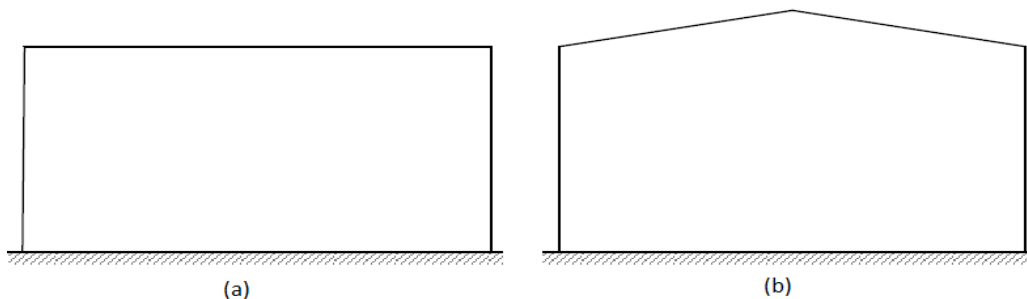


Figure 4.1 typical one bay portal frame; (a) flat-roofed portal frame and (b) pitched-roof portal frame.

Single - storey pitched roof steel portal frames are a very economical form of structure for most

single-storey buildings for industrial, distribution, retail and leisure purposes. Single-storey portal frame design uses structural layouts and structural forms that are frequently different from those used in other types of single-storey or multi-storey structures. As a result, many of the calculations used for portal frame design differs from those commonly used for other types of building.[5]

4.2.3 Moment connections

Steel moment framework uses a series of columns and beams, where the attachments are formed using a combination of welding and bolting. These connections are called "moment connections". A Moment Connection in structural engineering is a joint that allows the transfer of bending moment forces between a column and beam (or any other two members). If a child member (a beam) has some internal moment, the connection should be able to transmit the load due to that moment. With no releases to the joint when it is structurally analysed. The various connection methods used to achieve these connections have evolved throughout the decades, but as welding techniques and bolt strength have improved, the welded flange connection became the moment frame joint connection of choice.[6]

4.3 Portal frame with WOB's structures as lateral resisting systems

Seismic codes specify a minimum beam span-to-depth ratio for moment resisting frame to ensure formation of plastic hinges at beam ends with adequate length. This minimum beam span to-depth limitation is at odds with the need for shorter spans to control lateral drifts in tall buildings, especially with tubular frames. [7] From literature and as reported by some researcher, where numerical results are in conformity with the test results, which verify the validity of the model. The PSD test shows that the tested frame can satisfy the design requirement and the web opening does not weaken its stiffness. In the quasi-static test, the failure mode of the tested frame is in conformity with the judgement, i.e., Vierendeel mechanism is formed in weakened areas due to web opening and brittle weld fracture is avoided, which results in an improvement of the aseismic behaviours of steel MRF. [9]

Another investigation based on experimental data and numerical outcomes. Where the performance of castellated beam-column end plate connections up to failure was investigated; subjected to monotonic and cyclic loading in vertical and horizontal direction. The effect of arranging the geometry and location of openings were also been investigated. Indicating that the castellated model behaved softer therefore dissipated more energy than normal plane beam to column connection. [8] The finding showing also that the joints should have adequate strength and

stiffness to resist the internal forces induced by the framing members and external force like earthquake and wind loadings.

BIBLIOGRAPHY

- [1] **Kazuhiko Kasai and Michael D. Engelhardt**; Advances in design of eccentrically braced frames; presented at the Pacific Structural Steel Conference, Auckland, August 1986.
- [2] **Hamburger, Ron. et al., (2009)**. Seismic Design of Steel Structures. National Institute of Standards and Technology. NIST GCR 09-917-3
- [3] **Andersen and Petersen, 2010**. Ulrik Andersen and Stefan Petersen. Bygningsingeniør: Halvdelen af undersøgte tage har fejl - 6.000 tage bør tjekkes. URL: <http://kortlink.dk/c3q7>, 2010. Downloaded: 15-02-2013
- [4] **the steel construction institute**; TthncD IReport ; SCI Publication P164
- [5] **Chia-Ming Uang, Rafael Sabelli, Michel Bruneau**, Ductile Design of Steel Structures/second edition.
- [6] Plastic Design of Portal frame to Eurocode 3/University of Sheffield; Worked example.
- [7] **Chantal Rudman**; investigation of the structural behaviour of the portal frames; master thesis; University of Stellenbosch; March 2009.
- [8] **Antonio De Luca, Ernesto Grande & Elena Mele**; Non-Linear Response of Concentric Braced Frames; Giuseppe Brandonisio Civil Engineering Department (D.I.C.), Second University of the Studies of Naples, Aversa (CE), Italy. Structural Analysis and Design Department (DAPS), University of Naples “Federico II”, Naples, Italy.
- [9] **Saeid Zahedi Vahid ; Siti Aminah Osman** ; Monotonic and cyclic loading simulation of structural steelwork beam to column bolted connections with castellated beam; [University Kebangsaan Malaysia](#), Journal of Engineering Science and Technology; August 2013 8(4):416-427.

C *HAPTER V:*

OVERVIEW ON USED SOFTWARE AND FEA

5.1 General

FEA is widely useful tool for studying the behaviour of various structural and mechanical designs. It can also be used to predict the ability of a design to withstand extreme loading conditions that cannot be duplicated in an experiment. Hopefully these extreme loading conditions will be considered early in the design process. An example of such a finite element analysis is the simulation of the ability of an offshore platform to withstand the forces produced by a storm.

With the advances in modern computing techniques, finite element analysis has become a practical and powerful tool for engineering analysis and design. In Structural Engineering, development of structural design code equations, their redeveloping is a continuous process and requires a wide range of experimental studies. However, performing many numbers of experiments is costly, time consuming and hence uneconomical. On the other hand, conducting experiments is a compulsion for the research to progress.

ABAQUS is a suite of powerful engineering simulation programs based on the Finite Element Method, sold by Dassault Systems as part of their SIMULIA Product Life-cycle Management (PLM) software tools. Abaqus is a software package that is widely used in various industries and in the field of construction to solve a wide variety of problems in structural mechanics. It allows the implementation of very complex and customized material behaviours, up to the definition of failure criteria. The problem gets enormously simplified with the use of ABAQUS 6.9 (2009). ABAQUS is a highly sophisticated, general purpose finite element program, designed initially to model the behaviour of solids and structures under various externally applied loadings.

5.2 Introduction to ABAQUS

The ABAQUS 6.14.1 software was used for the finite element analysis (FEA). Which is a general-purpose finite element analysis program, capable of handling non-linear static analysis and elasto-plastic materials. In addition, Abaqus allows to take into account very complex contact behaviours that consider large rotations and friction.

Designed as a general-purpose simulation tool, ABAQUS can be used to study more than just structural (stress/displacement) problems. It can simulate problems in such diverse areas as heat transfer, mass diffusion, thermal management of electrical components (coupled thermal-

electrical analyses), acoustics, soil mechanics (coupled pore fluid-stress analyses), and piezoelectric analysis.

ABAQUS contains an extensive library of elements that can model virtually any geometry. It has an equally extensive list of material models that can simulate the behaviour of most typical engineering materials including metals, rubber, polymers, composites, reinforced concrete, crushable and resilient foams, and geotechnical materials such as soils and rock.

ABAQUS includes the following features:

- Capabilities for analysing both static and dynamic problems;
- The ability to model very large changes in shape of solids, in both two and three dimensions;
- A very extensive element library, including a full set of continuum elements, beam elements, shell and plate elements.
- A sophisticated capability to model contact between solids
- An advanced material library, including the usual elastic and elastic– plastic solids; models for foams, concrete, soils, piezoelectric materials and many others
- Capabilities to model a number of phenomena of interest, including vibrations, coupled fluid/structure interactions, acoustics, buckling problems and so on.

ABAQUS is simple to use and offers the user a wide range of capabilities, even the most complicated analyses can be modelled easily.

5.3 Modelling sequence

Every complete finite-element analysis consists of 3 separate stages:

Pre-processing or modelling: this stage involves creating an input file, which contains an engineer's design for a finite-element analyser (also called "solver").

Processing or finite element analysis: This stage produces an output visual file.

Post-processing or generating report, image, animation, etc. from the output file: This stage is a visual interpretation stage.

In fact, ABAQUS/CAE is capable of pre-processing, post-processing, and monitoring the processing stage of the solver; however, the first stage can also be done by other compatible CAD software, or even a text editor.

ABAQUS/Standard, ABAQUS/Explicit or ABAQUS/CFD is capable of accomplishing the processing stage. Assault Systems also produces ABAQUS for CATIA for adding advanced processing and post processing stages to a pre-processor like CATIA.

As shown in the picture below, 11 modules are implanted in ABAQUS CAE which have to be used one after the other in order to modelling, loading, defining boundary conditions and finally analysis and then showing the results, diagrams and etc. These 11 modules are named: Part-Property-Assembly-Step-Interaction-Load-Mesh-Optimization-Job-visualization-Sketch.

In the following, some details will be provided for each module:

- **PART MODULE:** This module allows the creation of the geometry required for the problem. Prior to create a 3-D geometry, the creation of 2-D must be performed and then manipulate it to obtain the solid geometry.

- **PROPERTY MODULE:** For defining material properties for the analysis and assigning them to available parts.

- **ASSEMBLY MODULE:** For assembling created parts together. Even with a single part, assembly is needed.

- **INTERACTION MODULE:** Permits to rely different parts by Tie, Rigid body, etc.

- **STEP MODULE:** To select the kind of analysis to be performed and define the parameters associated with it. variables to include can be also selected. in the output files in this module. Load is applied over a step; the sequence of loads creates several steps and define the loads for each of them. Most complex analysis are likely to have a sequence of steps. An analysis step during which the response is nonlinear is called general analysis step. An analysis step during which the response is linear is called a linear perturbation step. A linear perturbation analysis step provides the linear response of the system about the base state i.e. the state at the end of the last nonlinear analysis step prior to the linear perturbation step.

- **LOAD MODULE:** Allows to define the loads and boundary conditions of the model for a particular step (indicated in the toolbar below).

- **MESH MODULE:** The mesh module controls how to mesh your model: the type of element, their size etc.

- **JOB MODULE:** To submit the model for analysis.

- **VISUALIZATION MODULE:** To look at the deformed model. A plot of values of stress, displacement, reaction forces, etc. with the possibility of using contours, surface, vectors or tensors.

- **MODEL TREE:** Provides a graphical overview of the model and the objects that it contains, such as parts, materials, steps, loads, and output requests. In addition, the Model Tree provides a convenient, centralized tool for moving between modules and for managing objects. If the model database contains more than one model, Model Tree can be used to move between models.

- **RESULTS TREE:** provides a graphical overview of your output databases and other session-specific data such as X–Y plots. When more than one output database is open in the session, the Results Tree can be used to move between output databases.

N.B. There is no inherent set of units used in ABAQUS. It is up to the user to decide on a consistent set of units and use that units.

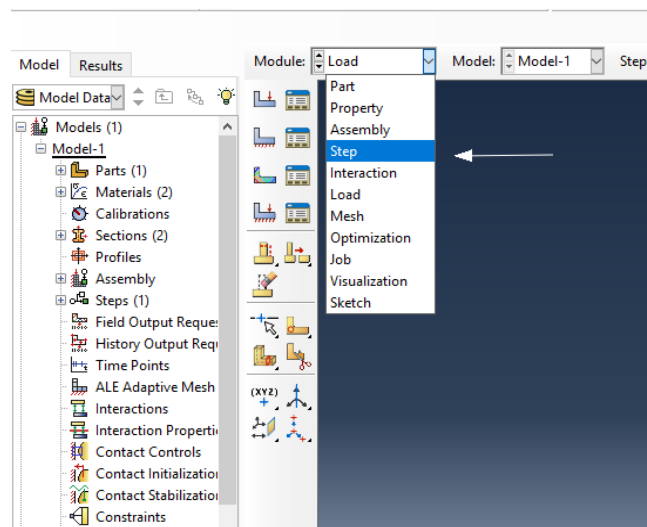


Figure 5.1: ABAQUS Modules.

5.4 Elements in ABAQUS

5.4.1 Element types

Wide range of elements in the ABAQUS/Explicit element library are available and provides flexibility in modeling different geometries and structures.

–Each element can be characterized by:

- Family: Continuum, shell, membrane, rigid, beam, truss elements, etc. Figure 5.2
- Number of nodes: Element shape and Geometric order. Figure 5.3
- Linear or quadratic interpolation
- Degrees of freedom: Displacements, rotations, temperature: translation towards 1; translation towards 2; translation direction 3; rotations around the axis 1; rotations around the axis 2; rotations around the axis 3.

Directions 1, 2 and 3 correspond to the global directions 1, 2 and 3, respectively; unless a local coordinate system has been defined at the nodes. Figure 5.4

- Formulation: Small and finite strain shells, etc.
- Integration: Reduced and full integration

Each element in ABAQUS has an assigned name: S4R, B31, M3D4R, C3D8R and C3D4 and the element name identifies primary element characteristics.

Each element can be differed by family, number of nodes, and Degrees of freedom.

- Family: solid (Continuum), shell, membrane, rigid, beam, truss elements, etc.

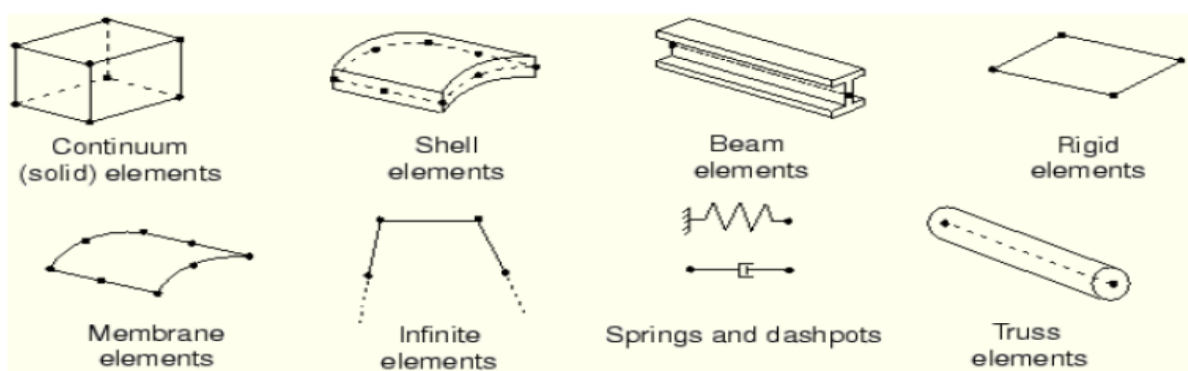


Figure 5.2: Family of element in ABAQUS.

- Number of nodes

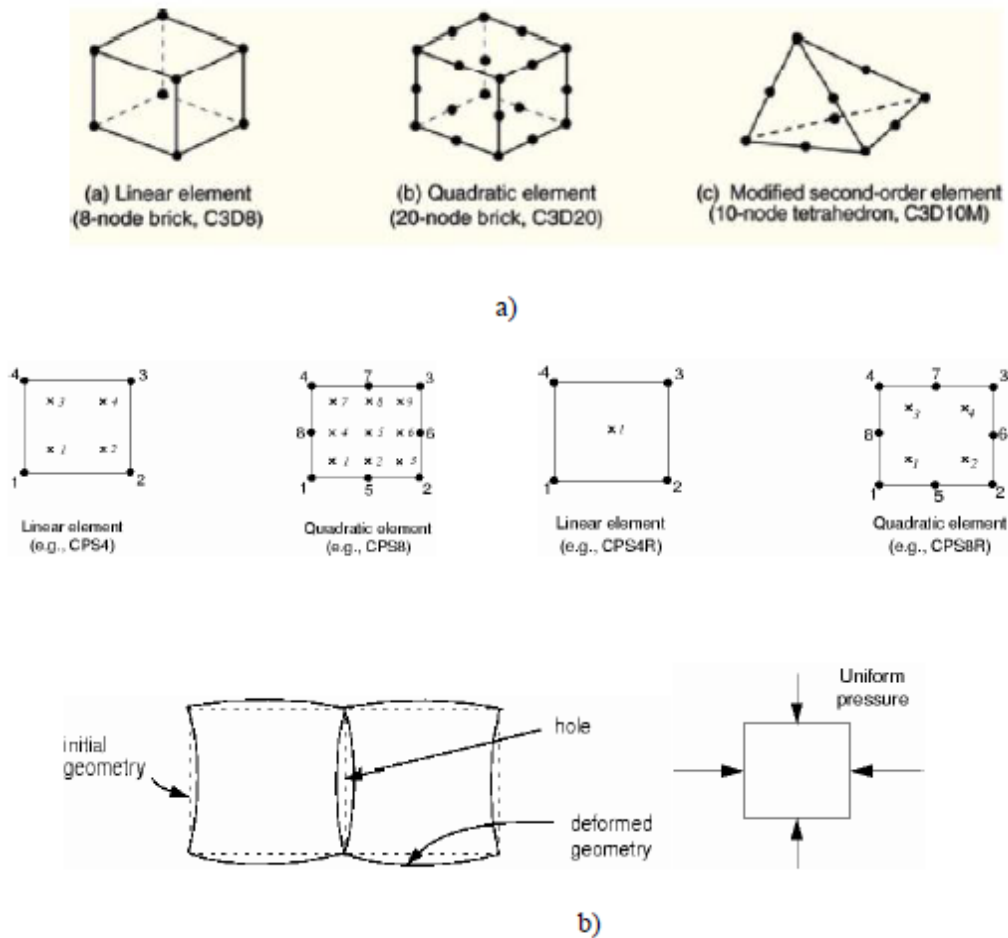


Figure 5.3: Number of nodes of element in ABAQUS

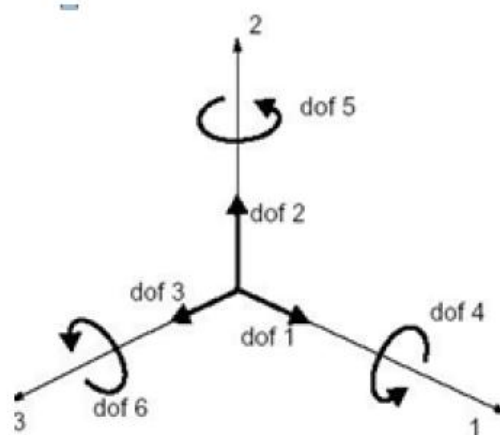


Figure 5.4: Displacement and Rotational degrees of freedom.

5.4.1.1 Shell element overview

Shell elements are needed for out-of-plane loading. Shell elements can also be used where the loading is planar but the material is made of composites. Since shell elements by definition allow for through thickness variation of material properties these are the appropriate elements to be used in these cases.

The ABAQUS shell element library provides elements that allow the modelling of curved, intersecting shells that can exhibit nonlinear material response and undergo large overall motions (translations and rotations). ABAQUS shell elements can also model the bending behaviour of composites.

The library is divided into three categories consisting of general-purpose, thin, and thick shell elements. Thin shell elements provide solutions to shell problems that are adequately described by classical (Kirchhoff) shell theory, thick shell elements yield solutions for structures that are best modelled by shear flexible (Mindlin) shell theory, and general-purpose shell elements can provide solutions to both thin and thick shell problems. All shell elements use bending strain measures that approximate those of Koiter-Sanders shell theory. While ABAQUS/Standard provides shell elements in all three categories, ABAQUS/Explicit provides only general-purpose shell elements. For most applications the general-purpose shell elements should be the user's first choice from the element library. However, for specific applications it may be possible to obtain enhanced performance by choosing one of the thin or thick shell elements. It should also be noted that not all ABAQUS shell elements are formulated for large-strain analysis.

The general-purpose shell elements are axisymmetric elements SAX1, SAX2, and SAX2T and three-dimensional elements S3, S4, S3R, S4R, S4RS, S3RS, and S4RSW, where S4RS, S3RS, and S4RSW are small-strain elements that are available only in ABAQUS/Explicit. The general-purpose elements provide robust and accurate solutions in all loading conditions for thin and thick shell problems. Thickness change as a function of in-plane deformation is allowed in their formulation. They do not suffer from transverse shear locking, nor do they have any unconstrained hourglass modes. Furthermore, in geometrically nonlinear analyses in ABAQUS/Standard the cross-section thickness of finite-strain shell elements changes as a function of the membrane strain based on a user-defined “effective section Poisson's ratio,” ν . In ABAQUS/Explicit, the thickness change is based on the “effective section Poisson's ratio” for all shell elements in large-deformation

analyses, unless the user has specified that the thickness change should be based on the element material definition. The thickness change based on the “effective section Poisson's ratio”.

SHELL181 is a 4-node 3-D shell element with 6 degrees of freedom at each node. The element has full nonlinear capabilities including large strain and allows 255 layers. The layer information is input using the section commands rather than real constants. Failure criteria is available using the FC commands.

5.4.2 Element Shapes

There are various kinds of element shapes in ABAQUS:

- Quad: Use exclusively quadrilateral elements.
- Quad-dominated: Use primarily quadrilateral elements, but allow triangles in transition regions. This setting is the default.
- Tri: Use exclusively triangular elements.
- Hex: Use exclusively hexahedral elements. This setting is the default.
- Hex-dominated: Use primarily hexahedral elements, but allow some triangular prisms (wedges) in transition regions.
- Tet: Use exclusively tetrahedral elements.
- Wedge: Use exclusively wedges elements.

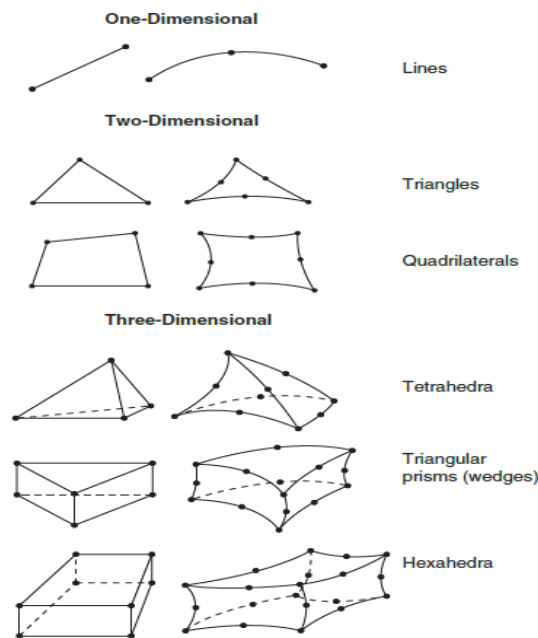


Figure 5.5: Elements Shapes in ABAQUS

5.5 Numerical Techniques used for Solving Nonlinear Problems with ABAQUS

The standard approach used to solve non-linear finite element problems has been the implicit iterative formulation in which the equilibrium equations between the external (P) and internal (I) forces are resolved iteratively until convergence [9]. Implicit schemas have become important tools for the study of multi-scale phenomena described by the non-linear partial derivative equations. The two main methods for implicit resolution are the incremental method Newton-Raphson iterative for general use, and the arc length method also known as the Riks method for buckling and post-bifurcation analysis. For these two methods, the overall tangent stiffness matrix of the system is computed at each stage of the analysis and successive iterations are made in order to respect the criterion of convergence. The latter can be based on forces, displacements or their combinations.

In the case of the Newton-Raphson method, the solution of a nonlinear problem requires an incremental/iterative technique, provided with such a technique approximates the actual solution to the nonlinear problem with:

$$P - I = 0.$$

There is generally no exact solution to these equations, so ABAQUS solves it iteratively by using the Newton-Raphson method to find an approximate solution that minimizes the residuals which represent the magnitude and distribution of extra external force at each degree of freedom needed to bring the structure into equilibrium. Hence, Newton-Raphson locates a displaced shape in which the residuals are zero.

Using Abaqus load-history versus time is defined as a sequence of steps. Each step is broken up into a sequence of time increments, which is part of a step. In static problems, the total load applied in a step is broken into smaller increments so that the nonlinear solution path may be followed. Each increment usually requires several iterations to achieve convergence.

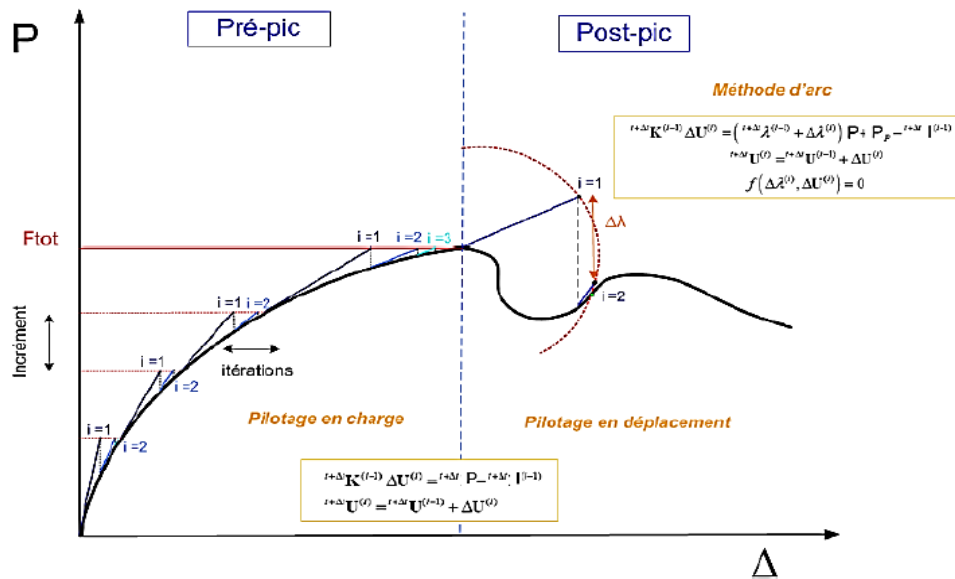


Figure 5.6: Resolution methods using implicit formulation.

5.5.1 Non-linear numerical modelling tools

5.5.1.1 General

Since the use of the finite element method in non-linear computation, the numerical simulation requires a very precise description of the physical and mechanical problems encountered during the various phases of the process. The need to solve the problem of non-linearity in its three forms: Material, geometrical and contact non-linearity, aims at evaluating the behaviour of the structures until failure. Each form of non-linearity has its specific characteristics to distinguish it from others. Indeed, it is necessary to understand the circumstance of these three varieties in order to ensure the wholeness of the actual possible nonlinear behaviour in the numerical simulation of structures. The difference between linear and nonlinear material in analysis can easily be shown. Incorporating nonlinear properties of materials not only allows for accurate calculation of stress distribution but also make it possible to verify certain load-bearing capacity aspects of the model like plastic collapse.[2][11]. Some details will be provided, for each for of nonlinearity, in the subsequent sections

5.5.1.2 Material Non-linearity

In structural mechanics, material non-linearity is directly associated with the characteristics of the mechanical behaviour of the used material, as well as with the existence of geometrical factors related to the shape and deformation of the structure. Indeed, structures built from ductile materials, say the steel, are recognised to have an additional strength beyond the elastic limit, which in turn, depends upon several factors among which the form of the shape of their cross-section. Nowadays, the design and safety verification of structures must take into account several aspects of the non-linear behaviour of structures, which are incorporated in modern structural codes of practice [3] [4].

Material nonlinearity is characterized by the dependence of stress on current strain. Some of its effects: Plasticity; Plastic hinge formation and plastic collapse; Necking; Rubber nonlinear elasticity; Cracking, crushing.[6]

5.5.1.2 Geometric non-linearity

Geometric non-linearity is due to the actual displacement of the structure. In fact, when these displacements become important, the equilibrium can no longer be described in the initial unreformed configuration (first order deformation of the displacements) but must be studied in the deformed configuration (second order deformation of the displacements). Within this category, one can distinguish between large displacements and moderate rotations on the one hand and large displacements and large rotations on the other hand. In this case, non-linear effects are associated with equilibrium equations that take into account the deformed configuration and the deformation-displacement ratio. [5] We can summarize that Geometric nonlinearity is characterized by nonlinear relationship between displacement increments, strain increments, and Integration over current (unknown) volume. [6]

The basis for the geometrical nonlinear analysis of structures has its theoretical foundations in the nonlinear elasticity of solid mechanics. The geometric nonlinearity appears in the theory of elasticity in the equilibrium equations written using the deformed configurations of the body and in the relationships strain-displacement, which include non-linear terms in displacements and their derivatives.[10]

5.5.1.3 Boundary conditions

In finite elements, the interaction between two or more bodies is configured when there is penetration of one body into another, i.e. when there are at least two points belonging to different bodies occupying the same spatial position. In the case of civil engineering structures, this challenge covers almost all aspects of the structural system, i.e. the structural constituent model, boundary conditions, geometric non-linearities, etc. One aspect of particular interest is the treatment of the interface of the elements of the structure., [6]

➤ **Contact:**

The problem of contacts is a relevant topic in solid mechanics because it introduces several times the interaction between bodies, forces and local deformations. This problem presents a high degree of complexity because it deals with the phenomena of geometric and material nonlinearity, even for materials considered with a linear elastic behaviour. Indeed, contact problems are of great importance in the field of civil engineering. These problems cover particular elements when analysing 3D joints in steel structures. These problems have a non-linear and irreversible character and consequently difficult to deal with.

➤ **Friction:**

The presence of friction adds variables to the contact problem but also numerical instabilities to the resolution. This instability results from the change of a contact point in the interface from a non-slip status to a sliding status or the opposite. The result is a numerical instability, which requires a specific treatment in order to reduce its influence on the convergence quality of the computation [8]. The Friction modelling consists of establishing a relationship between the tangential contact force and the relative sliding velocity. It is difficult to consider friction because of the very wide range of behaviours and the precision required. This leads to the formulation of several friction models [7].

Bibliography

- [1] **ABAQUS** standard analysis user's manual 5ersion 6.14-, 2018.
- [2] **Robert D. Cook**; FINITE ELEMENT MODELING FOR STRESS ANALYSIS. February2015.
- [3] **ABICHOU. H.**, "Simulation ; I 'emboutissage à froid par une Méthode asymptotique Numérique.", Thèse de doctorat, uni5ersité de Metz, 2001.
- [4] **Cra5eur. J.C.**, "Modélisation des éléments finis : Cours et exercices corrigés.", Livre, 3éme édition, DUNOD, 2008.
- [5] **ROBERT. F.**, "contribution à l'analyse non linéaire géométrique et matérielle des ossatures spatiales en génie ci5il : application aux ou5rages d'art.", Thèse de doctorat, institut national de sciences appliquées de Lyon, 1999.
- [6] ABAQUS user's manual 'Obtaining a Con5erged Solution with Abaqus'.
- [7] **BUSSETTA. P.**, "Modélisation et résolution du problème de contact mécanique", thèse Doctorat, l'uni5ersité du Québec à Chicoutimi, Canada,2009
- [8] **KALLEL. A.**, "Une modélisation du contact par l'approche mortier – application à la mise en forme ", thèse Doctorat, Uni5ersité de Technologie de Compiègne, 2014.
- [9] **Ben Ftima. M.**, "utilisation de la méthode des éléments finis non-linéaires pour la conception des structures en béton armé : application aux structures massives. », Thèse de doctorat, université de Montréal, 2013.
- [10] Abaqus Handout MANE 4240/ CI5L 4240: Introduction to Finite Elements Professor Suvrano Department of Mechanical, Aerospace and Nuclear Engineering/Rensselaer Polytechnic Institute.
- [11] The ABAQUS FAQ/ university Cambridge/ department of engineering.

*C*HAPTER VI:

MODELLING

6.1 Introduction

Finite element models were developed to simulate the structural behaviour of steel beams with web openings. In order to remain faithful to the basic philosophy that a simulation must be validated by comparing the numerical results with those from the experimental tests. These models were calibrated by experimental results from the literature performed by Redwood and Mccutcheon [5].and Juliet Warren [6]. In order to simulate the behaviour of perforated steel beams up to failure. In addition, the literature review showed that only cellular beams articulated at their ends have been the subject of theoretical, numerical and experimental studies. And from it, comparisons were made between experimental and numerical results for the moment-deflection curves for Redwood and Mccutcheon tested beams, and the load-deflection curves for Juliet Warren tested beams. Then we present the results obtained from a series of (number of our models) numerical simulations. (Moreover, more details if we decided to use other shape or stiffened openings etc...)

6.2 modelling properties of tested beams

In order to simulate the structural behaviour of steel beams with circular web openings for both single [4] and multiple openings [5]. A finite element model was established with material non-linearity incorporated into the finite element model which is capable of fully mobilising the moment capacities of the tee-sections under co-existing axial and shear forces due to global action. A bi-linear stress–strain curve was adopted in the material modelling of steel together with the Von-Mises yield criteria. Moreover, with geometric non-linearity incorporated into the finite element model, large deformation in the model may be accurately predicted, allowing load redistribution in the web across the opening after initial yielding. hence, the Vierendeel mechanism with the formation of four plastic hinges in both the tee-sections above and below the web openings may be investigated in detail.

Note that some applications (such as nonlinear finite elements analysis programs) require that the material properties be described in terms of true stress and strains (i.e., calculating stresses using the actual cross-section taking into account the Poisson effect, and strains using the actual length after elongation), rather than engineering stresses and strains (calculated using the initial cross-sectional area and length). These values can be obtained by the following relationships: [1]

- $\sigma_{\text{True}} = (1 + \epsilon_{\text{Engineering}}) \sigma_{\text{Engineering}}$.
- $\epsilon_{\text{True}} = \ln(1 + \epsilon_{\text{Engineering}})$.

In addition, Abaqus requires the use of plastic stress and strain. True plastic strain is defined by the following equation: $\epsilon_{\text{pl}} = \epsilon_{\text{t}} - \epsilon_{\text{te}} = \epsilon_{\text{t}} - \frac{\sigma_{\text{t}}}{E}$

Where ϵ_{te} : true elastic strain. [2]

6.2.1 Beams tested by Redwood and Mccutcheon

The simulated steel beams 2A and 3A with a single opening adopted the values present in Redwood and Mccutcheon experiments. The materials nonlinearity was considered by a bilinear elasto-plastic behaviour with a 205,000 MPa Young's modulus, a 5% strain hardening, and a 0.3 as the poisson's ration value.

Figure 6.1, tables 6.1, and 6.2 shows the characteristics, which is, adopted herein the test specimen with their geometric details and material properties. The loads and supports present in the experimental steel beams were simulated by using restrictions on appropriated nodes in the numerical model. All the modelled beams adopted a simply support configuration.

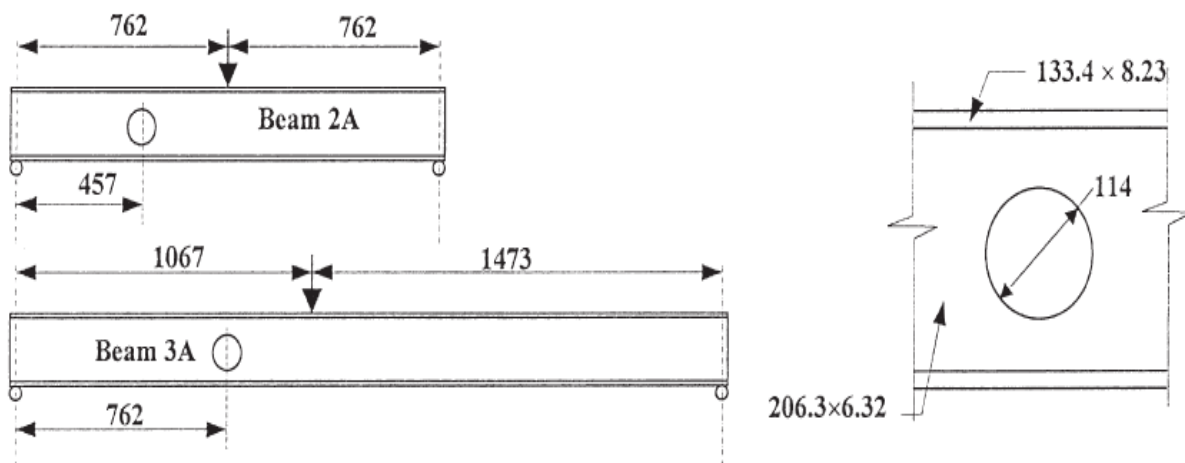


Figure 6.1: Beam models geometry [4]

Table 6.1: steel sections yield and ultimate stresses (m MPa) [4]

Beam	2A		3A	
Property	fy	fu	fy	fu
flange	352	503	311	476
web	376	512	361	492

Table 6.2: steel sections geometrical properties. [4]

Beam	Span (mm)	Flange width(mm)	Flange thickness(mm)	Web height (mm)	Web thickness (mm)
2A	1524	133.4	8.23	206.3	6.32
3A	2540	133.4	8.23	206.3	6.32

6.2.2 Beams tested by warren. J

The beams noted 1A and 3B considered are part of eight cellular beams tested by Warren, at the University of Natal, South Africa. These cellular beams were manufactured from hot-rolled I-beams of the UB 203×133×25 and 305x102x25 I beam. These sizes were chosen, as they are conveniently small sections, and ensured that the capacity of the testing equipment in the laboratory would not be exceeded series. Two loading conditions were chosen viz. midpoint and third point loading. The span of the beams, the distance between centres and the diameter of the openings have been carefully selected to avoid premature collapse due to shear buckling or buckling of the web post. The actual average properties measured from the uniaxial tensile tests on specimens taken from the beams are given in the table below. One lateral support system was implemented to prevent LTB of the beams. Beams 1A were tested in three-point bending. Beam 3B was tested in four-point bending. Each of the two concentrated loads is applied to a distance of 2.9 m from the nearest support. The loads were applied monotonously in stages to ruin by means of a hydraulic

cylinder controlled in force. the three-point bending test equipment as well as the supports are illustrated in figure 6.2.

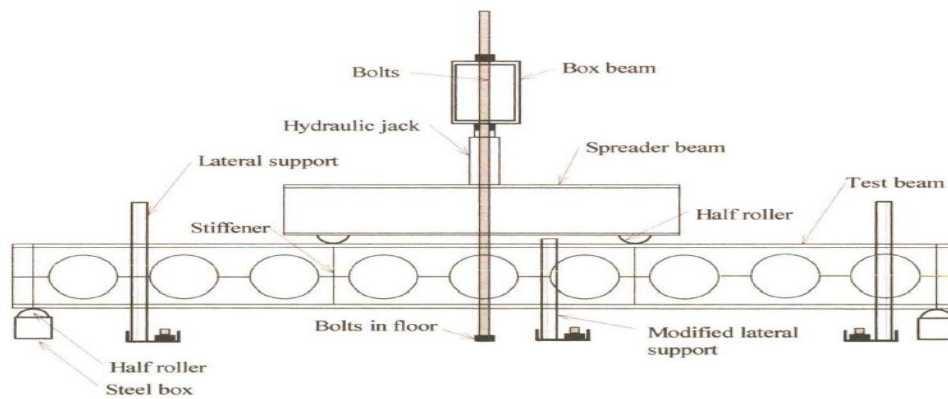


Figure 6.2: Typical test beam setup.[5]

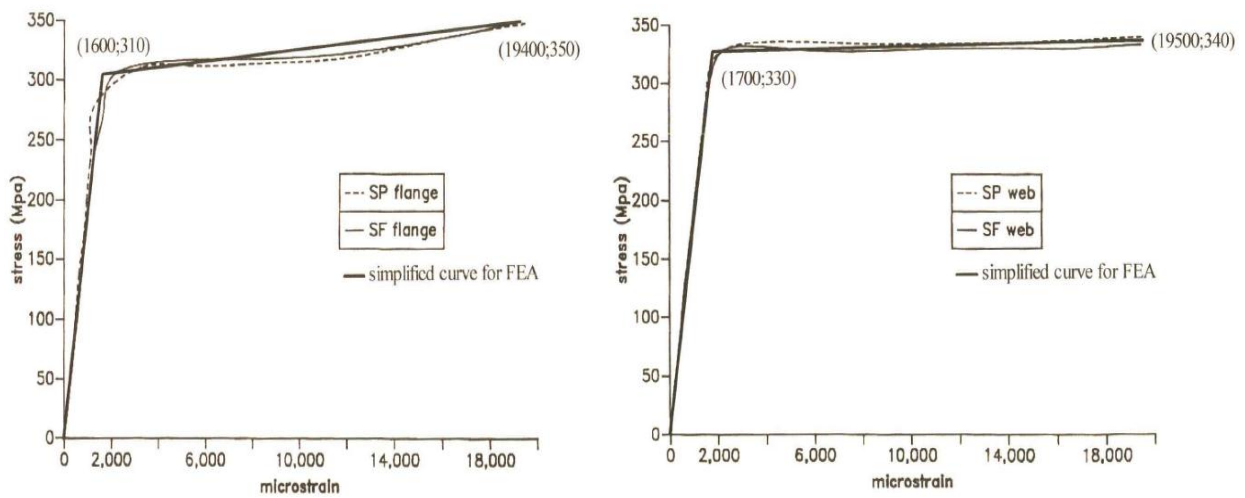


Figure 6.3: Stress vs strain curves used for FEA material properties.

Table 6.3: steel sections yield and ultimate stresses.[5]

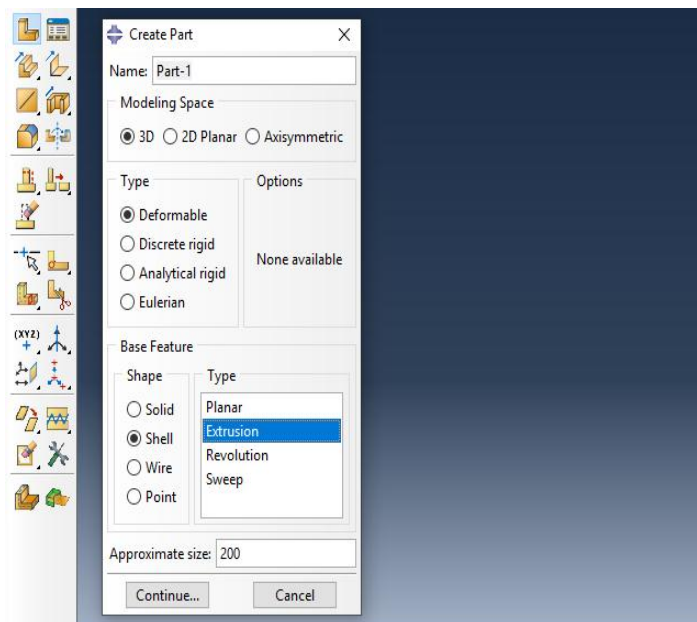
Property	f_y (MPa)	f_u (MPa)	E (GPa)
flange	310	350	200.5
web	330	340	201

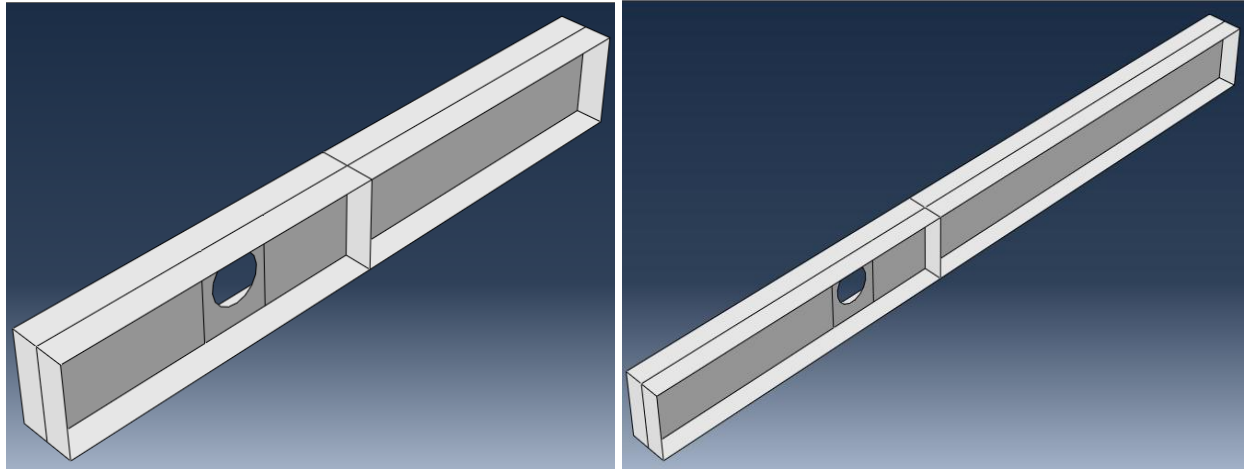
Table 6.4: steel sections geometrical properties in (mm). [5]

Beam	Span	Flange width	Flange thickness	Web height	Web thickness	openings Spacing	Opening diameter
1A	3100	133.4	7.8	289.9	5.8	300	200
3B	4200	101.6	6.8	435	5.8	450	300

6.3 Numerical simulations

The numerical simulations to reproduce the behaviour of the beams observed during the tests, which are part of the experimental programs described above, were carried out using the Finite Elements ABAQUS/Standard software version 6.14. In a large deformation analysis, the effect of geometric nonlinearity can be significant. Use the NLGEOM option with the STEP keyword to take into account the changes in geometry during the analysis. Then the stiffness matrix is calculated using the current configuration i.e. using the current position of the nodes.

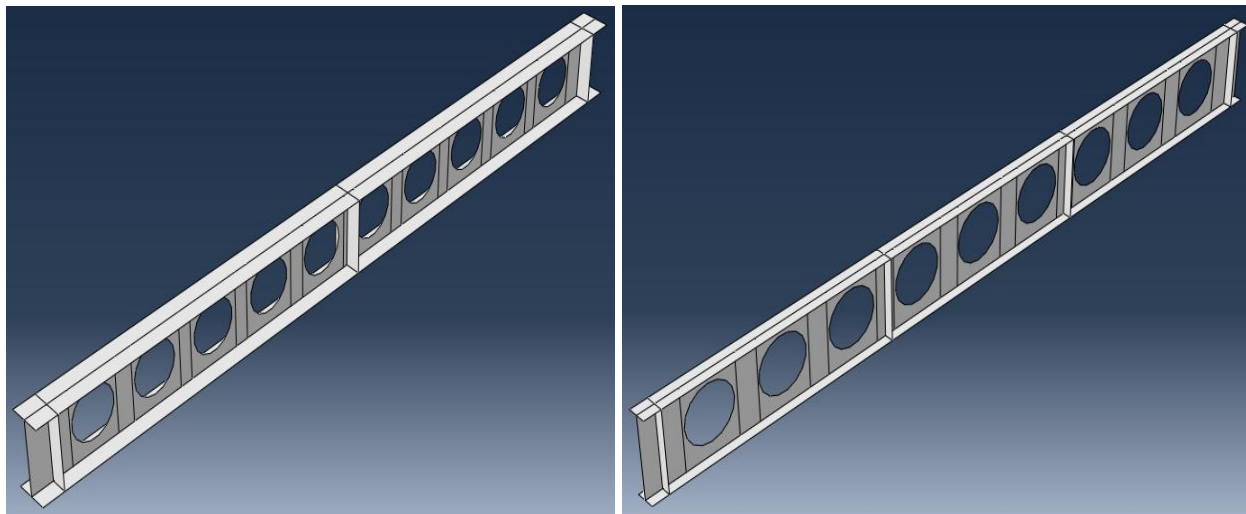
**Figure 6.4:** Creating of a shell element for modelling of beams



(a) Beam 2A

(b) Beam 3A

Figure 6.5: Creating part element for modelled Redwood and Mccutcheon beams [4].



(a) Beam 1A

(b) Beam 3B

Figure 6.6: creating part element for modelled Warren.J beams [5].

6.3.1 The applied loads

With regard to beams tested by Redwood and Mccutcheon [4] the collapse load at each of the load application points where applied at mid-pan for beam 2A ant at a distance for beam3A. For beams tested by warren [5] two loading conditions were chosen, midpoint and third point loading.

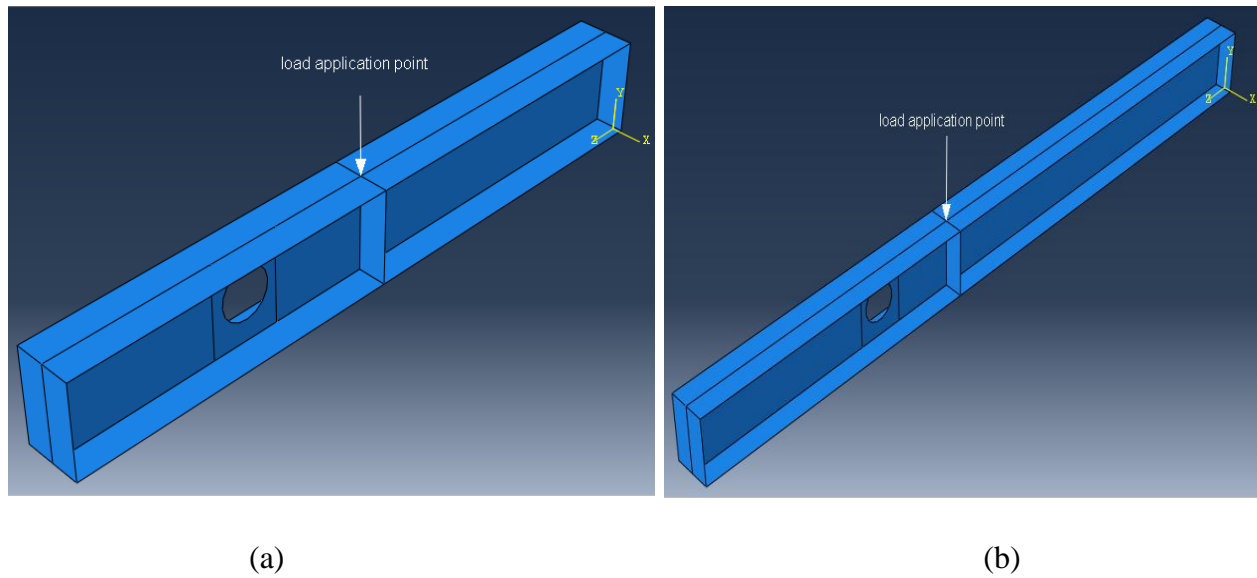


Figure 6.7: Loading position for (a) 2A and (b) 3A beams [4]

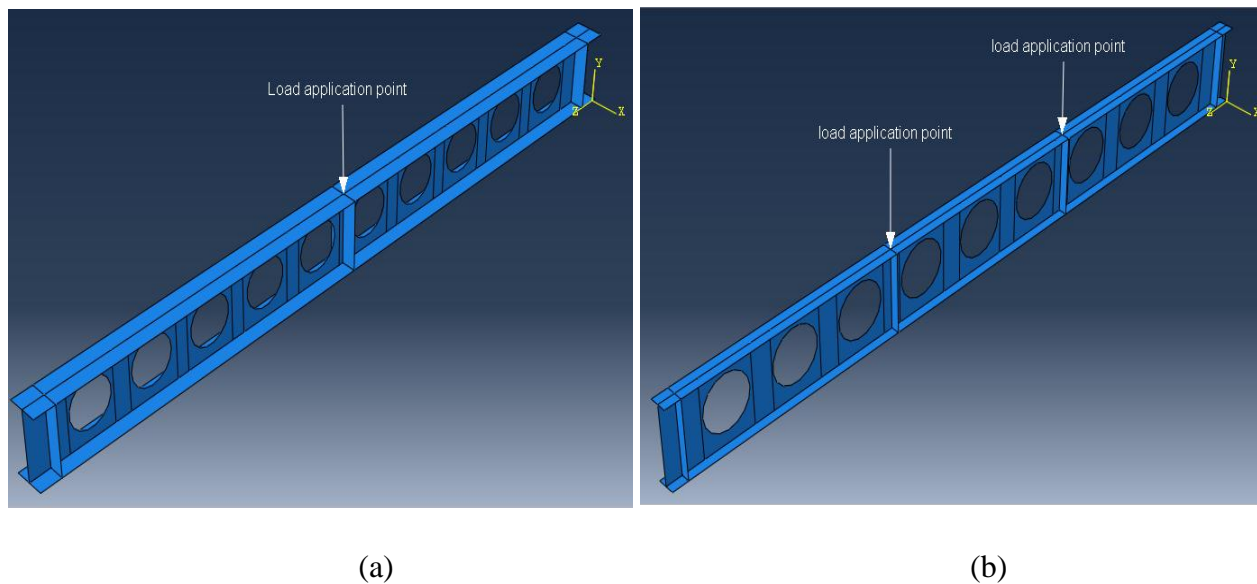


Figure 6.8: Loading position for (a) beam 1A and (b) beam 3B [5]

6.3.2 Boundary conditions

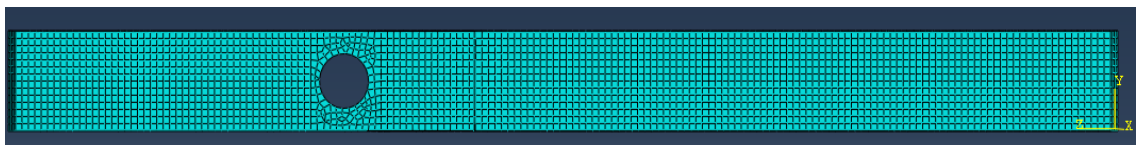
During the numerical investigation, it was necessary to ensure that the model collapse was not associated to lateral torsional buckling or to a local buckling at the load application point or supports. This was made by restricting the lateral displacements of the top flange along the beam span and using transverse stiffeners at the load application point and supports. All the modelled beams adopted a simply support configuration. In order to take into account large displacements

(P- Δ effect), the cinematic description of the elements in the non-linear geometric analysis used in the ABAQUS software is based on the updated Lagrangian formulation. Within each increment, the non-linear equilibrium equations are solved by the full Newton-Raphson approach. The web opening is free from any boundary effect or point load.

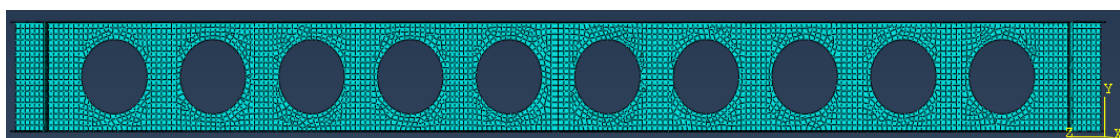
6.3.3 Meshing

Meshing is the way to divide the study subject (beams with web openings) into small particles with the exact same properties (size, type, geometry, etc.) to examine each particle alone[3]. Combining all these small particles give us the mesh. While mesh convergence is one of the most neglected issues affecting the accuracy of finite element models. The degree of stress change is dictated by the degree of change in the load or geometry in the region of interest. In the models, the most interesting areas are the vicinity of the web openings and the actual element size was carefully considered. Hence increasing the number of elements in the model will cause the solution to approach the analytical solution of the equations that govern the response.

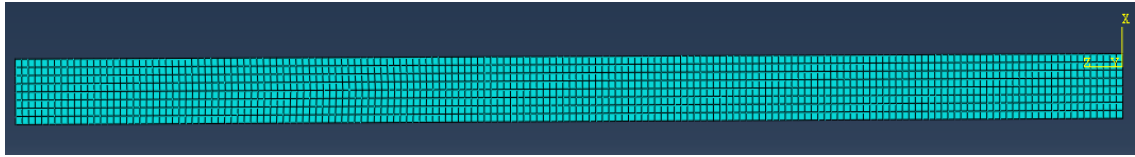
In this study, we have used a quad-dominated, which uses quadrilateral elements, providing six degrees of freedom per node and provides accurate solutions for most relevant applications, and allow some triangular prisms (wedges) in transition regions. Namely S4R (a 4-node doubly curved thin or thick shell, reduced integration, hourglass control, finite membrane strains) with six DOF per node, *i.e.*, translations and rotations on the X, Y, and Z axis, respectively. This special configuration where chosen from the ABAQUS element library due to the facility of applying and retrieving results with the minor errors. With refined mesh configuration in order to avoid discontinuities in stress contours across element boundaries



(a)



(b)



(c)

Figure 6.9: Meshing type example for (a) Redwood and Mccutcheon, (b) Warren.J and (c) flanges mesh generation for both.

6.4 Validation of the results and discussion of the primary studies

6.4.1 Study of single WOB tested by Redwood and Mccutcheon

6.4.1.1 General

As previously mention, and prior to any incursion in a very advanced concept using nonlinear FEA predicting the inelastic behaviour of web-opening structures, some basics applications must be executed and compared with previous work outcomes adopted by other studies in literature are remodelled and analysed to verify the reliability of the assumed numerical model of this study, including mesh and element types as follows presenting for validation of the Finite Element Model. Therefore, finite element models were first developed for Redwood's beams to simulate the inelastic structural behaviour of steel beams with single web openings. In fact, in this study, a three- dimensional nonlinear finite element 3D model is developed using ABAQUS Package version 6.14. Firstly, a discussion of the results of FEA coming up from this study in terms of bending moment-deflection curves as illustrated in Figures 6.10. Then a comparative discussion in terms of deflection vs. bending moment at mid-span section of the outcomes of FEA (ANSYS and others) and experimental results in [redwood] and other comparison of FEA results from literature as depicted in Figures 6.11 and 6.12. Then, these models were calibrated against numerical investigation made by Chung and Flavio.R and against experimental results performed by Redwood and Mccutcheon. It is worth to note that the wholes beams considered in this study have no stiffeners and no reinforcement at all in the vicinity of the opening.

6.4.1.2 Beam 2A and 3A

As well known, during FEA process, any structure must be divided into small and simple elements to assess the individual deformation. There are three types of meshing generations in

ABAQUS, when a shell element was selected; Quad, Quad-dominated and Triangular. It should be mentioned that all three types of mesh provide the same behaviour and value in terms of stress distribution and displacement. Except that the triangular type provides almost twice the number of elements and nodes compared to the other two types. While increasing number of elements at the openings edges which is the high stress area results in a slight difference in stress value. Quad-dominated elements are selected in the modelling of cellular beams, it was found that over, 3371 elements, and 13480 nodes were required to model beam 2A. With 5416 elements and 21660 nodes for beam 3A. Symmetric properties can be used in order to model only a half of the full beam model.

As in previous research works, that is Chung and Flavio.R, used two distinct strain hardening slopes when modelling the Redwood's results, 2% and 5% respectively, the idea has come to introduce in two different models these values to see the effect of strain hardening. In the following, a discussion of results concerns the effect of the slope values of strain hardening used in ABAQUS and a comparison with results available in literature.

It is worth to remind that the two beams having the same section along with it but using actual mechanical values of steel grades similar mechanical properties, along with the same applied load and the same opening geometrical characteristics and position. However, a major difference between the two beams: slenderness ratio, influencing the whole inelastic behaviour, and then this parameter is being the major parameter to be investigated.

Figure 6.10 depicting the linear and nonlinear behaviour of Beam 2A and Beam 3A coming up from the present study of FEA outcomes with the effect of strain hardening different slopes. Figure 6.14(a) is representing the FEA nonlinear behaviour outcomes of Redwood's beam for different values of the slope of the strain hardening, with the value of 2 and 5%, while Figure 6.14(b) concerns Beam 3A.

Broadly speaking, and as far as Beam 2A is concerned, it can be easily been seen in Figure 6.10(a) which has two main branches with a small transient part representing the elasto-plastic behaviour. The first branch of the curve shows a linear relationship between the transverse displacement and bending moment representing the linear elastic behaviour of the beam. No remarkable differences in the slope of plotted curves in values as consequence of changing the value of strain hardening slope. The bending moment increases as the loading rises until a yielding point at an approximate value of 55 KN.m under a deflection of 5 mm, indicating a yielding as the curve begins to have a nonlinear form.

Some differences can be seen and as the beam section is getting more plasticised, the differences become more and more evident, which indicated the impact of strain hardening on the inelastic behaviour of the beam. The nonlinear branch showing a clear nonlinear behaviour of the beam with very small slope and no collapse has been reached according to FEA model under a bending moment of approximately 66 KN.m with a transverse deflection of 19 mm. This nonlinear response of beams is represented by a ratio of 1.20 from first yielding to the final step in FEA model, which does not show any collapse of the beam 2A. Where the two curves have the same shape showing a distinct nonlinear behaviour.

Concerning Beam 3A, typical same remarks can be made as depicted in Figure 6.10(b) Similar remarks can be made for the second modelled beam, i.e. Beam 3A, excepting that the value corresponding to the first yielding becomes 69 KN.m vs. 8 mm. For the last step of FEA, a value 74 KN.m vs. 25 mm. The slope of about 1.07.

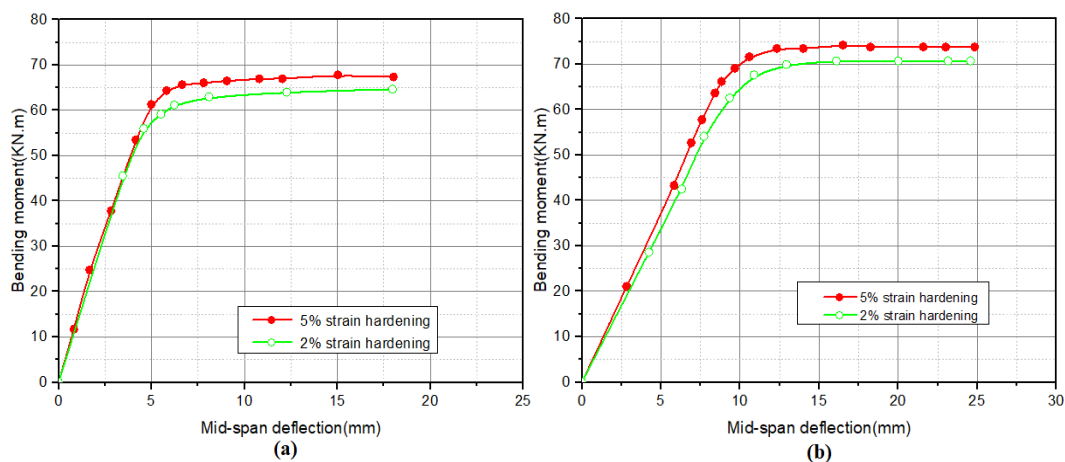


Figure 6.10: Finite element results (a) Beam 2A (b) Beam 3A

Figure 6.11 represents sections of the von Mises stress distribution of beam 2A under failure load. While the upper part of red curve reflects the plasticization in the steel areas. Noting that the level of plasticization varies from one beam to another. In this beam, the plastic areas are located in the region of the concentrated load and the openings edges, with 377.5 and 382.1 MPa stress value for 5% and 2% strain hardening respectively.

As previously highlighted by Chung [1] it is interesting to observe the stress contours representing the stress field of the beam which are plotted in figure 6.16 near the perforated section for beam 2A at the onset of yielding and at the collapse stage for 2% strain hardening slope value. The yielding begins at the web of the “Tees” at sections with $\alpha = 30^\circ$ and $\alpha = -45^\circ$. At the same

time a shear yielding at the web of the “Tees” at sections with $\alpha = 0^\circ$ is also noticeable. However, this yield does not generate a collapse mechanism and the beam is still able to sustain additional loads until the Vierendeel bending is sufficient to cause an extensive yielding on the “Tees”[1].

At failure, both the webs and the flanges of the tee sections at the HMS are extensively yielded. Furthermore, there is also extensive shear yielding in the webs of the tee sections with minimum web depth (i.e. $j = 0^\circ$). However, at the LMS, only the webs of the tee sections are yielded while the stress level of the flanges reaches only 60% of the yield strength. As a result, Beam 2A is failed with the formation of two full plastic hinges at the HMS but with only two partial plastic hinges at the LMS. This is probably due to the fact that at failure, extensive yielding occurs in the tee sections with minimum web depth which reduces the effectiveness of load re-distribution across the web openings.[1]

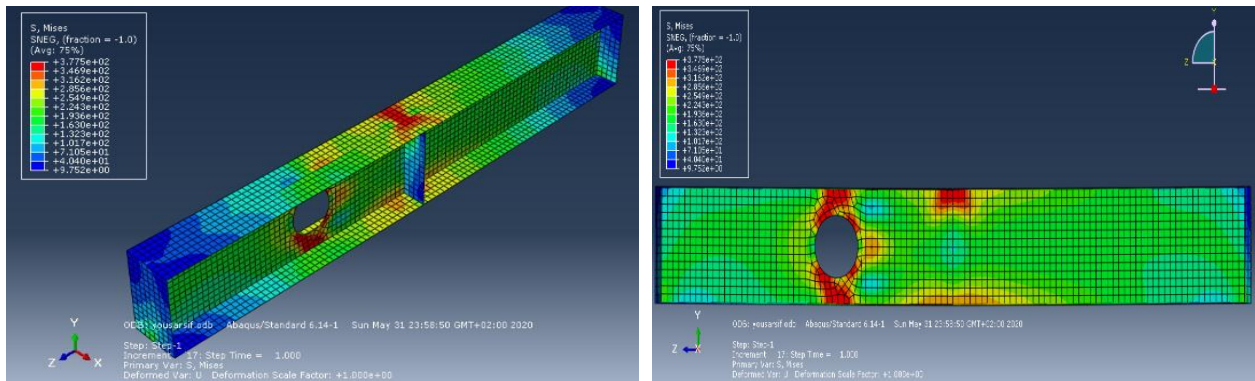


Figure 6.11: Von Mises equivalent stress contour distribution for 5 % strain hardening

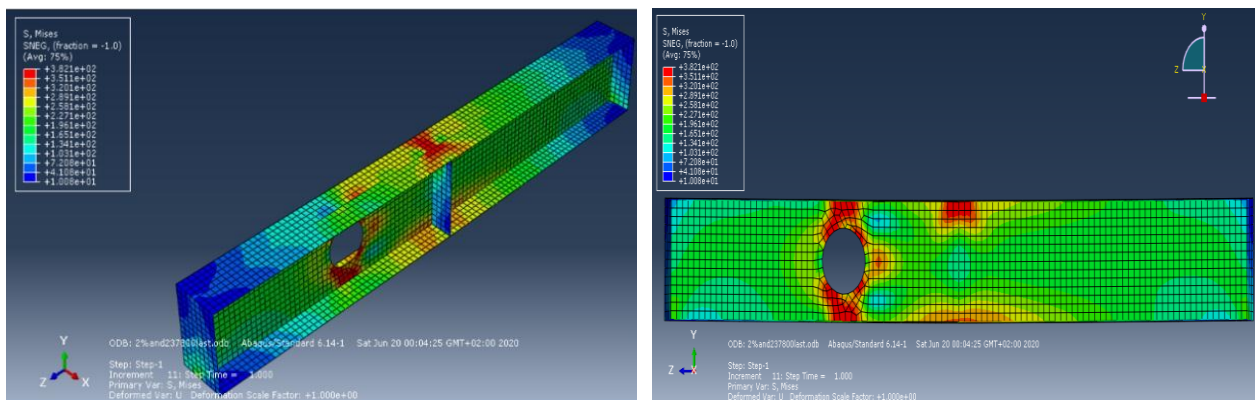


Figure 6.12: Von Mises equivalent stress distribution contour for 2 % strain hardening.

For Beam 3A, the location of the opening, the span of the beam gives rise to a different behaviour and stress distribution from that in Beam 2A. Figure 6.13 shows a high local stress developed at opening edges and the flanges with two full plastic hinges at LMS. The failure was due to the formation of four plastic hinges indicating Vierendeel mechanism. Where it starts to yield later than Beam 2A.

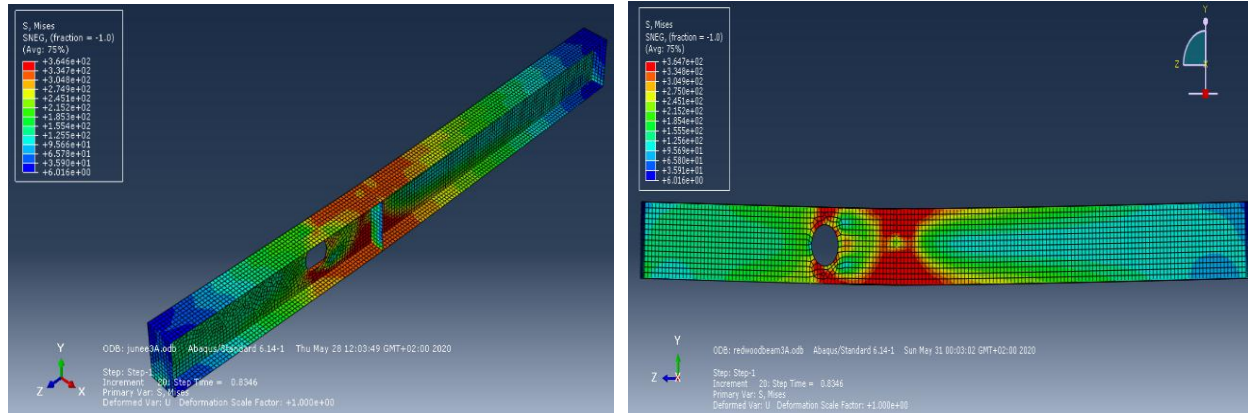


Figure 6.13: Von Mises equivalent stress distribution for 5 % strain hardening.

Calibration of the developed models was also carried out using comparative graphs presents in figure below; containing the experimental results produced by Redwood and McCutcheon test outcomes. Where the curves indicate that there was considerable agreement with the experiments, particularly in the elastic domain. In the plastic range, a small deviation between the numerical and experimental results was observed. For Redwood's, curve where initial yield pattern was observed at 44 KN.m with 4 mm deflection and 50 KN.m with 7 mm deflection for beam 2A and 3A respectively. For the last increment, it was noticed at 63 KN.m vs 21mm deflection with 68 KN.m vs 25mm deflection, for beam 2A and 3A respectively.

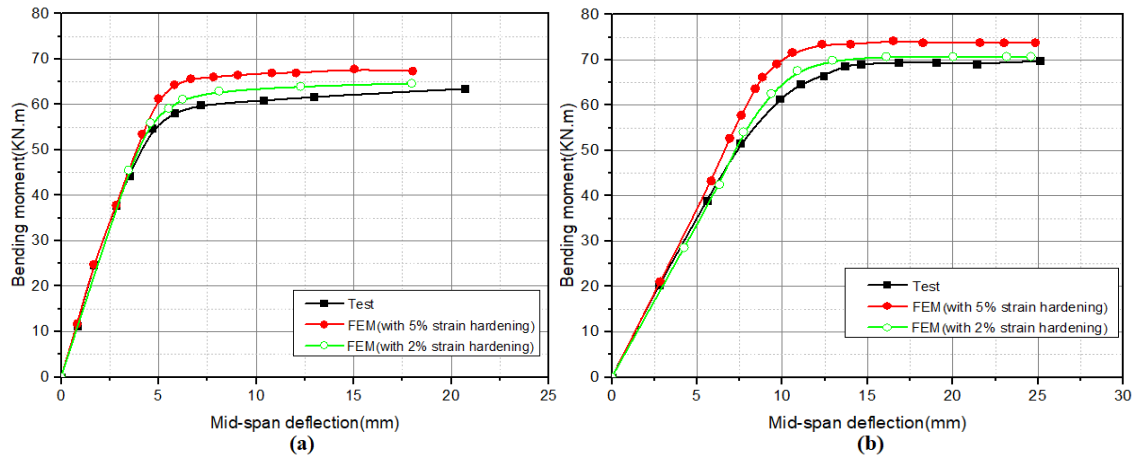


Figure 6.14: Comparison of finite element and experimental model results

(a) beam 2A (b) beam3A

Figure 6.15 show all the comparative graphs with the present study outcomes. Where the cures for both beam 2A and 3A plotted with 5% strain hardening was closer to Flacio.R results. Hence the curves plotted with 2% strain hardening was similar to chung results.

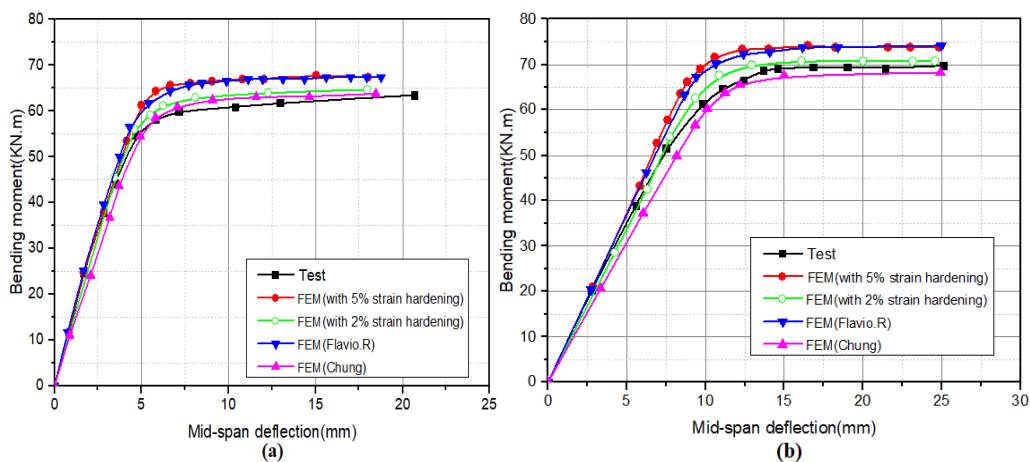
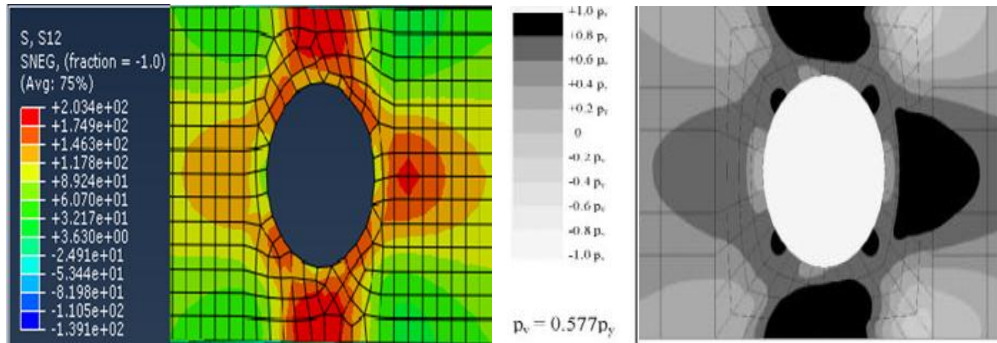


Figure 6.15: Comparison of several finite element and experimental model results

(a) beam 2A (b) beam3A



(a) (b)

Figure 6.17: Shear stress distribution contour in Beam 2A

(a) Present study (b) Chung

LMS	HMS	
		(a)
		(b)
<p>S, Mises SNEG, (fraction = -1.0) (Avg: 75%)</p> <ul style="list-style-type: none"> +3.775e+02 +3.469e+02 +3.162e+02 +2.856e+02 +2.549e+02 +2.243e+02 +1.936e+02 +1.630e+02 +1.323e+02 +1.017e+02 +7.105e+01 +4.040e+01 +9.752e+00 		(c)

Figure 6.16: Von Mises stress distribution contour in Beam 2A

(a) Chung, (b) Flavio.R and (c) present study.

6.4.2 Study of beams tested by Warren.J**6.4.2.1 General**

In this, section a presentation and a general discussion of the results obtained from both an experimental and numerical study of the nonlinear behaviour of steel beams with multiple openings reported by Warren. J. Full-scale destructive tests were carried out for the investigation on eight cellular beams. Failure load, failure mode and deflections were obtained for each beam.

Firstly, a discussion of the FEM outcomes from the present study, then a comparative discussion in terms of deflection vs load at mid-span section of the Test results and a FEM plotted with LUSAS software. For the modelled beams namely 1A and 3B, where loaded at mid-span and at the third points respectively it should be stated that all web openings are concentric to the mid-height of the sections and symmetric about the mid span of the beam. Whereas the openings have no stiffeners. A quad-dominated mesh of elements was selected. Where give a number of about 7108 and 10676 elements for beam 1A and 3B respectively. The mesh was coarser, i.e., larger elements towards the end of the beam and more refined near the centre where the stresses are higher and where failure finally occurs.

6.4.2.2 Beam 1A

As reported by Warren.J for beam 1A, test loading was in increments of 11,4 kN up to 80,1 kN then in increments of 5,7 kN to failure. Buckling of the flange above the centre opening was observed at a load of 114 kN, and at a load of 119,5 kN the beam continued to deflect under a constant load. This load was taken as the failure load. The failure was fully plastic Vierendeel failure in one of the openings adjacent to the load. (Figures 2.9 and 2.10) The beam moved horizontally between the lateral supports by 2,15 mm. A horizontal movement of 2.62 mm at the unsupported end was observed after which the horizontal movement stopped. This indicated that settlement was taking place rather than buckling.

As presented in Figure 6.18 the linear and nonlinear behaviour of Beam 1A coming up from the present FEA results where the elasto-plastic behavior was noticed. At the value of 110 KN corresponding to about 7.5 mm deflection indicating that the curve begins to have a nonlinear

form. A straight branch pointed out that the beam continues to deflect under a constant load where takes the value of 130 KN with about 14 mm transverse deflection. This nonlinear response is represented by a ratio of 1.18 from first yielding to the final step in FEA model, which does not occur any collapse of the beam 1A. So as reported by Warren the failure loads predicted by the FEA method are all significantly greater than the experimental values. It was noted in the FEA models that large plastic deflections occurred before the beam failed, whereas only small plastic deformations were observed in the experimental beams at failure. This may be attributed to the fact that, in experimental work, mechanical properties are not to be put, it utilises the actual data, whereas in a theoretical modelling, values, i.e. yielding and ultimate stresses, strain hardening etc., must be introduced and then the outcomes will be in terms of these latter values.

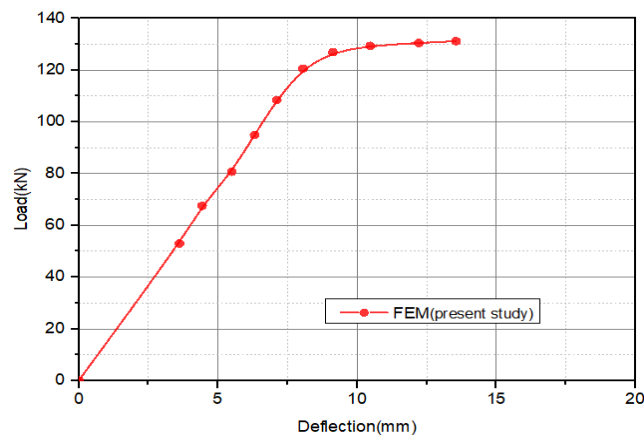


Figure 6.18: Beam 1A finite element model results.

The comparison of the ABAQUS simulation results for model 1A with the laboratory test in figure 6.19(a), carried out by Warren.J showed that the load-displacement curves were similar, with a slight agreement at the elastic range. However, in the plastic range, a noticeable deviation between the numerical and experimental results was observed as natural consequence of the input data which may not be very accurate. As reported by Warren, the relationship between stress and strain is assumed to be linear and dependent on Young's modulus. When the strains become plastic, this no longer true and an increase in the rate of change of stress is indicated.

Figure 6.19(b) show a direct comparison of the present results with Warren.J, FEM outcomes plotted with LUSAS software. The initial linear elastic analysis gave a good indication of the load at which the beam was likely to yield. So the findings indicate a good agreement

between both Warren.J and present study graphs, specifically at the elastic domain. For Warren.J graph and in the plastic domain where the beam start to yield exactly at the same value of the present results but with a maximum deflection equal to 15.2 mm. The fact of the difference between the outcomes may be attributed to the boundry condition and the load appling method.

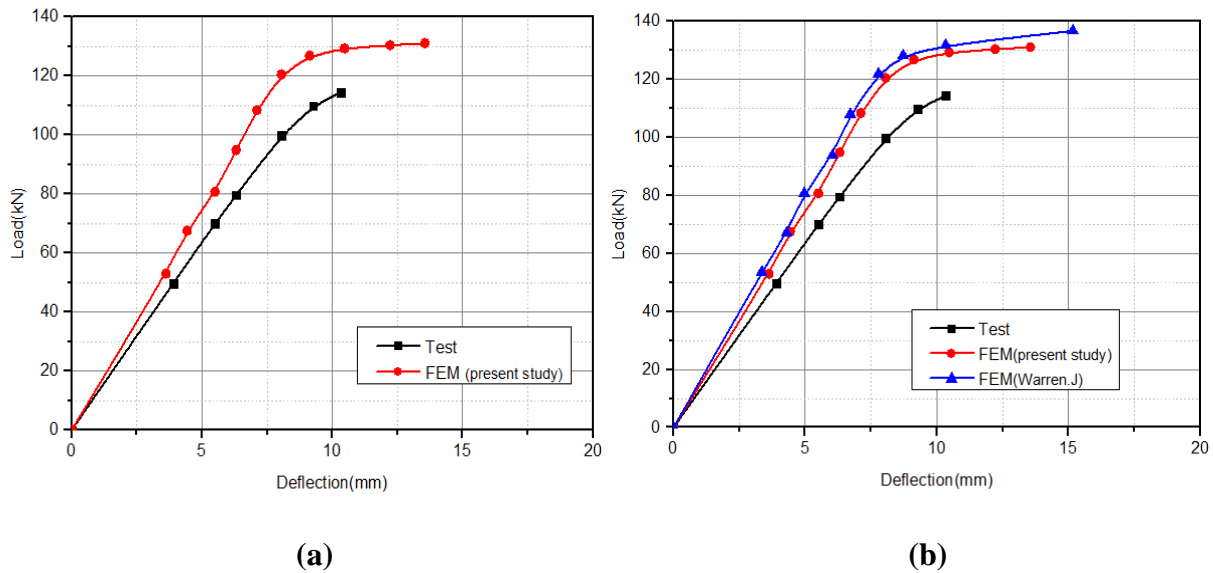


Figure 6.19: Beam 1A finite element and experimental model results comparison.

Figure 6.20 Present Von Mises stress distribution. While the red region reflect the plasticization steel areas. Noting that the level of plasticization varies from one opening to another. As shown in the figures below and with maximum value of 335 MPa, the higher stress where located at the load application point and at the centre openings near the load. With the formation of two full plastic hinges at the LMS, with only two partial plastic hinges at the HMS. Moreover, it continues to decrease until it reaches the farthest opening. For these reasons the failure mode where associated to Vierendeel deflections across the openings.

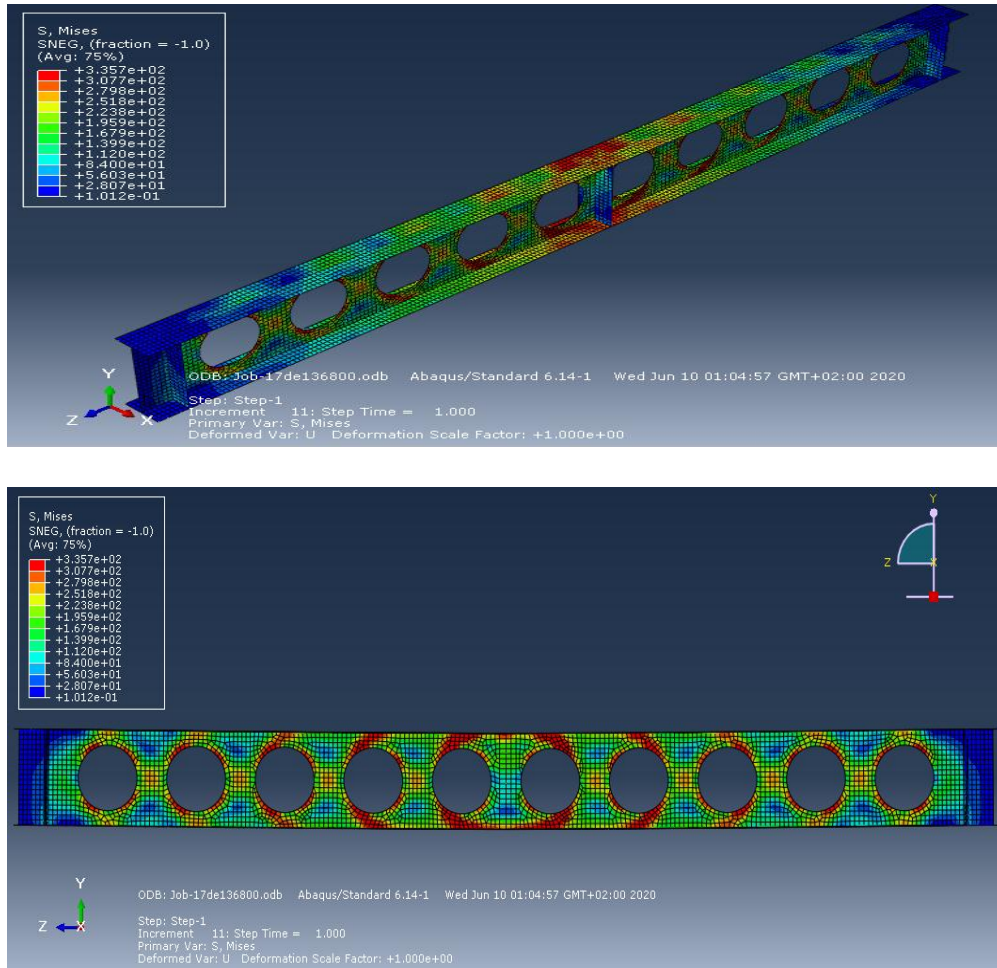


Figure 6.20: Von mises stress distribution contour at last stage

6.4.2.3 Beam 3B

As reported by Warren and during the two preliminary tests no excessive lateral displacements were measured. The beam was loaded in increments of 11,4 kN. The rate of lateral displacement increased in the centre and at the ends of the beam, and at a load of 151 KN, the test was halted. The beam recovered when the load was removed. An extra lateral support was added to each end of the beam and the test procedure repeated. The beam deflected laterally throughout the test and at a load of 174 kN a large lateral displacement was noted and the test was halted. The beam made only a partial recovery with unloading and a 5 mm lateral distortion remained. Two additional lateral supports were used in the final test. The beam was inverted so that the buckled compression flange became the tension flange. The lateral supports in the middle section of the beam were to one side of the centre so the beam was rotated horizontally to give lateral support to

the buckled section. No gap was left between the lateral support uprights and the flange of the beam at the beginning of the test. At a load of 140 kN the beam began to buckle in an S shape between the supports. It was decided to continue the test and at a load of 193 kN the beam continued to buckle laterally at a constant load. Failure was deemed to have taken place.

Figure 6. Introduce load-deflection curve coming up from FEM results. the linear and nonlinear behaviour of Beam 3B is shown, where the elasto-plastic behavior was noticed. At the value of 175KN corresponding to about 15 mm deflection indicating that the curve begins to have a nonlinear form. A straight branch pointed out that the beam continues to deflect under a constant load where takes the value of 195KN with about 30 mm transverse deflection. This nonlinear response is represented by a ratio of 1.11 from first yielding to the final step in FEA model, which does not occur any collapse of the beam 3B.

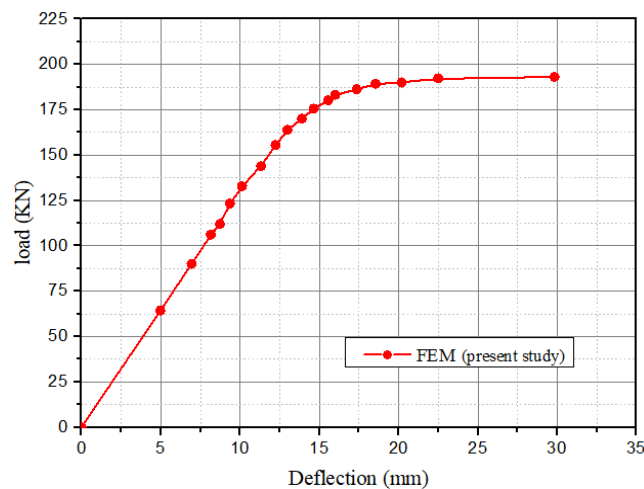


Figure 6.21: Beam 3B finite element model results.

Comparison of FEA and experimental work undertaken by Warren is shown in Figure 6.22(a), as presented the agreement at the elastic range. Where the indication of first yielding was also at the load of 175KN and 15 mm transverse deflection.

Figure 6.22(b) show a direct comparison of the present results with Warren.J, FEM outcomes plotted with LUSAS software. The two graphs were comparable. The initial linear elastic analysis gave a good indication of the load at which the beam was likely to yield. So the findings indicate a good agreement between both Warren.J and present study graphs, specifically at the elastic domain. For Warren.J graph and in the plastic domain where the beam start to yield exactly at the

value of 180KN with about 18mm deflection. Until the beam reach the value of 206 KN where it continue to deflect under constant load.

Von Mises stress distribution countour is illustrated in the figure below. With maximum value of 347 MPa, where the height stress area located at the two load application points and the circular opening edges. According to the difference of the load application method, a completely different behaviour from that in the beam 1A was clearly noticed, specifically for the openings located between the two point load where the bending moment equal to zero.

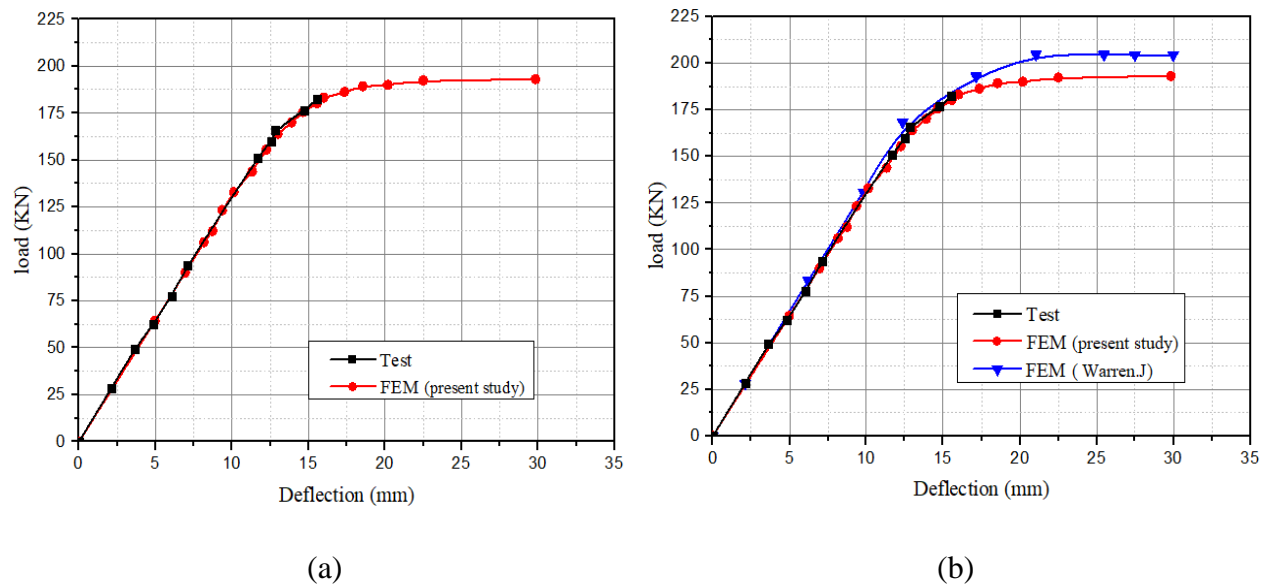
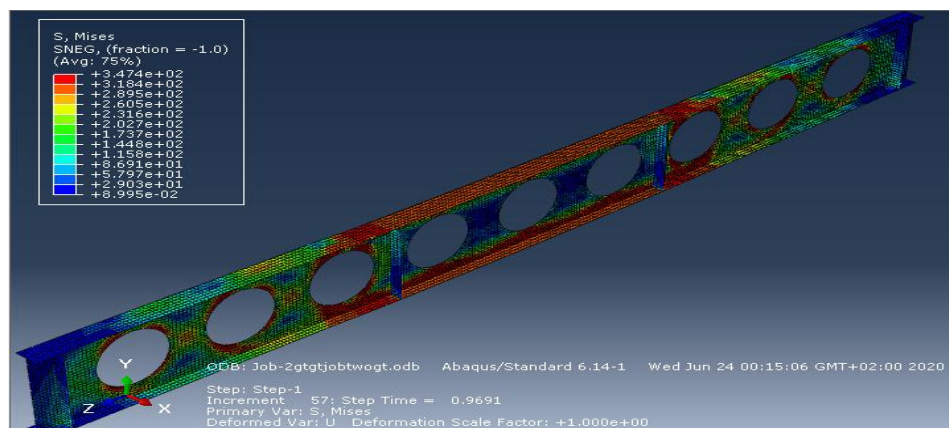


Figure 6.22: Comparison of finite element and experimental model results for Beam 3B



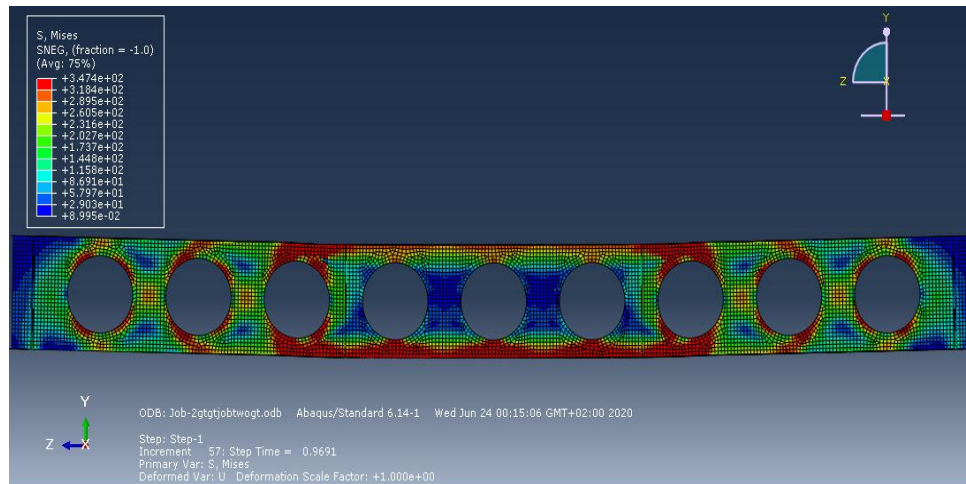


Figure 6.23: Von Mises stress distribution contour for beam 3B

6.4.3 Summary of the obtained results

Despite the fact that details on the experimental works were missing, especially concerning the experiments setup and the real mechanical properties of the steel used, and the boundary conditions, the modelling beams associated to Redwood and Mccutcheon data with single web openings, has shown that the obtained failure mode where associated to Vierendeel bending with the formation of four plastic hinges at the opening edges, which is a local mode. These obtained results agree with what was already presented and discussed in Chapter 2.

The same general remarks can be made for the modelling beams with with multiple web openings associated with Warren tested beams data are showing a good agreement for what have been also mentioned in chapter 2, the failure mode observed was associated to the formation of four plastic hinges indicating the presence of Vierendeel bending. This mode of failure may occur near high or very high openings. close to each other, mainly through shear force. Each Tee is subjected to a shear combination which has the effect of reducing their axial capacity and moment resistant. Additional failure modes should be also considered as they relate to web post buckling between two adjacent openings. And the top flange buckle locally under points loads. It is also clear that the failure by buckling of the web posts does not exclude the appearance of plastic areas. The formation of plastic zones is probably closely related to the mechanical slenderness of the beam sides as well as to the shape and dimensions of the web openings.

As a concluding main remark from the study undertaken in this part of the research program in this master dissertation, one can say that the results of the models proposed are in good agreement with the published results, which encourage to carry on a parametric study taking into account the keys parameters influencing the nonlinear behaviour of WOB, such as the shape of opening, their diameters and position etc. This parametric analysis will be fully presented and discussed in the forthcoming chapter intiled, Chapter VII: NUMERICAL PARAMETRIC ANALYSIS OF KEY PARAMETERS ON THE NONLINEAR BEHAVIOURS OF WOB.

Bibliography

[1] **ABICHOU. H.**, "Simulation de l'emboutissage à froid par une Méthode asymptotique Numérique.", Thèse de doctorat, université de Metz, 2001.

[2] **Craveur. J.C.**, "Modélisation des éléments finis : Cours et exercices corrigés." , Livre, 3ème édition, DUNOD, 2008.

[3] **ROBERT. F.**, "contribution à l'analyse non linéaire géométrique et matérielle des ossatures spatiales en génie civil : application aux ouvrages d'art.", Thèse de doctorat, institut national de sciences appliquées de Lyon, 1999.

[4] **Redwood, R.G. and Mccutcheon, J.O.** (1968) Beam Tests with Unreinforced Web Openings. Journal of the Structural Division, **94**, 1-17.

[5] **Warren, J.**, "Ultimate load and deflection behaviour of cellular beams", MSc thesis, School of Civil Engineering, University of Natal, Durban, South Africa, 2001.

C ***HAPTER VII***

***ANALYSIS OF KEY PARAMETERS ON THE
NONLINEAR BEHAVIOURS OF WOB's.***

7.1 General and scope

In the previous chapter, details were given on some studied cases dealing with the effect on the behaviour of beams with the presence of single and multiple circular openings in steel structures.

In fact, a validation was made for two experimental data tested by Redwood and Mccutcheon, Warren.J respectively and finite elements analysis outcomes by ABAQUS. The results show a good agreement throughout several plots depicted in different graphs where the results were compared to experimental and numerical results from literature.

Because of the success of the first part of this study, it has been decided to carry out a comprehensive study dealing with several parameters thought to highly influenced the carrying capacity of beams with web-openings. Indeed, a parametric study was then conducted to investigate the influence of geometrical parameters (shape of opening, height of opening etc) on the load carrying capacity and the failure mode mechanism. Highlighting the influence of opening height with different shapes and presence of different stiffeners configurations.

Furthermore, in this work the study is then extended to cover the behaviour of four portal frames, with different boundary conditions., an attempt has also been made to better understanding the elastic and inelastic behaviour of web opening structure WOS in a one bay single portal storey frame through four models. Furthermore, the investigation examines whether the failure mode of the whole structure is similar as per Eurocode3. The portal frames the beams and columns have similar geometrical properties provided in Table 7.4 with different boundary conditions.

In this section, presentation of the results obtained from a series of 16 numerical simulations carried out isolated beams having WOB's. Table 7.3 identifies the investigated parameters.

The use of steel grade 355 as per EC3 and the hot-rolled section IPE 450 steel profile as detailed in table 7.1 and 7.2 where selected in all the modelled beams having 6 m of length, which is a reference length in steel structure.

7.2 Parametric study and modelling of isolated beam

7.2.1 Properties of modelled beams

Analysis of key parameters on the nonlinear behaviours of WOB's.

Table 7.1: Profile geometrical details

profile	Flange width(mm)	Flange thickness(mm)	Web height (mm)	Web thickness(mm)	Steel grade
IPE450	190	14.6	450	9.4	S355

Table 7.2: Perforated profile details

profile	Flange width(mm)	Flange thickness(mm)	Web height (mm)	Web thickness(mm)	Steel grade
IPE450	190	14.6	672	9.4	S355

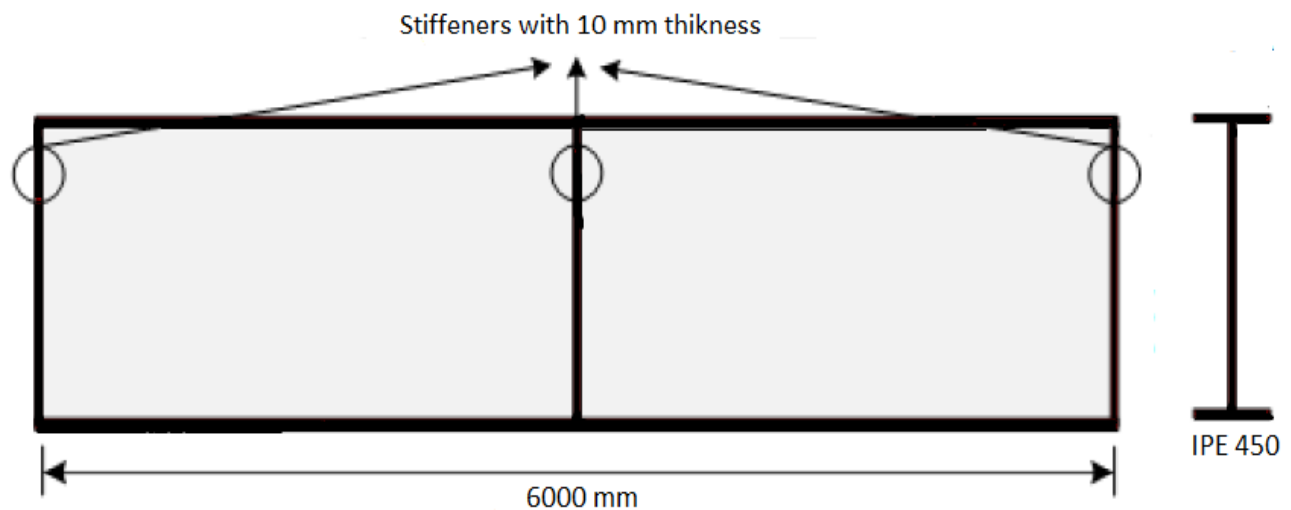
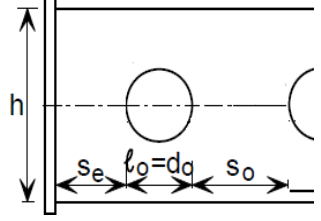
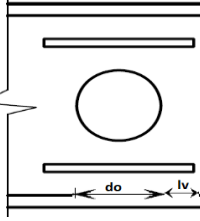
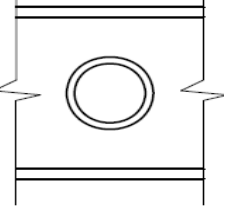
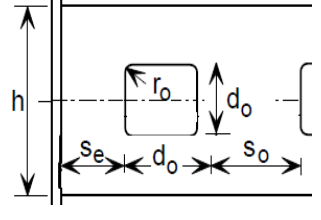
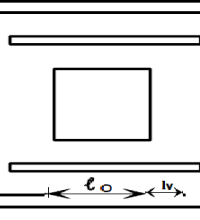
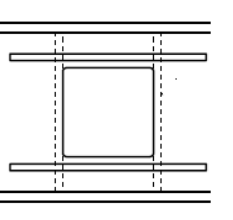
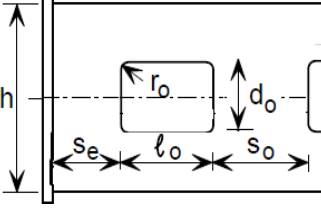
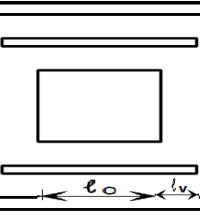
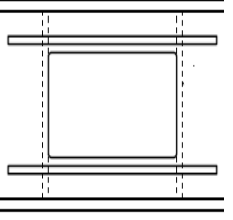
**Figure7.1:** Plain web beam with global geometrical characteristics

Table 7.3: parametric modelling variables

openings details	Unstiffened Configuration 1	Unstiffened Configuration 2	Stiffened opening Configuration3	Stiffened opening Configuration 4
	<p>- IPE450</p> <p>-h = 642 mm</p> <p>-do = 0.7 h</p> <p>- Se ≥ do</p>	<p>- IPE450</p> <p>-h = 642 mm</p> <p>-do = 0.5 h</p> <p>-Se ≥ do</p>		
	<p>- IPE450</p> <p>-h = 642 mm</p> <p>-do = 0.7 h</p> <p>-Se ≥ do</p> <p>-ro = 15 mm</p>	<p>- IPE450</p> <p>-h = 642 mm</p> <p>-do = 0.5 h</p> <p>-Se ≥ do</p>		
	<p>- IPE450</p> <p>-h = 642 mm</p> <p>-do = 0.7 h</p> <p>-lo ≤ 2do</p> <p>-Se ≥ lo</p> <p>-ro = 15 mm</p>	<p>- IPE450</p> <p>-h = 642 mm</p> <p>-do = 0.5 h</p> <p>-lo ≤ 2do</p> <p>-Se ≥ lo</p>		

7.2.2 Cases studied model geometrical features

- Cases 1 and 2 (Figures 7.2)

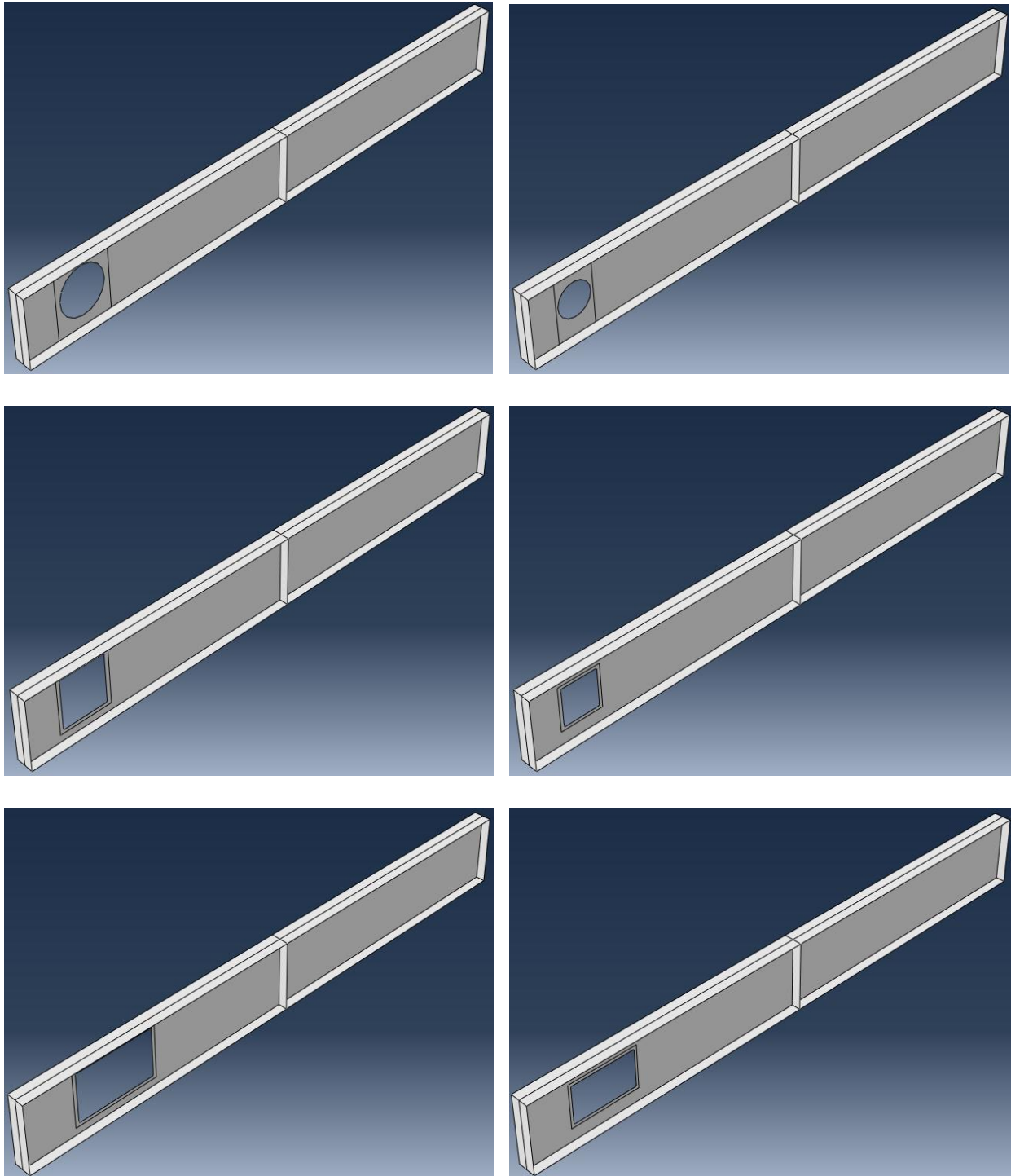


Figure 7.2: Basic geometry models layout without reinforcements cases 1 and 2

- **Cases3 and 4 (Figure 7.3)**

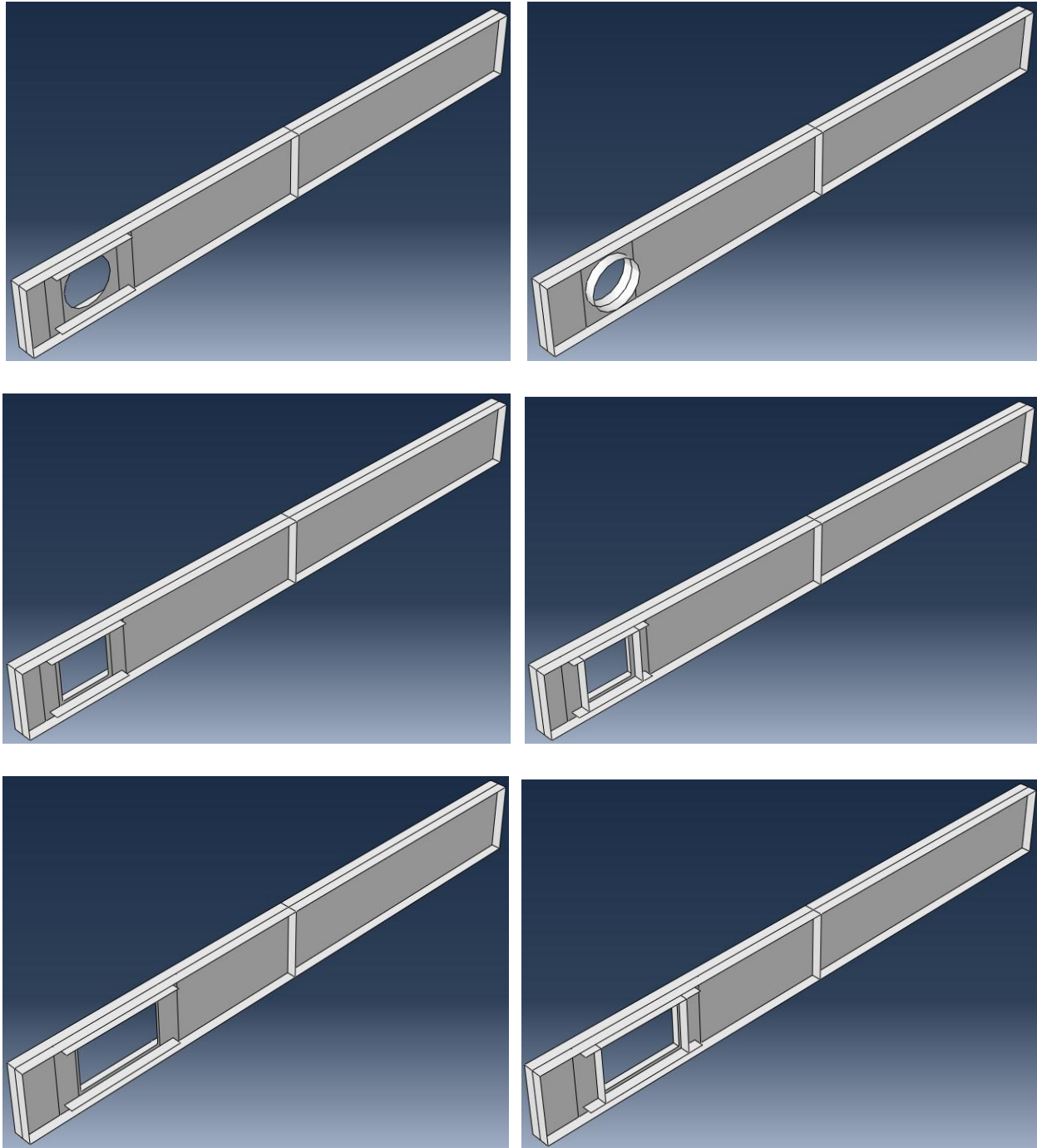


Figure 7.3: Basic geometry models layout without reinforcements cases 3 and 4

7.2.3 Boundary conditions and meshing for isolated beams

For the modelled beams are assumed to simply supported with a restriction of the top flanges to ensure that the failure mode of the structures will not be associated to lateral buckling that is lateral torsional buckling (LTB) or to a local buckling (LB) at the load application point or supports. In addition, the openings are free from any boundary restrictions.

Four noded shell elements were selected for the simulations with a Quad-dominated meshing type where more details are in section 6.3.3. The mesh was coarser, i.e., larger quadrilateral elements towards the end of the beam and more refined triangles near the centre where the stresses are higher and where failure finally occurs.

7.2.4 Results and discussion of isolated beam cases

As the chapter is devoted to a parametric study of parameters that been thought to influence the linear and nonlinear behaviours of beams with web-openings as series of nonlinear models have been built-up in ABAQUS. The overall results are being presented as plots of Displacements vs. Loads. In all plots, two distinct branches can be seen. The first branch is describing the linear behaviour, while the second one is relating to the nonlinear behaviour. An inspection of the results presented in figure below indicate that opening geometry significantly influences the steel beams behaviour and load carrying capacity.

- Case 1

For the case of beam made from IPE450 hot-rolled section, characterised by six-meter span and a web opening of 0.7 h, the load-deflection curves are plotted.

The first parameter investigated is being the height of the opening, i.e. beams having an openings height about to 0.7 h with different geometrical shapes. As clearly remarkable from Figure 7.4, nonlinear performance can be clearly observed. Also, can be seen from Figure 7.4 that comparable ultimate loads were reached despite the form circular or square opening for beam with, being close to the ultimate load of beams without openings. Figure 7.5 shows that curves associated to beam without and with circular opening start to yield at load of 480 KN with about 20 mm transverse deflection and it continue to deflect under constant load. For beam with square opening where it presents a slightly different with 97% load carrying capacity. The plot indicates where the first yielding occurs at 460 KN corresponds to about 35 mm deflection. While the beam with rectangular opening shows weaker behaviour presents a relatively smaller ultimate loads, as its ultimate load has a value about 50% of that of the others beams, this has been stated similarly

(Flavio.2011). This represents a significant reduction on its load carrying capacity. At a load of 198 KN a nonlinear branch of the curve begins corresponding to 10 mm deflection and finishes at 88 mm.

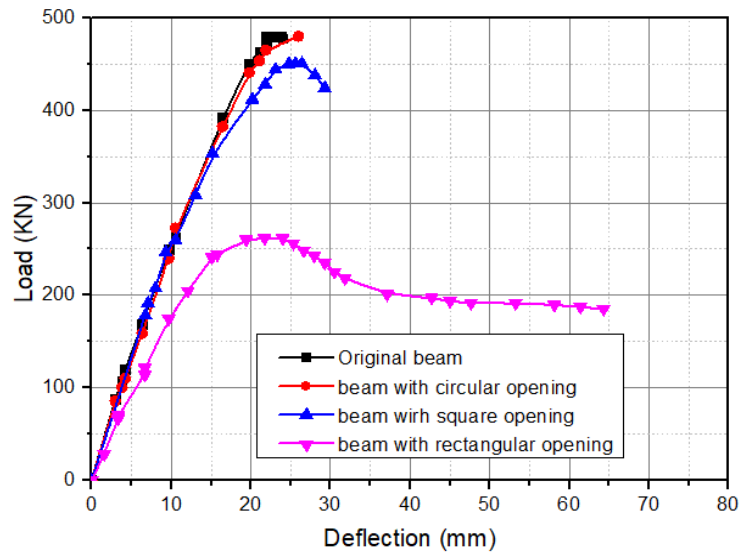


Figure7.4: Load-deflection curves for case1

Nonlinear finite element analysis using ABAQUS results provide also stresses contours, and deformed shape of specimens. These contours will be presented and discussed in the following respectively. In fact, there are two yield failure criteria implanted in Abaqus, namely: the maximum shear stress criterion (Tresca), states that the material failed when the shearing stress on the component has reached the yield shear strength of the material, which is derived from the tensile test of the material specimen. and the maximum distortion energy criterion (Von Mises), generally accepted world-wide in steel constructions design codes.

Accordingly, Von Mises stress distribution where obtained for circular, square and rectangular opening. As shown in figure 7.5 for circular, square and rectangular openings respectively, and despite the adopted corner concordance radius, stress concentration location is formed at the corner of the openings of beams with square and rectangular geometries. Stresses where distributed across the holes of the corners and deflection of the beam increases. Also, Vierendeel collapse mechanism was observed in all the beams with the formation of four plastic hinges at the opening's edges. This is easily explained by the fact that the formation of the Vierendeel mechanism is directly associated with the shear

force at the opening, i.e. the increase in the shear force magnitude at the opening reduces the collapse load of the beam.

It can be concluded that the beams with circular openings presenting higher ultimate loads than the other investigated opening geometries. As mentioned above, the use of an appropriate radius of concordance in the region of the edge of the beam web aperture is extremely important for square and rectangular aperture beams, as it reduces stress concentration.

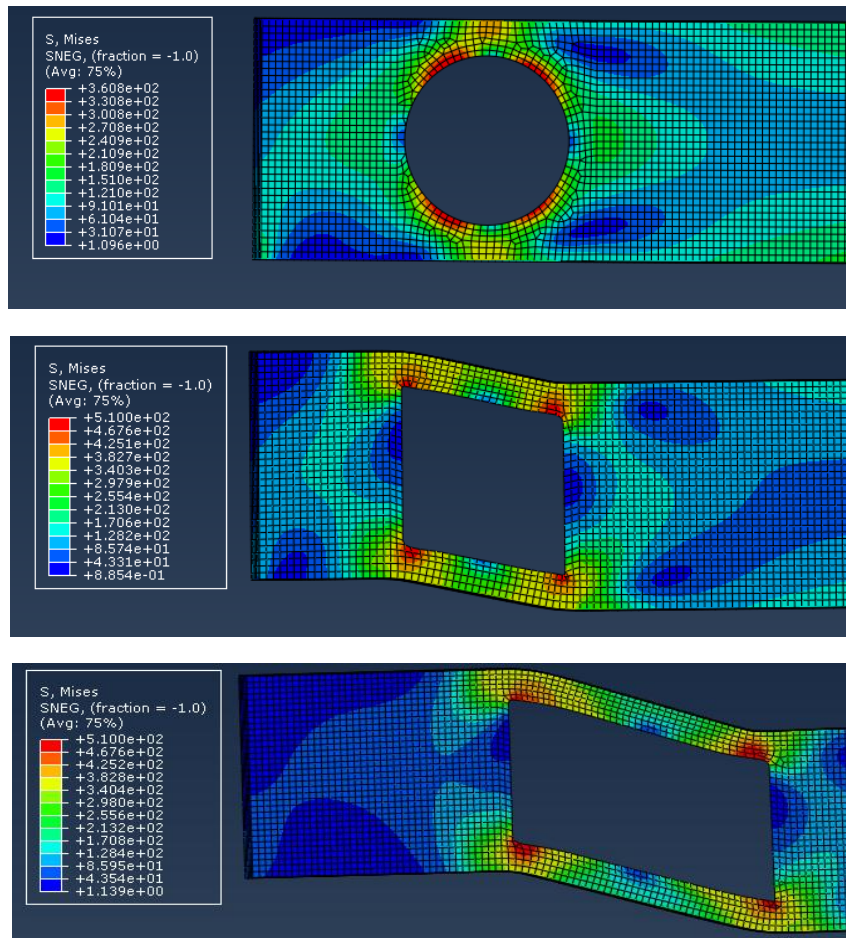


Figure 7.5: Von Mises combined stress distribution contour for case 1

- Case 2

The effect of reducing the opening height from 0.7 H to 0.5 H was the second parameter investigated. The load deflection curves were presented in Figure 7.6.

Broadly speaking, Figure 7.6 shows relatively same curves for the three studied cases. As can be noticed from Figure 7.6 that for circular opening the first yielding starts at 480 KN with a corresponding transverse deflection about 13. For beam with square opening shows alike behaviour of that of the circular opening the plot indicates that the first yielding occurs at 480 KN when the transverse deflection reaches the magnitude of 15 mm. Rectangular opening also reaches the ultimate load but with the maximum deflection being equal to 18 mm. With using an opening height of 0.5 H, similar ultimate loads were reached for all beam regardless the shape of the opening, that is circular, square and rectangular opening. Compared to case 1, the rectangular opening presents roughly the same global behaviour as others.

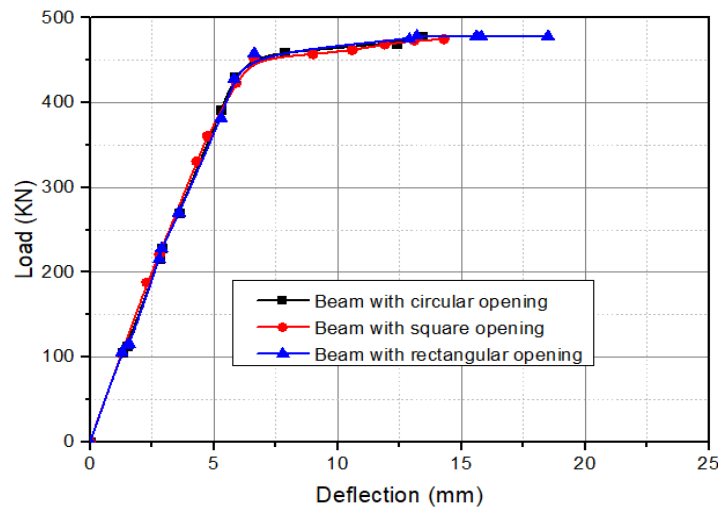


Figure 7.6: Load-deflection curves associated to case 2.

As far as combined stresses are concerned, Figure 7.7 illustrates the ultimate distribution of Von Mises criteria. By the variation of openings height to 0.5 H, different behaviours were observed from that discussed in case 1. It is worth to recall that less stress concentration zone, with reduced values of equivalent stress of Von Mises for the case of circular opening have been noticed, showing clearly the effect of the height of the opening. Unlike circular opening for which no clear plastic pattern was formed and stresses being less than the yield value. Square and rectangular opening are showing similar plastic pattern. That is to say that for both situations, the plasticisation areas indicate the that four plastic hinges formed at the corners showing therefore the occurrence

of Vierendeel bending. It is interesting to mention that these plastic hinges are more significant for the case of rectangular opening and the plastic area is more spread for the latter case.

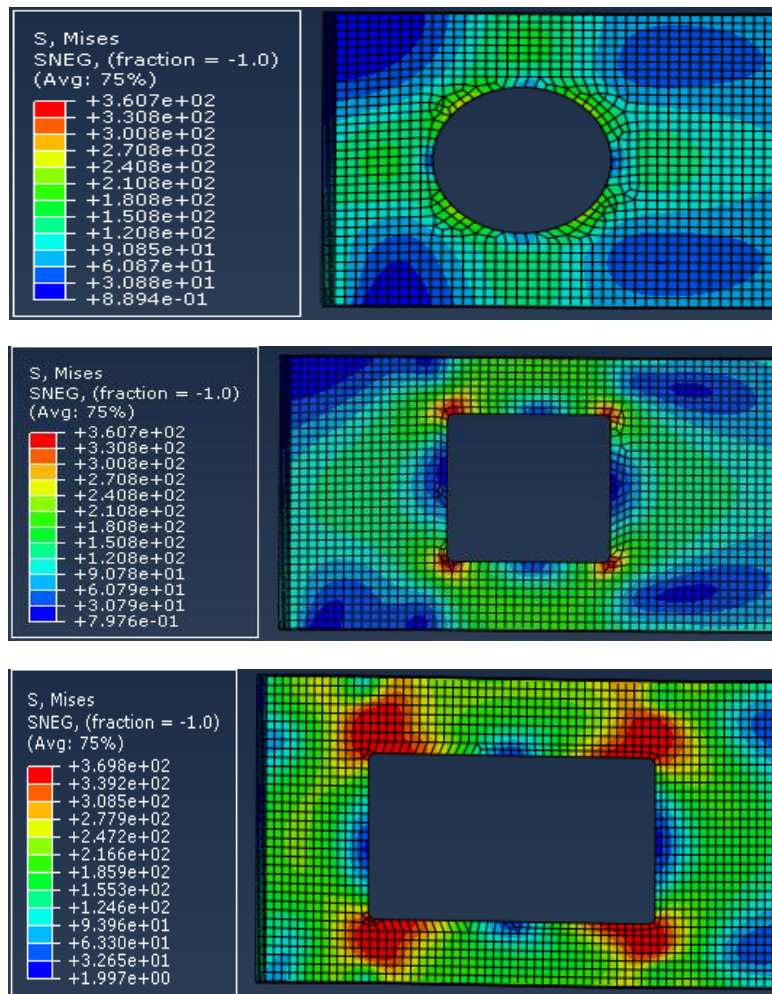


Figure 7.7: Von Mises combined stress distribution contour for case 2

- Case 3

The behaviour of beams analysed in the preceding paragraphs does not have any kind of reinforcements. Case 3 take into account the effect of adding stiffeners on the overall behaviour of WOB to improve and to quantify the beneficial effect of stiffeners the performance of the beams and increase their resistance capacity and to prevent premature buckling to be checked according to EC3 provisions. Accordingly, in order to quantify the importance of reinforcing the opening evaluating and the influence of geometry shape of the beam with opening web, case 3 has been studied. Indeed, a double-sided longitudinal reinforcement was used to illustrate this parameter

studied in this section as well as the rules presented in section N.2.2 of EC3. Particular provision concerning the length l_v should satisfy as per section N.2.2.5 of EC3: $l_v \geq 0.25l_0$.

The finding indicates that a significantly improved behaviour compared to case1 has been noticed, where all beams reach the ultimate load with a deflection of 14 mm, 16 mm and 28 mm for circular, square and rectangular openings respectively, see Figure 7.8. A Noticeable decrease in stress values were also reached by this case.

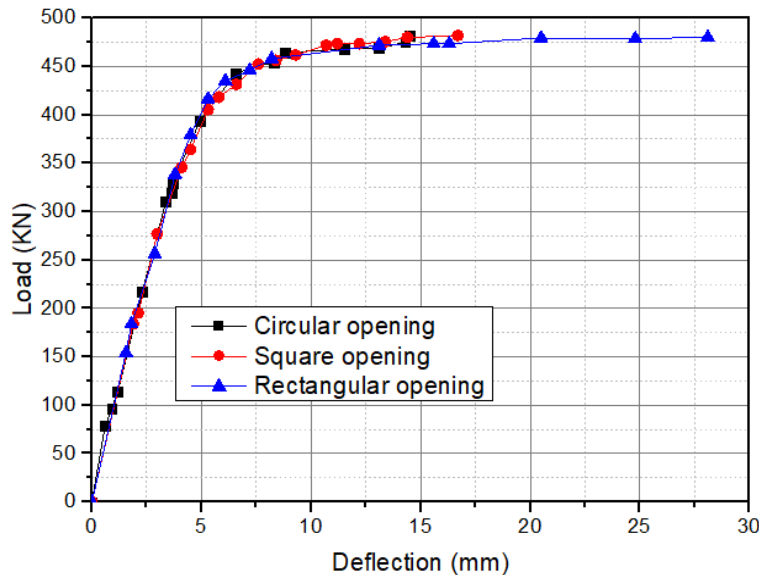
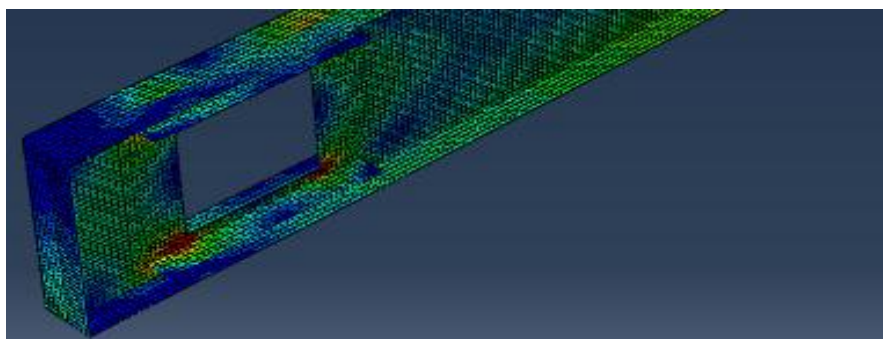
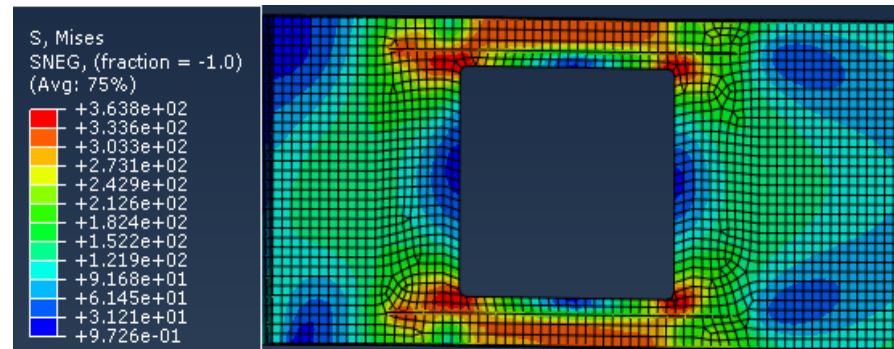
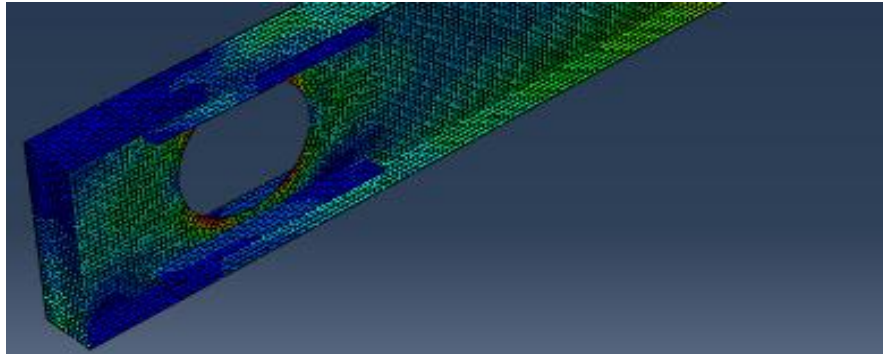
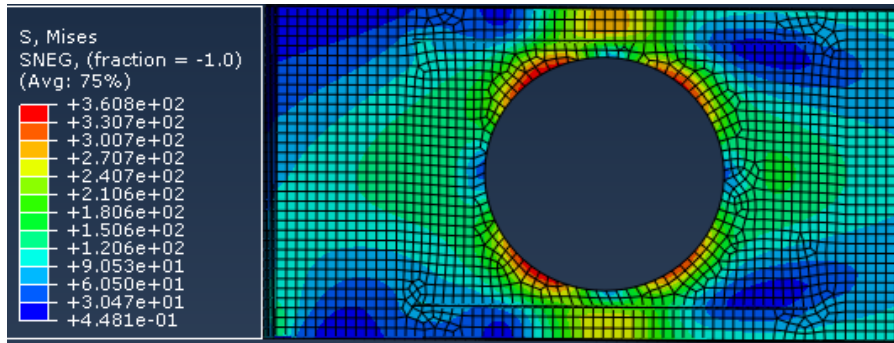


Figure 7.8: Load-deflection curve for case 3.

To investigate the stress distribution around the openings and along the stiffeners, Von Mises stress distribution are provided as plots in Figure7.9, showing the loading history for the last step, that is the ultimate state. Significant deformation is observed at the corners of the stiffened opening and along the stiffener. The results stated that the presence of the longitudinal stiffeners enables a better stress redistribution along the web openings with comparison to results presented in figure7.6 contributing for an increase of the beams load carrying capacity. Despite this beneficial effect, The Vierendeel mechanism was still the main collapse mode associated to specimens



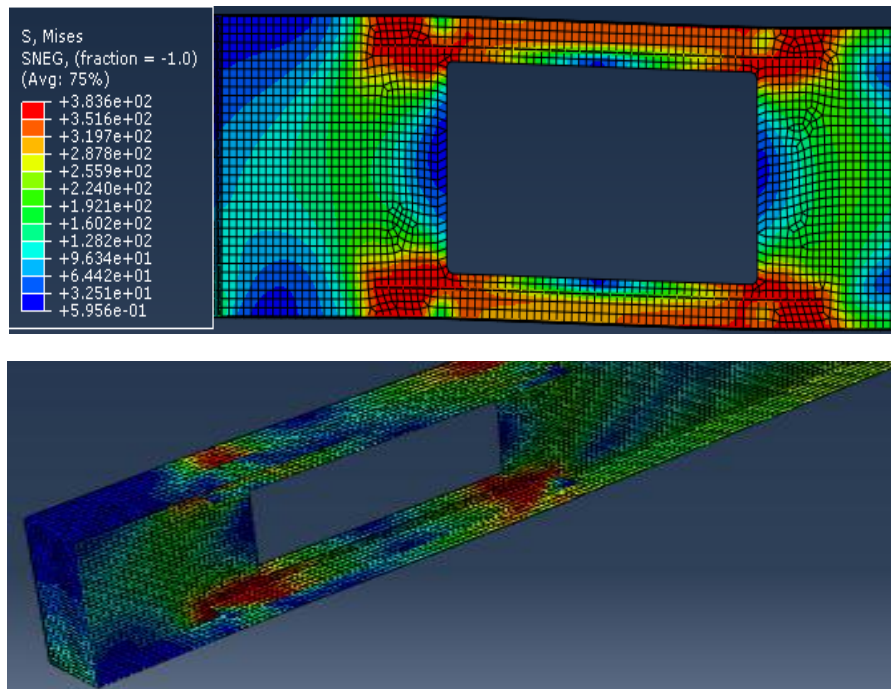


Figure 7.9: Deformed shape and Von Mises stress distribution for case 3

- Case 4

In this particular study, an additional stiffening reinforcement case has been provided to distinguish the difference in terms of global behaviour between cases 3 and 4.

Circular reinforcement for the circular opening has been considered in an appropriate location. Transverse reinforcement on the vertical edges were added to the square and rectangular opening beams to prevent buckling of the compression flange in the plane of the web. The obtained load-deflection graph shows, a slight decrease in deflection with 13mm, 15 mm and 23mm for circular, square and rectangular opening respectively as presented in the relative Figure 7.10.

Figure 7.11 illustrates the distribution of stresses along the reinforcements. As can be seen in Figure 7.11, the upper flange does not achieve any plasticizing behaviour, and remain elastic for all stages of loading, especially for beams having circular and square openings. This complies with the statement mentioned above where this case contributes to prevent buckling of the compression flange. Moreover, a noticeable decrease of stress value was obtained.

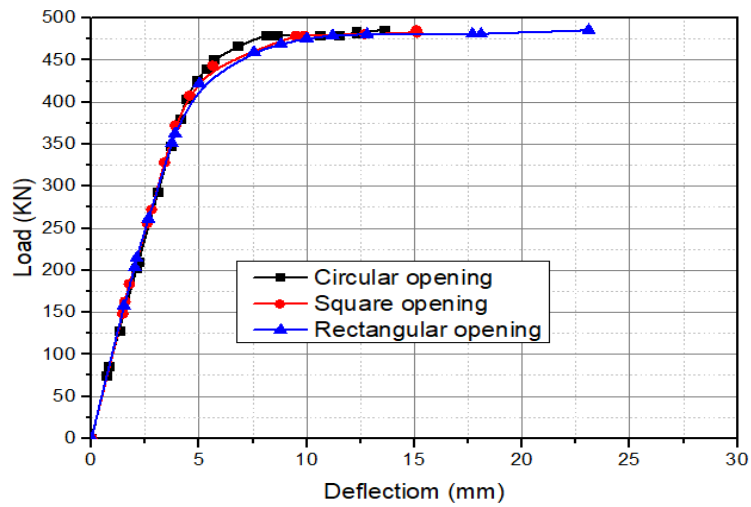
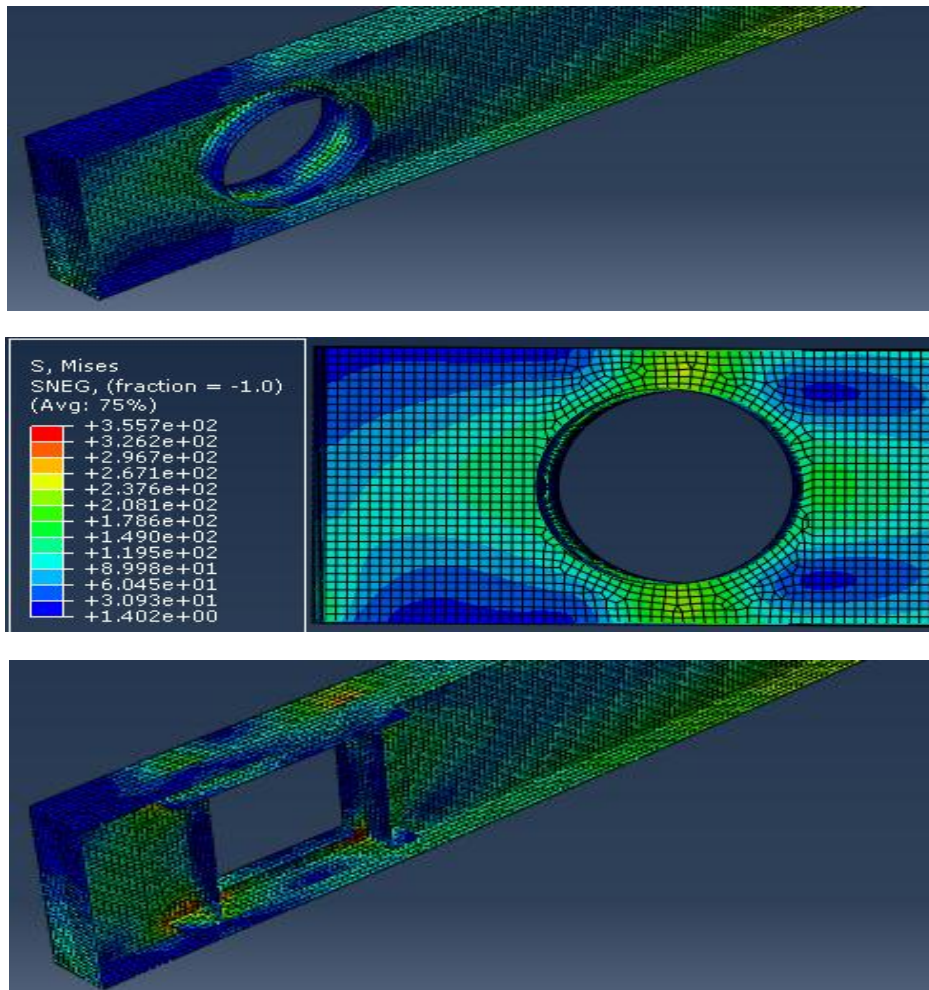


Figure 7.10 Load-deflection curve associated to case 4



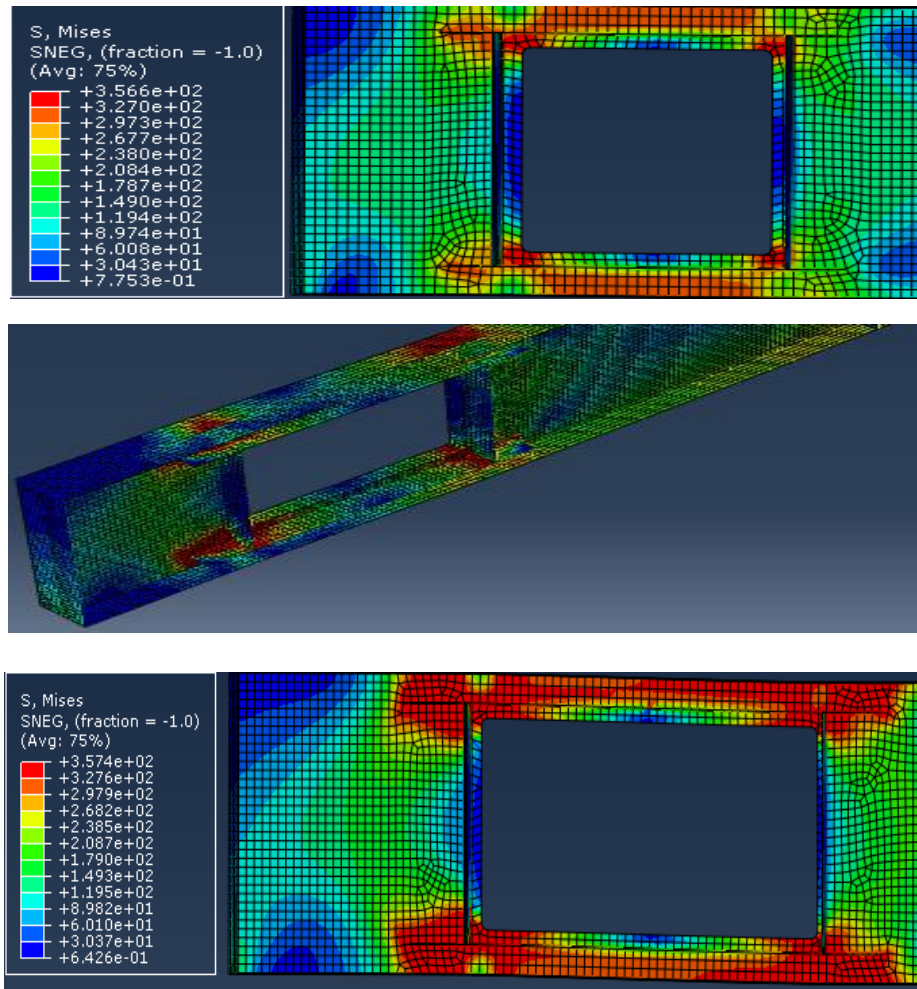


Figure 7.11: Deformed shape and Von Mises stress distribution for case 4

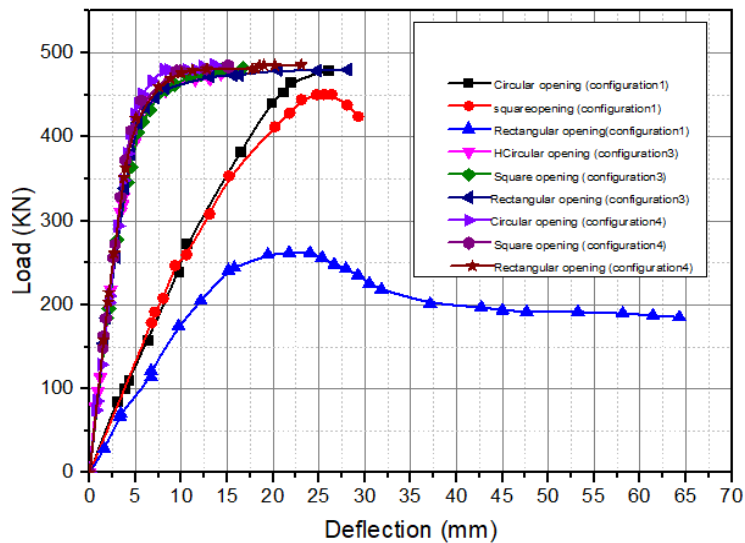


Figure 7.12: Load-deflection comparative curves

Comparative graphs were plotted, see Figure 7.13, in order to show the difference between parameters investigated in cases 1,3 and 4.

7.3 Parametric study and modelling of portal frames

7.3.1 Model description

This section aims to evaluate the performance of steel structural members in order to examine the behaviour of WOBs when associated with columns in moment-resisting steel frames.

A series of four portal frame single story single bay has been investigated. Geometrical properties, support conditions at the bottom of columns are shown in Table 7.4. Basic geometry layout of models of the portal single storey one bay with cellular beams is shown in Figure 7.13. The main focus of the study deal with the simulation of a series of beams were modelled in section 6.4.2 (Warren.J tested beams including 1A and 3B) embedded in portal frame structures associated to columns. Four models where the beams are connected to columns with tie constrains.

Table7.4: portal frames models

Models	Column length	Beam used	BC
Model 1	3.5m	1A	ENCASTRE
Model 2	3.5m	1A	Pinned-Rolled
Model 3	4.6m	3B	ENCASRE
Model 4	4.6m	3B	Pinned-Rolled

7.3.2 Boundary conditions and meshing for the portal frames

Two boundary conditions at the base section have been selected for the modelled portal frames. Firstly, both the extremities of the columns where restrained symmetrically fixed. Then, a hinged support was chosen to restrict the bottom left side with pinned support and the bottom right side with rolled support. Thus, Quad-dominated mesh type were used to simulate the four models of the portal frames, with Four noded shell elements namely S4R

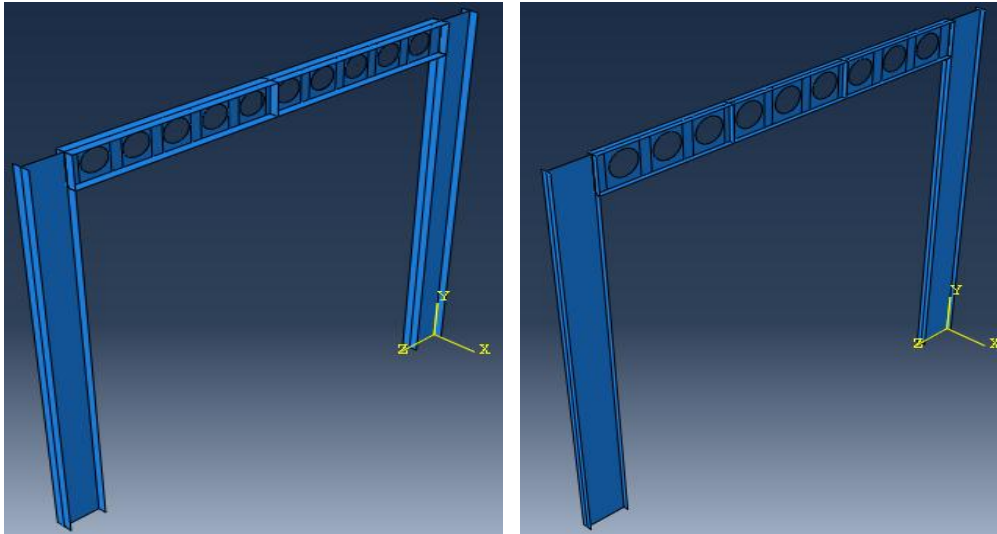


Figure 7.13: Basic geometry layouts of models of the portal single storey one bay with cellular beams.

- **Model 1**

Figure 7.14 describes FEA results concerning the linear and nonlinear behaviours of Models through different branches linear and nonlinear elasto-plastic can be noticed. At the value level of 120 KN corresponding to about 5 mm deflection indicating that the curve begins to have a nonlinear form, that is the first yielding state. A no-straight branch pointed out that the ruin occurs under a constant load where takes the value of 130 KN with about 9.3 mm transverse deflection. This nonlinear response can be quantified by a ratio of 1.08 (i.e. 8%) from first yielding to the final step.

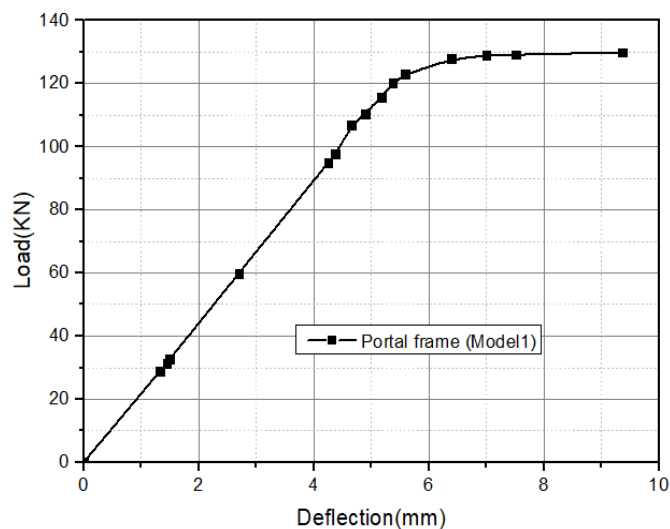
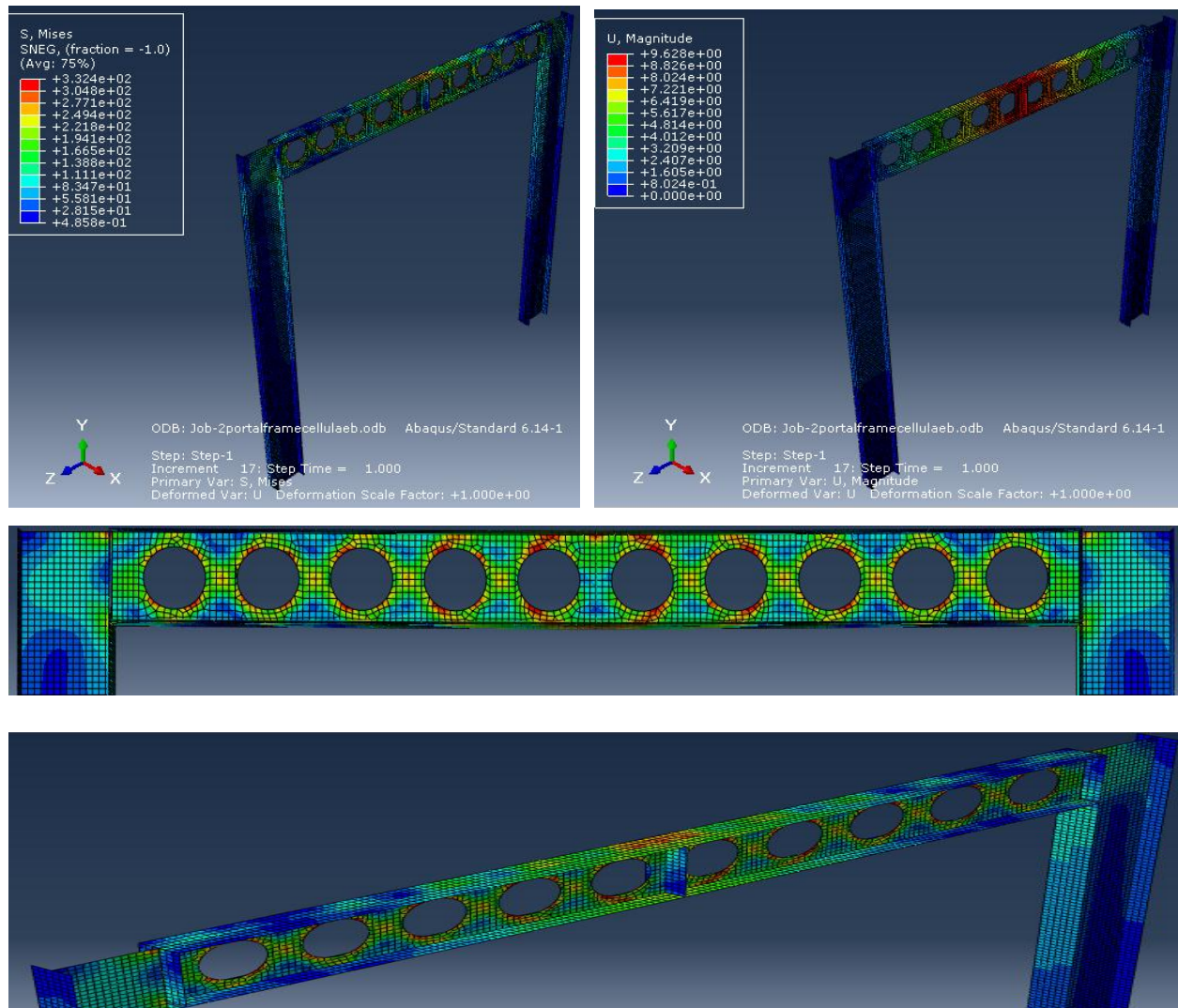


Figure 7.14: Load-deflection curve for model 1.

Analysis of key parameters on the nonlinear behaviours of WOB's.

The results were also presented by introducing the Von-Mises stress contour, and as noted, a significantly reduced stress value to 332 MPa was reached near the openings. Whereas the red regions were also downplayed. The connection area between the beams and the column reflects with two red zones indicating the value of the height stress. Vierendeel bending was the primary mode of failure, and the upper flange buckle locally at the point of load application.



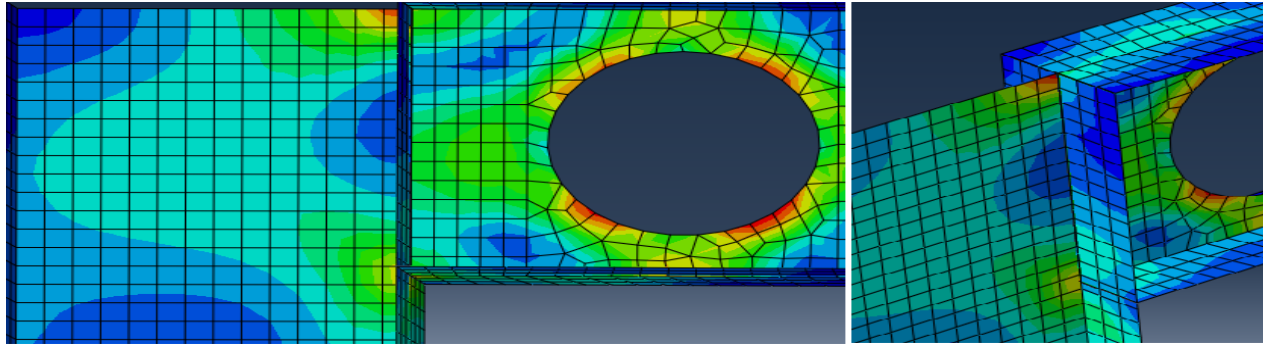


Figure 7.15: Deformed shape and Von Mises Equivalent Stress contour for model 1 with some other details in different interesting sections.

- Model 2

Model 2 is investigated to proof the effect of boundary conditions on the overall behaviour of the frame. As presented in Figure 7.16, the elasto-plastic behaviour of model is clearly observable. It is worth to note that the performance of model 2 is influenced compared to model 1 by the change made in the boundary conditions from fully restrained (encasté) to pinned-rolled conditions. At the value of 110 kN which corresponds roughly to 6 mm vertical deflection indicating that the curve begins to have a nonlinear form. At plastic range, the beam continues to deflect under a constant load, and then a slow increase in the applied load with a value of 130 kN which produces 11.95 mm of transverse deflection.

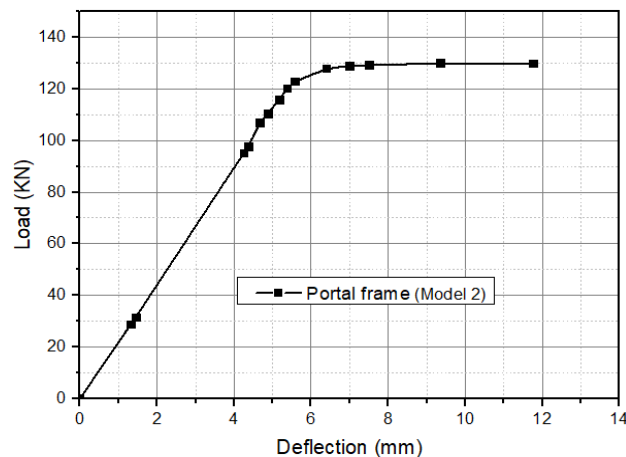
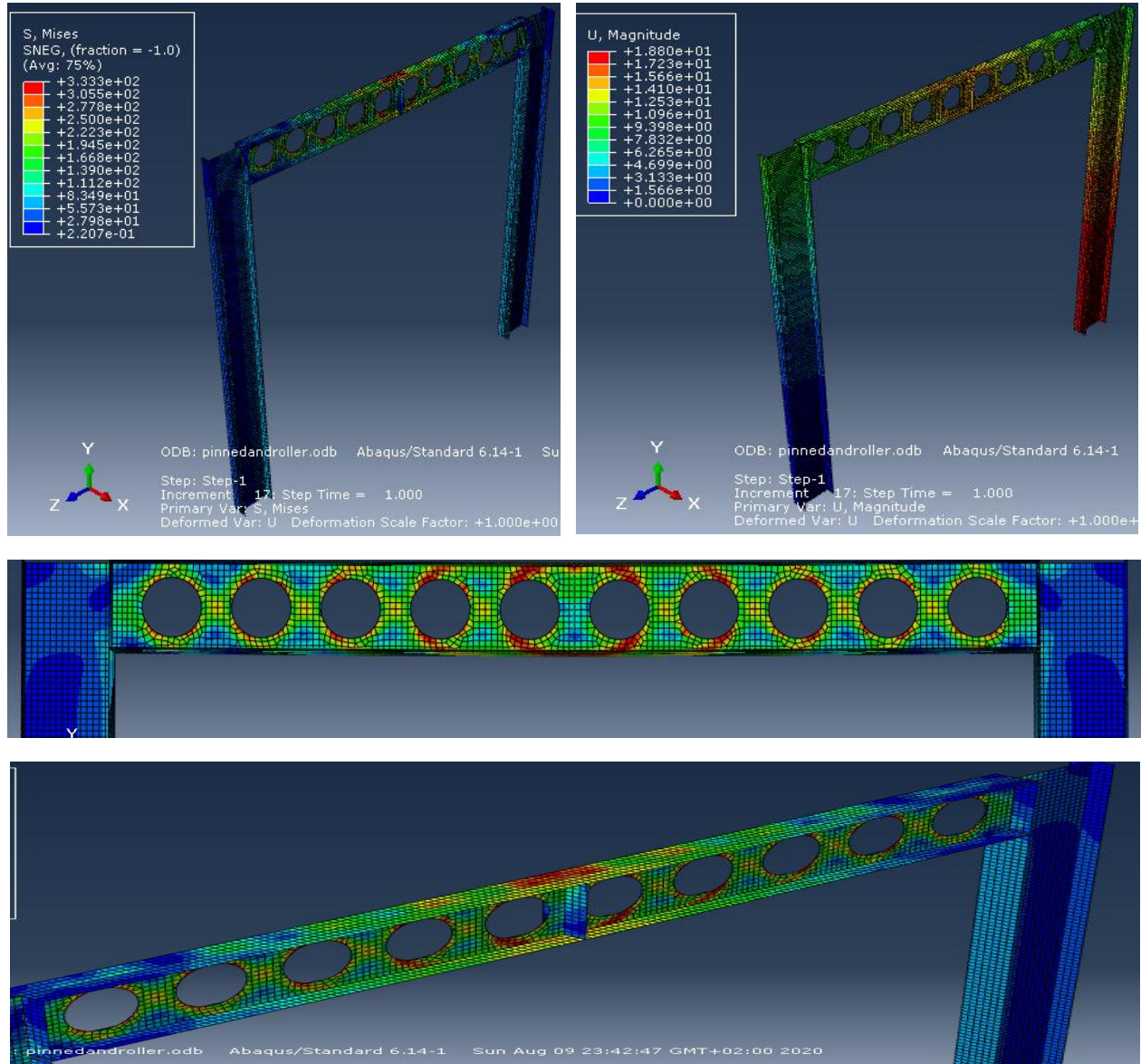


Figure 7.16: Load-deflection curve for model 2.

The deformed configurations located in the most critical sections are shown in Figure 7.17. Von Mises stress contour shows a maximum value of 333 MPa, which is approximately the value

of yield stress, and it is also visible that the location of the high stressed zone was close to the circular openings with a slight increase compared to Model 1. Obviously, this is due to the new boundary conditions which are pinned-rolled instead of fully restrained. Also, four plastic hinges have been formed around the opening, signifying clearly the existence of a Vierendeel bending mechanism. It has been noticed that the upper flange of the beam buckles locally under concentrated loading.



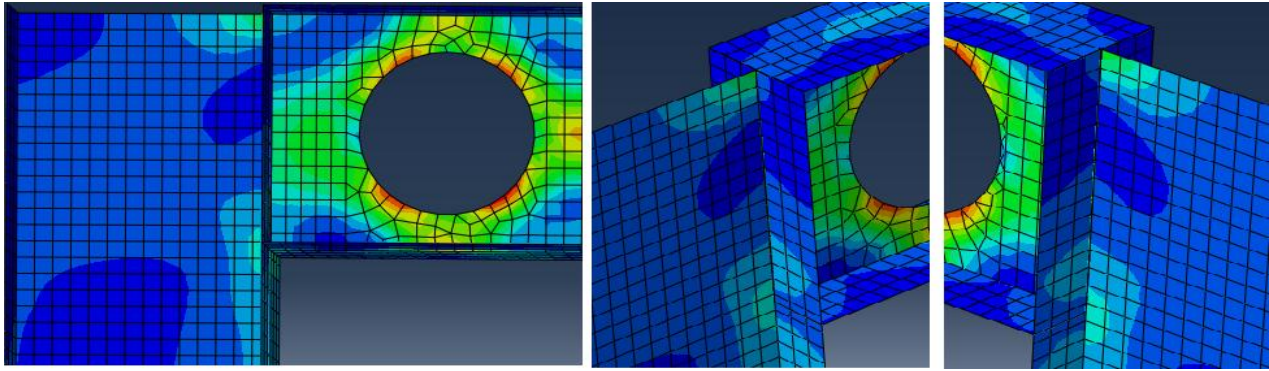


Figure 7.17: Deformed shape and Von Mises Equivalent Stress contour for model 2 with some other details in different interesting sections.

- Model 3

For model 3, the beam named 3B behaves differently when integrated into a portal frame. In the Load-deflection curve plotted in Figure 7.18, two branches representing respectively the linear and nonlinear behaviour of the structure. The first yielding occurs at 170 KN under a transverse deflection of 8 mm, indicating the beginning of an elasto-plastic behaviour. The curve reaches an ultimate applied load of around 192KN under 15mm transverse deflection.

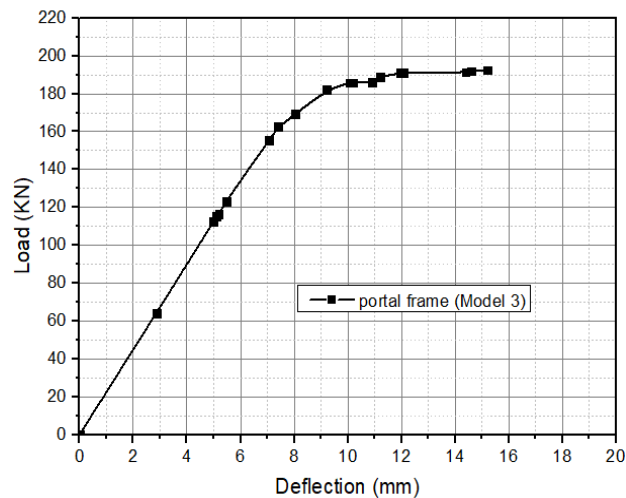


Figure 7.18: Load-deflection curve for model 3.

With respect to the results obtained, Figure 7.19 displays the distribution of stress for mode 13, for which similar remarks can be made as it was Model 1, including the decrease in stress values and reduction in the high stressed regions. As can be seen in Figure 7.19, the beam to column connection were presents also plasticization zones. With a maximum stress value of 334 MPa. The mode of failure is definitely associated to Vierendeel bending accompanying with a local buckling of the upper flange.

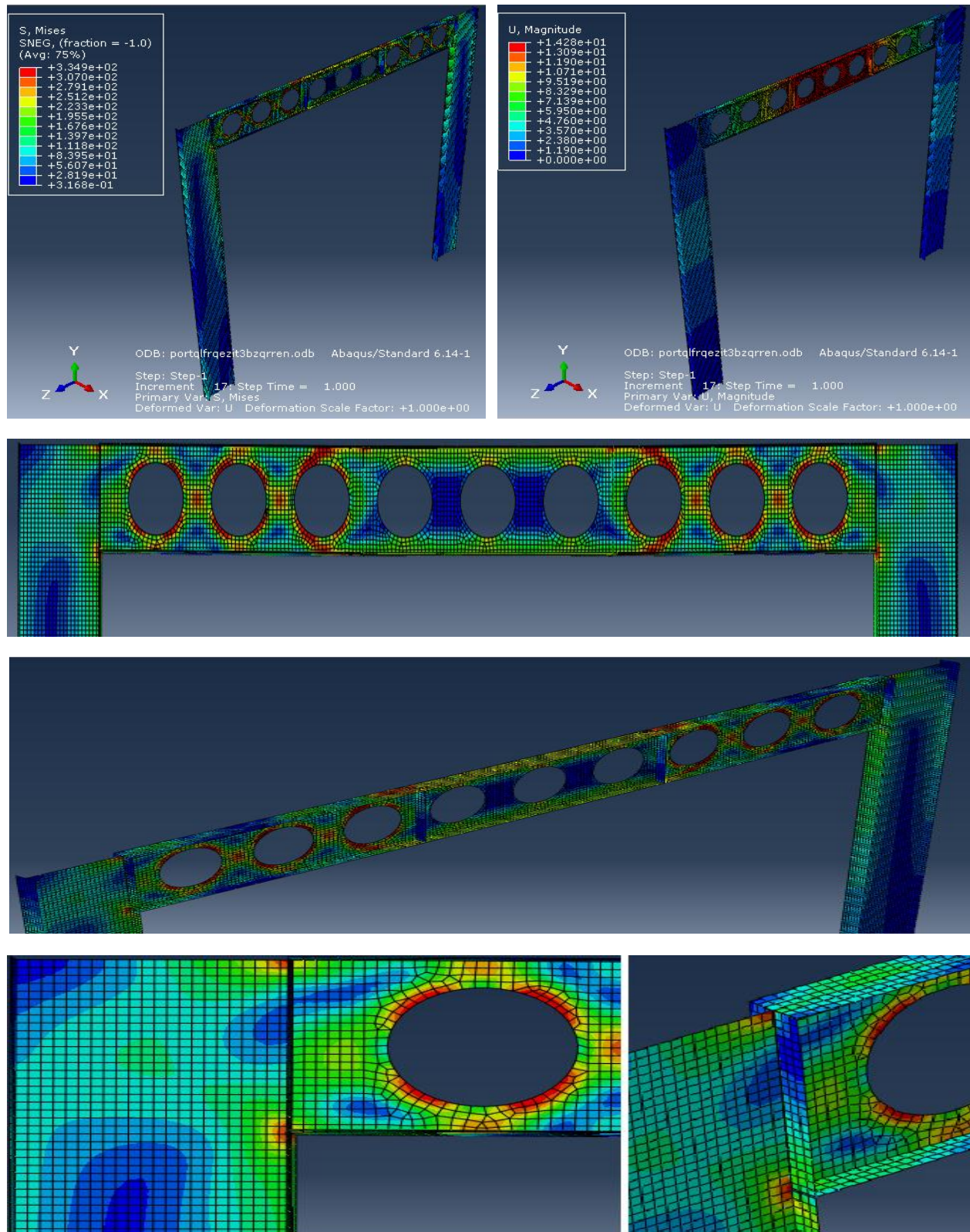


Figure 7.19: Deformed shape and Von Mises Equivalent Stress contour for model 3 with some other details in different interesting sections.

Analysis of key parameters on the nonlinear behaviours of WOB's.

- Model 4

By varying the boundary conditions, a noticeable difference between model 3, model 4 and the tested beam 3B is also remarkable. Figure 7.20 illustrates the linear and nonlinear behaviours of model 4. The first yielding appears at load equal to 170kN associated to 7 mm transverse deflection. The ultimate load was about 193 kN under deflection of 19.5mm, representing the last step of loading.

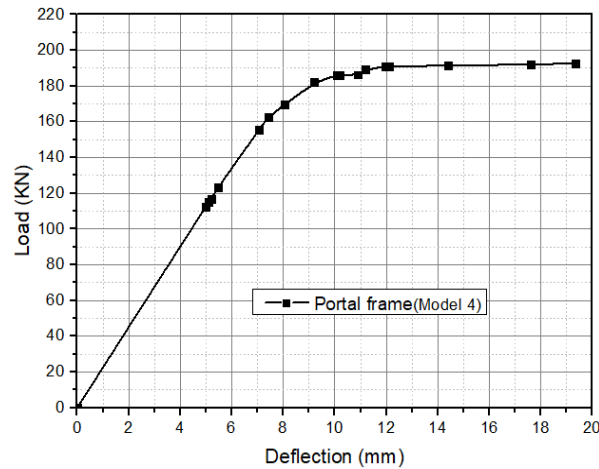
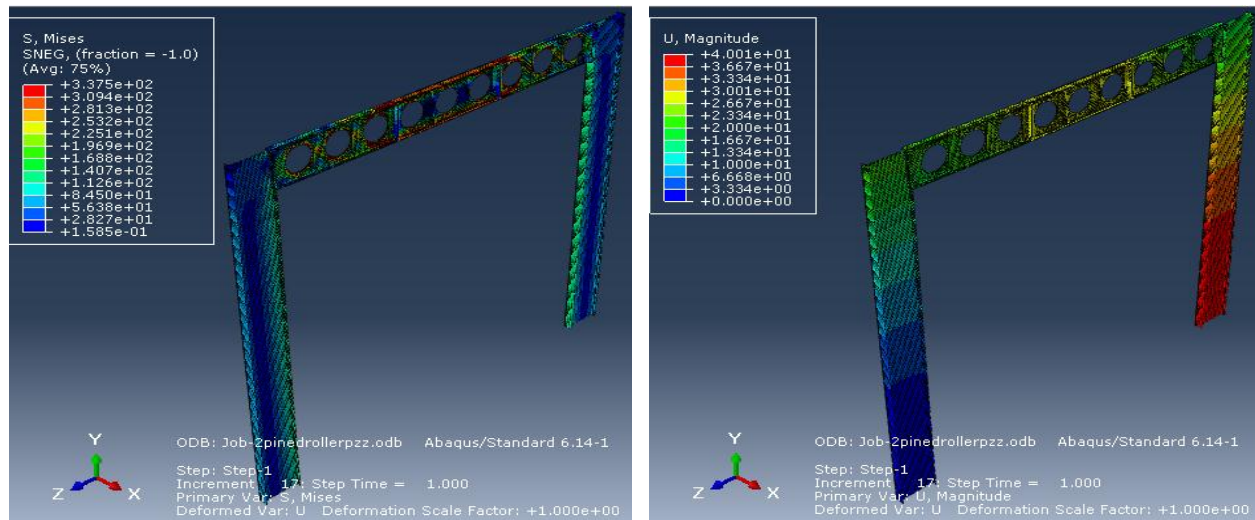


Figure 7.20: Load-deflection curve for model 4.

Von-Mises stress distribution plotted in figures below, shows the same patterns of stress contours with an augmentation of the stress areas from that in model 3 where achieved. With a value of 337 MPa.



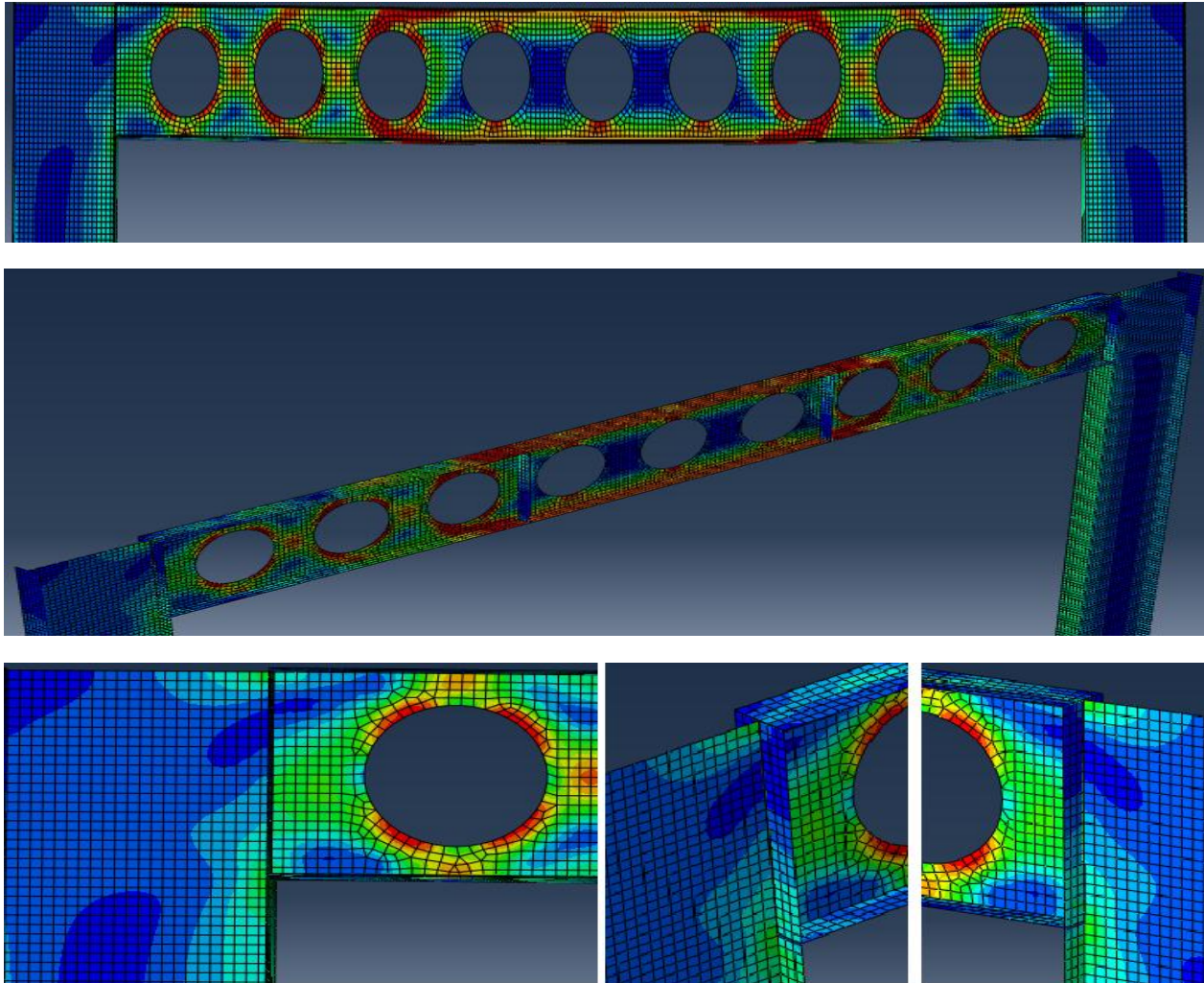


Figure 7.21: Deformed shape and Von Mises Equivalent Stress contour for model 4 with some other details in different interesting sections.

7.4 Summary of the obtained results:

The results found in this study fully discussed in previous sections demonstrates, once again, that the shape of the opening plays an important role affecting the failure mode and load carrying capacity for 0.7 h web-opening. A better performance has been noticed for the circular opening with nearer behaviour of the square opening. Whereas the rectangular opening has comparably, somewhat, the poorest performance. By reducing the height of the opening from 0.7h to 0.5h a significant difference in load carrying capacity was obtained along with a reduction in deflection and notable decrease in the maximum values of combined stresses from Von Mises Criteria.

As the first configuration shows really poor behaviour, especially for rectangular opening, stiffeners must be provided to delay the instability and increase the cross-sectional resistance significantly. Accordingly, the webs are stiffened by placing stiffeners on each side of the opening where the stress concentration is closer there leading to shear failure. To obtain better results in improving the efficiency of the stiffeners, another configuration was adopted, in which the results reported a difference with an improvement in stress distribution around the opening and along the stiffeners with a slight decrease in deflection.

The additional study carried out on four single storey one bay structures with multiple cellular beams taken from literature gives a number of interesting outputs including that the location of the critical sections were pointed at the opening's edges, concentrated loading and beam to column connections conditions, where the red regions reflects the presence of the height stress zones. One of the important remarks that can be made is that two different boundary conditions lead to different behaviour in terms of stresses and strains. Moreover, it was found that the modelled portal frames with fully restraints conditions gives a more valuable performance compared to models with rolled-pinned conditions classified as sway structures.

With Comparison between isolated beams and where it is embedded with columns, gives rise new stresses and deflections values indicating a different behaviour. The FE outputs shows that the isolated beams have the poorest performance compared either to portal frame with fixed or hinged BC. The major mode of collapse was associated with Vierendeel bending with the formation of four plastic hinges near the openings, and local buckling of the upper flange due to concentrated loading.

Bibliography

[1] European profiles/ Arcelor metal

[2] Arcelor metal-ACB

***SUMMARY, CONCLUSIONS AND RECOMMENDATIONS
FOR FUTURE WORK***

Throughout this Master academic's dissertation, several analyses on web-opening structures are described, conducted and discussed and gives an insight in the nonlinear behaviour of such structures. The dissertation was written over a 20-week period of time with full of difficulties arising from a pandemic situation relating to Covid-19 at the University of Tébessa, in Civil Engineering Department at Sciences and Technology Faculty. It must be mentioned that achieving the work described in this dissertation has needed lot of hard work and time consuming to obtain satisfactory results.

Broadly speaking, it can be asserted that the initial objectives of this study, which were to focus on the investigation of the non-linear behaviour of web opening sections as isolated beams and part of portal single storey frame were generally achieved. The characterization of their failure modes, carrying capacity and the effects on the nonlinear behaviour represented by the different load-deflection curves were fully discussed in the previous chapter. To study the influence of several parameters on the behaviour of WOS, a comprehensive numerical simulation has been performed throughout nonlinear models which were all implanted in ABAQUS software.

As several times mentioned, the present Master's dissertation aims to evaluate the nonlinear behaviour of web-opening structures in two important distinct parts. Firstly, a validation throughout a numerical modelling of two experimental data, available in literature, and compared to results coming from a series of previous others FE simulation works, also available in literature. The main difficulty was to overcome the lack of some information concerning the inputs file and details of the test procedure and set-up, especially for Redwood and Mccutcheon's data. Secondly, a parametric study was conducted to examine the effect of several parameters on the global and local behaviours of models built-up in ABAQUS, i.e. shape of the opening, dimension of the opening. Additionally; the favourable effect of reinforcements near the openings has been investigated, with the study of these beams associated with a portal single storey frame. For these purposes, 16 numerical FE simulations were implemented in ABAQUS, in which 12 models devoted to isolated beams and 4 other models for beams connected to columns (portal frame).

From this work, some main conclusions may be drawn to summarise the findings of the undertaken nonlinear analysis; and which will be presented in two parts, namely: the conclusions related to the validation of experimental data provided in literature with FEA models described earlier in this dissertation; and conclusions relative to the parametric analysis.

- **Part 1 Conclusions**

By using the experimental data Redwood and Mccutcheon to model numerically the behaviour of tested beams; some concluding remarks can be recalled:

- In all models studied, Load-Displacements curves have been extracted through an excel program and contain two branches: linear showing an elastic behaviour and a nonlinear branch describing an inelastic behaviour. This clearly shows a true behaviour of the models.

- The obtained results relative to beams 2A and 3A examined in this section are in good agreement with the major parameter studied, i.e. the effect of beam slenderness and strain-hardening with values of 5% and 2% respectively.

- When varying the length span from short one of 1.5 m to larger one of 2.54m; it has been noticed this variation affect significantly the inelastic performance by influencing Vierendeel bending failure mode and observed of an augmentation of stress values leading to the creation of large critical sections. Additionally, an increase in vertical deflection has be also remarked.

- The influence of the strain hardening input by adopting a value of 2%; which depends in fact on the thickness of section as per EC3, the outcomes of this study are in very good agreement with the work of Chung. Using the value of 5% the results cope very well with a more recent work of Flavio's. leading to an improvement of bending moment resistance capacity. Also, it is worth to recall that the author has used ABAQUS for modelling while the two earlier works, namely Chung and Flavio have been using other software leading to approximately similar results especially the combined stresses; that Von Mises outputs.

- The observed failure modes of all studied models, were restrained against any LTB's effect as specified in the experimental work set-up were all of type of Vierendeel bending with the formation of four partial plastic hinges near the openings. It must be reminder that in all models were. As far as

The validation of inelastic the numerical models implanted in ABAQUS for the work published by Warren was done. It is worth to point out that only one from four analyses of Warren's work has been used for the validation namely the experiment data and outcome of numerical LUSAS software. The idea behind the choice of beams 1A and 3B was to show the

differences by using many geometrical characteristics, i.e. the section of the profile, the number of openings, the spacing between the openings and the points of application of the load. The position of transverse loading effect has been investigated, at mid-span and at equal distance respectively, and because of the value of bending moments have led to some differences in terms of stress distributions configurations and deformations. Comparable results with Warren's published LUSAS modelling results were found by the author. Once again, as in Warren's results; Vierendeel failure occurred in the opening with the highest combined shear and moment for both the mid span and third point load cases.

- **General conclusions from the parametric study**

Because of the satisfactory results described in the upper section, in which the performed numerical modelling analysis have shown agreement with experimental data along with other FEA modelling, it was decided to carry out a parametric study on the factors thought to be affecting the global behaviour of WO structures. Indeed, checking out as stated in many researches works in literature, that the mechanical behaviour of these structures is strongly depending on several parameters, in particular the shape of the openings, the position, and the dimensions of the openings. From this parametric analysis, one can draw some main concluding remarks:

For case 1, the opening geometry influences significantly the beams load carrying capacity the values of stresses and strains. As expected, the beams with rectangular shape openings presented the smaller ultimate loads, which is about 50% lesser than their equivalent beams with square or circular openings. While the beam with circular opening demonstrates that despite the higher shear force acting at the openings, their circular geometry enables the beams to sustain higher ultimate loads, similar to the ultimate loads of plane beams without openings. Also, it was demonstrated in this particular study that the structural efficiency of unstiffened steel beam with circular web openings by showing a more satisfactory behaviour over their equivalent unstiffened solutions with square and rectangular openings.

For case 2 in which the dimensions of the openings are reduced from 0.7 h to 0.5 h, it was noticed an increase in load carrying capacity and a small reduction of the transverse deformations was achieved.

By placing stiffeners around the opening, which are frequently used, as per EC3, for circular, square and rectangular openings are frequently used, an improving of performance of the beam compared to the unstiffened one was noticed.

In addition, it was found that the use of longitudinal stiffeners along the opening area showed a benefit over beams with unreinforced opening solutions. Equipping beams with longitudinal stiffeners increased the ultimate load carrying capacity of beams by about twice as much as the non-reinforced beams with rectangular and square openings, respectively.

The use of adequate edge concordance radius in beams with rectangular and square openings is very important parameter to be taken into account for a better distributing steel beam web stress.

Accordingly, the Vierendeel collapse mechanism was observed in all the beams combined with locale buckling, namely local buckling of flanges, under the concentrated loading.

- Portal frame study:

Once again, it should be mentioned that the lack of knowledge on the mechanical behaviour of WOB's embedded into a whole structure impedes the understanding of the influence of web openings in beams connected to columns. That the reason for choosing very simple cases to try to better understand portal frame having web opening behaviour.

the assembly of the beams and columns into a single bay portal frame has shown a better performance in terms of stresses and deformations compared to isolated beams, namely with the decrease of the plasticization zones.

By changing the boundary conditions at the bottom of columns has led to different stress values around the openings and at the beam to column connection. Additionally, the fixed end supports shows advantageous behaviour compared to pinned ends.

Even for a portal frames, Vierendeel bending seems to be the main mode of failure, which is caused by the transferred shear force passing through the openings combined with local buckling of the compressed flange.

the main findings of this work can be summarised as expected, that single web opening beams present best performance in regard to Vierendeel bending and stress concentration compared to beams with multiple web openings. Where the strain hardening, the beam span and the location of the applied load play major roles for this section. According to results obtained in the parametric study, the opening shape and size have a significant effect on the load carrying capacities and stress distribution. Stiffeners may be required in the previous cases. A clear difference in behaviour was

obtained by the adoption of two different configurations when dealing with the main failure mode, which is Vierendeel bending. The outcomes from the simulated portal frames have shown an advantageous performance in terms of stresses and strains with both fixed or pinned ends.

To conclude this research topic, the following recommendations for future research works can be suggested:

1. Assessment of the linear and nonlinear of isolated beams having web-opening under dynamic loadings.
2. Evaluation of the linear and nonlinear of isolated beams having web-opening under fire conditions.
3. Investigation of the instability phenomenon namely Lateral Torsional Buckling on the static linear and nonlinear behaviours on WO structures.
4. The study of elastic and inelastic global behaviour of multi-storeys buildings under static and dynamic loadings.
5. Investigation of the seismic performance of steel buildings having WO Beams in low and moderate earthquake zones.